Eur. Phys. J. C (2016) 76:683
DOI 10.1140/epjc/s10052-016-4481-2

THE EUROPEAN PHYSICAL JOURNAL C

CrossMark

Regular Article - Experimental Physics

Search for squarks and gluinos in events with hadronically decaying tau leptons, jets and missing transverse momentum in proton–proton collisions at $\sqrt{s} = 13$ TeV recorded with the ATLAS detector

ATLAS Collaboration[⋆]

CERN, 1211 Geneva 23, Switzerland

Received: 21 July 2016 / Accepted: 7 November 2016 / Published online: 10 December 2016
© CERN for the benefit of the ATLAS collaboration 2016. This article is published with open access at Springerlink.com

Abstract A search for supersymmetry in events with large missing transverse momentum, jets, and at least one hadronically decaying tau lepton has been performed using 3.2 fb^{-1} of proton–proton collision data at $\sqrt{s} = 13$ TeV recorded by the ATLAS detector at the Large Hadron Collider in 2015. Two exclusive final states are considered, with either exactly one or at least two tau leptons. No excess over the Standard Model prediction is observed in the data. Results are interpreted in the context of gauge-mediated supersymmetry breaking and a simplified model of gluino pair production with tau-rich cascade decays, substantially improving on previous limits. In the GMSB model considered, supersymmetry-breaking scale (Λ) values below 92 TeV are excluded at the 95% confidence level, corresponding to gluino masses below 2000 GeV. For large values of $\tan\beta$, values of Λ up to 107 TeV and gluino masses up to 2300 GeV are excluded. In the simplified model, gluino masses are excluded up to 1570 GeV for neutralino masses around 100 GeV. Neutralino masses below 700 GeV are excluded for all gluino masses between 800 and 1500 GeV, while the strongest exclusion of 750 GeV is achieved for gluino masses around 1450 GeV.

Contents

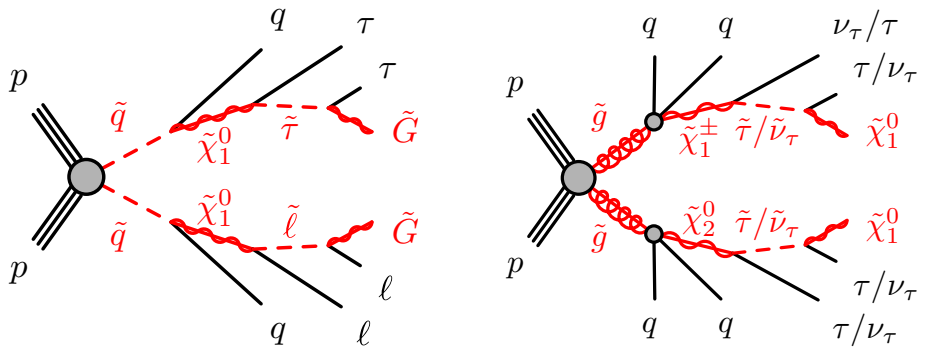
1 Introduction 1
2 The ATLAS detector 3
3 Data and simulation samples 3
4 Reconstruction of final-state objects 4
5 Event selection 5
6 Background estimation 7
6.1 Vector-boson and top quark backgrounds 8
6.2 Multi-jet background 11
7 Systematic uncertainties 12
8 Results 15
9 Summary 16
References 18

⋆ e-mail: atlas.publications@cern.ch

1 Introduction

Supersymmetry (SUSY) [1–6] introduces a symmetry between fermions and bosons, resulting in a SUSY partner (sparticle) for each Standard Model (SM) particle, with identical mass and quantum numbers, and a difference of half a unit of spin. Squarks ($\tilde{q}$), gluinos ($\tilde{g}$), sleptons ($\tilde{\ell}$) and sneutrinos ($\tilde{\nu}$) are the superpartners of the quarks, gluons, charged leptons and neutrinos, respectively. The SUSY partners of the gauge and Higgs bosons are called gauginos and higgsinos, respectively. The charged electroweak gaugino and higgsino states mix to form charginos ($\tilde{\chi}_i^{\pm}$, $i = 1, 2$), and the neutral states mix to form neutralinos ($\tilde{\chi}_j^0$, $j = 1, 2, 3, 4$). Finally, the gravitino ($\tilde{G}$) is the SUSY partner of the graviton. As no supersymmetric particle has been observed, SUSY must be a broken symmetry. In general, the minimal supersymmetric Standard Model (MSSM) allows couplings which violate baryon- and lepton-number conservation, leading to, for example, a short proton lifetime. To ensure accordance with established measurements, R-parity [7–11] conservation is often assumed. In this scenario, sparticles are produced in pairs and decay through cascades involving SM particles and other sparticles until the lightest sparticle (LSP), which is stable, is produced.

Final states with tau leptons are of particular interest in SUSY searches, although they are experimentally challenging. Light sleptons could play a role in the co-annihilation of neutralinos in the early universe, and models with light scalar taus are consistent with dark-matter searches [12]. Furthermore, should SUSY or any other physics beyond the Stan-



(a) GMSB **(b)** Simplified model

Fig. 1 Diagrams illustrating the two SUSY scenarios studied in this analysis. In the GMSB model, the scalar lepton $\tilde{\ell}$ is preferentially a scalar tau $\tilde{\tau}_1$ for high values of $\tan\beta$

dard Model (BSM) be discovered, independent studies of all three lepton flavours are necessary to investigate the coupling structure of the new physics, especially with regard to lepton universality. If squarks and gluinos are within the reach of the Large Hadron Collider (LHC), their production may be among the dominant SUSY processes.

This article reports on an inclusive search for squarks and gluinos produced via the strong interaction in events with jets, at least one hadronically decaying tau lepton, and large missing transverse momentum from undetected LSPs. Two distinct topologies are studied, with one tau lepton (1τ) or two or more tau leptons (2τ) in the final state. These mutually exclusive channels are optimised separately. The analysis is performed using 3.2 fb^{-1} of proton–proton (pp) collision data at $\sqrt{s} = 13$ TeV recorded with the ATLAS detector at the LHC in 2015. Two SUSY scenarios are considered: a gauge-mediated SUSY-breaking (GMSB) model, and a simplified model of gluino pair production. Previous searches based on the same final state have been reported by the ATLAS [13,14] and CMS [15] collaborations.

In GMSB models [16–18], SUSY breaking is communicated from a hidden sector to the visible sector by a set of messenger fields that share the gauge interactions of the SM. SUSY is spontaneously broken in the messenger sector, leading to massive, non-degenerate messenger fields. Gauginos acquire their masses via one-loop diagrams involving messengers. Squarks and sleptons, which do not couple directly to the messenger sector, get their masses from two-loop diagrams involving messengers and SM gauge bosons, or messengers and gauginos. The free parameters of GMSB models are the SUSY-breaking mass scale in the messenger sector (Λ), the messenger mass scale (M_{mes}), the number of messenger multiplets (N_5) of the $\mathbf{5}+\bar{\mathbf{5}}$ representation of SU(5), the ratio of the two Higgs-doublet vacuum expectation values at the electroweak scale ($\tan\beta$), the sign of the Higgsino mass term in the superpotential ($\text{sign}(\mu) = \pm 1$), and a gravitino-mass scale factor (C_{grav}). Masses of gauginos and sfermions are proportional to Λ, and scale as N_5 and $\sqrt{N_5}$, respectively. The M_{mes} scale is required to be larger than Λ, to avoid tachyonic messengers and charge- and colour-breaking vacua, and lower than the Planck mass to suppress flavour violation. The latter condition implies that the lightest supersymmetric particle is a very light gravitino. The C_{grav} parameter, which results from the mechanism communicating SUSY breaking to the messengers, mainly affects the decay rate of the next-to-lightest supersymmetric particle (NLSP) into the LSP.

As in previous ATLAS searches [13,14], the GMSB model is probed as a function of Λ and $\tan\beta$, and the other parameters are set to $M_{\text{mes}} = 250$ TeV, $N_5 = 3$, $\text{sign}(\mu) = 1$ and $C_{\text{grav}} = 1$. For this choice of parameters, the NLSP is the lightest scalar tau ($\tilde{\tau}_1$) for large values of $\tan\beta$, while for lower $\tan\beta$ values, the $\tilde{\tau}_1$ and the superpartners of the right-handed electron and muon ($\tilde{e}_{\text{R}}$, $\tilde{\mu}_{\text{R}}$) are almost degenerate in mass. The squark–antisquark production mechanism dominates at high values of Λ. A typical GMSB signal process is displayed in Fig. 1a. The value of C_{grav} corresponds to prompt decays of the NLSP. The region of small Λ and large $\tan\beta$ is unphysical since it leads to tachyonic states.

The other signal model studied in this analysis is a simplified model of gluino pair production [19] in an R-parity-conserving scenario. It is inspired by generic models such as the phenomenological MSSM [20,21] with dominant gluino pair production, light $\tilde{\tau}_1$ and a $\tilde{\chi}_1^0$ LSP. Gluinos are assumed to undergo a two-step cascade decay leading to tau-rich final states, as shown in Fig. 1b. The two free parameters of the model are the masses of the gluino ($m_{\tilde{g}}$) and the LSP ($m_{\tilde{\chi}_1^0}$). Assumptions are made about the masses of other sparticles, namely the $\tilde{\tau}_1$ and $\tilde{\nu}_\tau$ are mass-degenerate, and the $\tilde{\chi}_2^0$ and $\tilde{\chi}_1^\pm$ are also mass-degenerate, with

$$m_{\tilde{\chi}_1^\pm} = m_{\tilde{\chi}_2^0} = \frac{1}{2}(m_{\tilde{g}} + m_{\tilde{\chi}_1^0}),$$
$$m_{\tilde{\tau}_1} = m_{\tilde{\nu}_\tau} = \frac{1}{2}(m_{\tilde{\chi}_1^\pm} + m_{\tilde{\chi}_1^0}). \quad (1)$$

Gluinos are assumed to decay to $\tilde{\chi}_1^{\pm} q\bar{q}'$ and $\tilde{\chi}_2^0 q\bar{q}$ with equal branching ratios, where q, q' denote generic first- and second-generation quarks. Neutralinos $\tilde{\chi}_2^0$ are assumed to decay to $\tilde{\tau}\tau$ and $\tilde{\nu}_\tau \nu_\tau$ with equal probability, and charginos $\tilde{\chi}_1^{\pm}$ are assumed to decay to $\tilde{\nu}_\tau \tau$ and $\tilde{\tau}\nu_\tau$ with equal probability. In the last step of the decay chain, $\tilde{\tau}$ and $\tilde{\nu}_\tau$ are assumed to decay to $\tau\tilde{\chi}_1^0$ and $\nu_\tau \tilde{\chi}_1^0$, respectively. All other SUSY particles are kinematically decoupled. The topology of signal events depends on the mass splitting between the gluino and the LSP. The sparticle decay widths are assumed to be small compared to sparticle masses, such that they play no role in the kinematics.

2 The ATLAS detector

The ATLAS experiment is described in detail in Ref. [22]. It is a multi-purpose detector with a forward–backward symmetric cylindrical geometry and a solid angle[1] coverage of nearly 4π.

The inner tracking detector (ID), covering the region $|\eta| < 2.5$, consists of a silicon pixel detector, a silicon microstrip detector and a transition radiation tracker. The innermost layer of the pixel detector, the insertable B-layer [23], was installed between Run 1 and Run 2 of the LHC. The inner detector is surrounded by a thin superconducting solenoid providing a 2T magnetic field, and by a finely segmented lead/liquid-argon (LAr) electromagnetic calorimeter covering the region $|\eta| < 3.2$. A steel/scintillator-tile hadronic calorimeter provides coverage in the central region $|\eta| < 1.7$. The end-cap and forward regions, covering the pseudorapidity range $1.5 < |\eta| < 4.9$, are instrumented with electromagnetic and hadronic LAr calorimeters, with either steel, copper or tungsten as the absorber material.

A muon spectrometer system incorporating large superconducting toroidal air-core magnets surrounds the calorimeters. Three layers of precision wire chambers provide muon tracking coverage in the range $|\eta| < 2.7$, while dedicated fast chambers are used for triggering in the region $|\eta| < 2.4$.

The trigger system, composed of two stages, was upgraded [24] before Run 2. The Level-1 trigger system, implemented with custom hardware, uses information from calorimeters and muon chambers to reduce the event rate from 40 MHz to a maximum of 100 kHz. The second stage, called the High-Level Trigger (HLT), reduces the data acquisition rate to about 1 kHz. The HLT is based on software and runs reconstruction algorithms similar to those used in the offline reconstruction.

[1] ATLAS uses a right-handed coordinate system with its origin at the nominal interaction point in the centre of the detector and the z-axis along the beam pipe. The x-axis points from the interaction point to the centre of the LHC ring and the y-axis points upward. Cylindrical coordinates (r, ϕ) are used in the transverse plane, ϕ being the azimuthal angle around the beam pipe. The pseudorapidity is defined in terms of the polar angle θ as $\eta = -\ln\tan(\theta/2)$.

3 Data and simulation samples

The data used in this analysis consist of pp collisions at a centre-of-mass energy of $\sqrt{s} = 13$ TeV delivered by the LHC with a 25 ns bunch spacing and recorded by the ATLAS detector from August to November 2015. Data quality requirements are applied to ensure that all sub-detectors were operating normally, and that LHC beams were in stable-collision mode. The integrated luminosity of the resulting data set is 3.16 ± 0.07 fb^{-1}.

Simulated Monte Carlo (MC) event samples are used to model both the SUSY signals and SM backgrounds, except multi-jet production, which is evaluated from data. All MC samples are generated at $\sqrt{s} = 13$ TeV. In addition to the hard-scattering process, soft pp interactions (pile-up) are included in the simulation using the Pythia 8.186 [25] generator with the A2 [26] set of tuned parameters (tune) and MSTW2008LO [27] parton density function (PDF) set. Generated events are reweighted such that the average number of pp interactions per bunch crossing has the same distribution in data and simulation. For SM background samples, the interactions between generated particles and the detector material are simulated [28] using Geant4 [29] and a detailed description of the ATLAS detector. In the case of signal samples, a parameterised fast simulation [30] is used to describe the energy deposits in the calorimeters.

The W+jets and Z+jets processes are simulated with the Sherpa 2.1.1 [31] generator. Matrix elements (ME) are calculated for up to two partons at next-to-leading order (NLO) and up to four additional partons at leading order (LO) in perturbative QCD using the OpenLoops [32] and Comix [33] matrix element generators, respectively. The polarisation of tau leptons in $W(\tau\nu)$+jets and $Z(\tau\tau)$+jets events is handled by the TauSpinner [34] program. The phase-space merging between the Sherpa parton shower (PS) [35] and matrix elements follows the ME+PS@NLO prescription [36]. The CT10 [37] PDF set is used in conjunction with dedicated parton-shower tuning. Simulated samples are generated in bins of the transverse momentum (p_{T}) of the vector boson. The inclusive cross sections are normalised to a next-to-next-to-leading-order (NNLO) calculation [38] in perturbative QCD based on the FEWZ program [39].

For the simulation of $t\bar{t}$ and single-top-quark production in the Wt- and s-channels, the Powheg- Box v2 [40] generator is used with the CT10 PDF set for the matrix elements calculation. Electroweak t-channel single-top-quark events are generated using the Powheg- Box v1 generator. This generator uses the four-flavour scheme for the NLO matrix element calculation together with the fixed four-flavour CT10f4

PDF set. For all top quark processes, top quark spin correlations are taken into account (for t-channel production, top quarks are decayed using MadSpin [41]). The parton shower, hadronisation, and underlying event are simulated using Pythia 6.428 [42] with the CTEQ6L1 [43] PDF set and the corresponding Perugia 2012 tune [44]. Cross sections are calculated at NNLO in perturbative QCD with resummation of next-to-next-to-leading logarithmic (NNLL) soft gluon terms using the Top++ 2.0 program [45].

Diboson production is simulated using the Sherpa 2.1.1 generator with the CT10 PDF set. Processes with fully leptonic final states are calculated with up to one (4ℓ, $2\ell + 2\nu$) or no partons ($3\ell + 1\nu$) at NLO and up to three additional partons at LO. Diboson processes with one of the bosons decaying hadronically and the other leptonically are simulated with up to 1 (ZZ) or 0 (WW, WZ) partons at NLO and up to 3 additional partons at LO. The generator cross sections are used for these samples.

The simplified-model signal samples are generated using MG5_aMC@NLO v2.2.3 [46] interfaced to Pythia 8.186 with the A14 tune [47] for the modelling of the parton shower, hadronisation and underlying event. The ME calculation is performed at tree level and includes the emission of up to two additional partons. The PDF set used for the generation is NNPDF23LO [48]. The ME–PS matching is done using the CKKW-L prescription [49], with a matching scale set to one quarter of the gluino mass. The GMSB signal samples are generated with the Herwig++ 2.7.1 [50] generator, with CTEQ6L1 PDFs and the UE-EE-5-CTEQ6L1 tune [51], using input files generated in the SLHA format with the SPheno v3.1.12 [52] program. The parton shower evolution is performed using an algorithm described in Refs. [50,53–55]. Signal cross sections are calculated at NLO in the strong coupling constant, adding the resummation of soft gluon emission at next-to-leading-logarithm accuracy [56–60]. The nominal cross section and the uncertainty are taken from an envelope of cross-section predictions using different PDF sets and factorisation and renormalisation scales, as described in Ref. [61].

4 Reconstruction of final-state objects

This analysis primarily requires the presence of jets, hadronically decaying tau leptons and missing transverse momentum in the final state. Jet b-tagging is used to separate the top quark background from vector bosons produced in association with jets (V+jets, where $V = W, Z$). Electrons and muons are vetoed in the 1τ channel, and muons are explicitly used in the 2τ channel for background modelling studies.

Primary vertices are reconstructed using inner-detector tracks with $p_{\mathrm{T}} > 400$ MeV that satisfy requirements on the number of hits in silicon tracking devices [62]. Primary vertex candidates are required to have at least two associated tracks, and the candidate with the largest $\sum p_{\mathrm{T}}^2$ is chosen as the primary vertex.

Jets are reconstructed with the anti-k_t clustering algorithm [63] with a distance parameter $R = 0.4$. Clusters of topologically connected calorimeter cells [64] with energy above the noise threshold, calibrated at the electromagnetic energy scale, are used as input. The jet energy is calibrated using a set of global sequential calibrations [65,66]. Energy from pile-up interactions is subtracted based on the jet area and the median energy density computed for each event [67]. Jets are required to have $p_{\mathrm{T}} > 20$ GeV and $|\eta| < 2.8$. The discrimination between hard-interaction jets and pile-up jets is achieved by a jet-vertex-tagging algorithm [68]. Events with jets originating from cosmic rays, beam background or detector noise are vetoed using the *loose* quality requirements defined in Ref. [69]. Jets containing b-hadrons (b-jets) are identified using a multivariate algorithm exploiting the long lifetime, high decay multiplicity, hard fragmentation, and large mass of b-hadrons [70]. The b-tagging algorithm identifies genuine b-jets with an efficiency of approximately 70% in simulated $t\bar{t}$ events. The rejection rates for c-jets, hadronically decaying tau leptons, and light-quark or gluon jets are approximately 8, 26 and 440, respectively [71].

Electron candidates are reconstructed from an isolated energy deposit in the electromagnetic calorimeter matched to an inner-detector track. They are required to have $p_{\mathrm{T}} > 10$ GeV, $|\eta| < 2.47$, and candidates reconstructed in the transition region between the barrel and end-cap calorimeters ($1.37 < |\eta| < 1.52$) are discarded. Electrons are required to satisfy a *loose* likelihood identification requirement [72,73] based on calorimeter shower shapes and track properties. The significance of the transverse impact parameter of the electron track is required to be less than five.

Muon candidates are reconstructed in the region $|\eta| < 2.5$ from muon spectrometer tracks matching ID tracks. Muons are required to have $p_{\mathrm{T}} > 10$ GeV and pass the *medium* identification requirements defined in Ref. [74], based on the number of hits in the ID and muon spectrometer, and the compatibility of the charge-to-momentum ratio measured in the two detector systems.

Hadronically decaying tau leptons are reconstructed [75] from anti-k_t jets with $E_{\mathrm{T}} \geq 10$ GeV and $|\eta| < 2.5$ calibrated with a local cluster weighting technique [76]. Tau candidates are built from clusters of calorimeter cells within a cone of size $\Delta R \equiv \sqrt{(\Delta\eta)^2 + (\Delta\phi)^2} = 0.2$ centred on the jet axis. Tau energy scale corrections are applied to subtract the energy originating from pile-up interactions and correct for the calorimeter response. Tau leptons are required to have $p_{\mathrm{T}} > 20$ GeV, and candidates reconstructed within the transition region $1.37 < |\eta| < 1.52$ are discarded. Tau leptons are required to have either one or three associated tracks, with a charge sum of ± 1. A boosted-decision-tree discrimi-

Table 1 Overview of the successive steps in the overlap removal algorithm

	Object discarded	Object kept	Matching condition
1.	Loose tau	Electron	$\Delta R < 0.2$
2.	Loose tau	Muon	$\Delta R < 0.2$
3.	Electron	Muon	Shared inner-detector track
4.	Jet	Electron	$\Delta R < 0.2$
5.	Electron	Jet	$\Delta R < 0.4$
6.	Muon	Jet	$\Delta R < 0.4$
7.	Jet	Loose tau	$\Delta R < 0.2$

nant is used to separate jets from tau leptons. It relies on track variables from the inner detector as well as longitudinal and transverse shower-shape variables from the calorimeters. The analysis makes use of *loose* and *medium* tau leptons, corresponding to identification working points with efficiencies of 60 and 55% for one-track tau leptons, respectively, and 50 and 40% for three-track tau leptons, respectively. Electrons mis-identified as 1-track tau leptons are rejected by imposing a p_{T}- and $|\eta|$-dependent requirement on the electron likelihood, which provides a constant efficiency of 95% for real tau leptons, with an inverse background efficiency (rejection factor) for electrons ranging from 30 to 150 depending on the $|\eta|$ region.

The missing transverse momentum vector $\vec{p}_{\mathrm{T}}^{\,\mathrm{miss}}$, whose magnitude is denoted by $E_{\mathrm{T}}^{\mathrm{miss}}$, is defined as the negative vector sum of the transverse momenta of all identified physics objects (electrons, muons, jets, and tau leptons) and an additional soft-term. Therefore, the $E_{\mathrm{T}}^{\mathrm{miss}}$ calculation benefits from the dedicated calibration for each final-state object. The soft-term is constructed from all the tracks with $p_{\mathrm{T}} > 400$ MeV originating from the primary vertex which are not associated with any physics object. This track-based definition makes the soft-term largely insensitive to pile-up [77].

After object reconstruction, an *overlap-removal* procedure is applied to remove ambiguities in case the same object is reconstructed by several algorithms. Tau candidates are discarded if they are found to overlap with a light lepton (electron or muon). If an electron and a muon are reconstructed using the same inner-detector track, the electron is discarded. For overlapping jets and electrons, the electron is kept. Light leptons in the vicinity of a jet are considered to originate from secondary decays within the jet and are discarded. Finally, in case a jet is reconstructed as a tau lepton, the tau candidate is retained. The successive steps of this procedure are summarised in Table 1. The final-state objects considered in the analysis are those surviving the overlap-removal algorithm.

5 Event selection

The trigger used in this analysis is the lowest-threshold missing transverse momentum trigger that was active without restrictions during the whole 2015 data-taking period. The efficiency of that trigger is measured using data collected by a set of single-jet triggers, with events containing at least two jets and one loose tau lepton. The trigger is found to have an efficiency greater than 99% when requiring $E_{\mathrm{T}}^{\mathrm{miss}} > 180$ GeV and a jet with $p_{\mathrm{T}} > 120$ GeV in the offline selection, which is referred to as *trigger plateau* conditions.

After trigger requirements, a pre-selection common to both channels is applied to ensure that only well-reconstructed events enter the analysis. Events containing no reconstructed primary vertex, mis-measured muon tracks, cosmic muon candidates, jets originating from calorimeter noise or reconstructed near inactive areas in the calorimeter, are vetoed. The presence of a second jet with $p_{\mathrm{T}} > 20$ GeV is required. To suppress the contribution from multi-jet events where large $E_{\mathrm{T}}^{\mathrm{miss}}$ would arise from jet energy mis-measurement, a minimum angular separation in the transverse plane is imposed between either of the two leading jets and the missing transverse momentum, $\Delta\phi(\mathrm{jet}_{1,2}, \vec{p}_{\mathrm{T}}^{\,\mathrm{miss}}) > 0.4$.

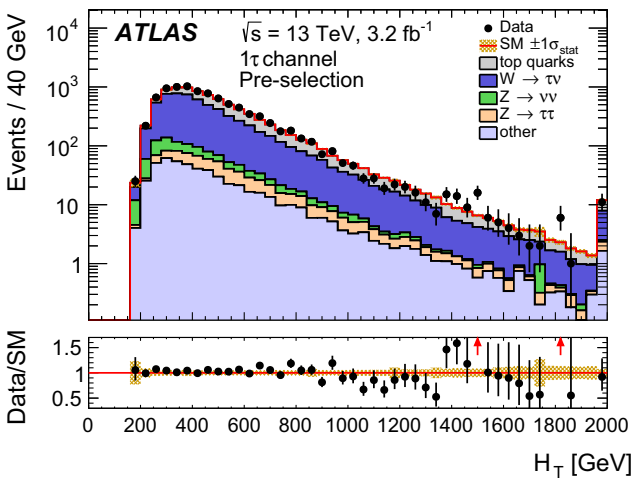
As part of the pre-selection in the 1τ channel, events are required to contain exactly one medium tau lepton and no light lepton. The veto against electrons and muons was used in Run 1 to ensure the 1τ channel did not overlap with the $e\tau$ and $\mu\tau$ channels, which are not part of the present analysis. The lepton veto does not affect the expected sensitivity to the simplified model, and has been kept in the 1τ channel. Events with two or more loose tau leptons are rejected to make the 1τ and 2τ channels statistically independent. In the 2τ channel, at least two loose tau leptons are required at pre-selection level. No veto is applied against light leptons, as this would cause a sizeable selection inefficiency for GMSB signals.

In each channel, signal regions (SRs) are defined for several signal scenarios. The following kinematic variables are found to provide discrimination between signal and background, or between backgrounds themselves:

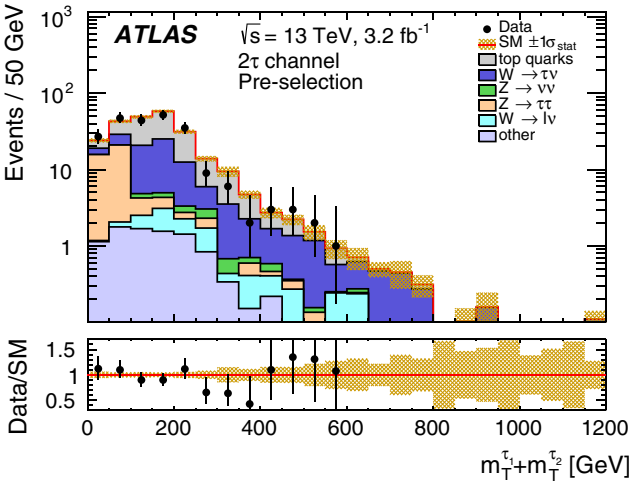
- the transverse mass of the system formed by $\vec{p}_{\mathrm{T}}^{\,\mathrm{miss}}$ and a lepton ℓ assumed to be massless,

$$m_{\mathrm{T}}^{\ell} \equiv m_{\mathrm{T}}(\ell, \vec{p}_{\mathrm{T}}^{\,\mathrm{miss}}) = \sqrt{2 p_{\mathrm{T}}^{\ell} E_{\mathrm{T}}^{\mathrm{miss}} (1 - \cos\Delta\phi(\ell, \vec{p}_{\mathrm{T}}^{\,\mathrm{miss}}))}\,. \quad (2)$$

  For events where the missing transverse momentum and the lepton originate from a $W \to \ell\nu$ decay, the m_{T}^{ℓ} distribution exhibits a Jacobian peak at the W boson mass. In the 1τ channel, the m_{T}^{τ} variable is used. In the 2τ channel, the $m_{\mathrm{T}}^{\tau_1} + m_{\mathrm{T}}^{\tau_2}$ variable based on the two leading tau



(a) H_{T} distribution in the 1τ channel



(b) $m_{\mathrm{T}}^{\tau_1} + m_{\mathrm{T}}^{\tau_2}$ distribution in the 2τ channel

Fig. 2 Kinematic distributions at pre-selection level, for the 1τ and 2τ channels. The last bin includes overflow events. The *shaded bands* indicate the statistical uncertainties in the background predictions. The contribution labelled as "other" includes diboson and multi-jet events, and the V+jets processes not explicitly listed in the legend. *Red arrows* in the data/SM ratio indicate bins where the corresponding entry falls outside the plotted range

leptons is used, and m_{T}^{μ} is used for specific selections requiring a muon;

- the scalar sum of the transverse momenta of all tau leptons and jets in the event, $H_{\mathrm{T}} = \sum_i p_{\mathrm{T}}^{\tau_i} + \sum_j p_{\mathrm{T}}^{\mathrm{jet}_j}$;
- the magnitude of the missing transverse momentum, $E_{\mathrm{T}}^{\mathrm{miss}}$;
- the effective mass, $m_{\mathrm{eff}} = H_{\mathrm{T}} + E_{\mathrm{T}}^{\mathrm{miss}}$;
- the $m_{\mathrm{T2}}^{\tau\tau}$ variable [78,79], also called *stransverse mass*, computed as

$$m_{\mathrm{T2}}^{\tau\tau} = \sqrt{\min_{\vec{p}_{\mathrm{T}}^{\,a}+\vec{p}_{\mathrm{T}}^{\,b}=\vec{p}_{\mathrm{T}}^{\,\mathrm{miss}}} (\max[m_{\mathrm{T}}^2(\tau_1, \vec{p}_{\mathrm{T}}^{\,a}), m_{\mathrm{T}}^2(\tau_2, \vec{p}_{\mathrm{T}}^{\,b})])}, \tag{3}$$

where (a, b) refers to two invisible particles that are assumed to be produced with transverse momentum vectors $\vec{p}_{\mathrm{T}}^{\,a,b}$. In this calculation, (a, b) are assumed to be massless. The $m_{\mathrm{T2}}^{\tau\tau}$ distribution has a kinematic endpoint for processes where massive particles are pair-produced, each particle decaying to a tau lepton and an undetected particle. In cases where multiple tau leptons are produced in a decay chain, there is no a-priori way to select the pair leading to the desired characteristic. For events with more than two tau-lepton candidates, $m_{\mathrm{T2}}^{\tau\tau}$ is hence calculated using all possible tau-lepton pairs and the largest value is chosen;

- the sum of the transverse masses of all jets and of the two leading tau leptons in the event, $m_{\mathrm{T}}^{\mathrm{sum}} = m_{\mathrm{T}}^{\tau_1} + m_{\mathrm{T}}^{\tau_2} + \sum_i m_{\mathrm{T}}^{\mathrm{jet}_i}$, where $m_{\mathrm{T}}^{\mathrm{jet}}$ is defined analogously to m_{T}^{ℓ};
- the total number of jets, N_{jet};
- the number of b-tagged jets, $N_{b\text{-jet}}$.

These variables are also used for the selection of control regions (CRs) and validation regions (VRs) in the context of background modelling studies, as discussed in Sect. 6.

Figure 2 shows example kinematic distributions at pre-selection level. The dominant backgrounds are $W(\tau\nu)$+jets and $t\bar{t}$ production in the 1τ channel, with subdominant contributions from $Z(\nu\nu)$+jets and $Z(\tau\tau)$+jets. In the 2τ channel, the pre-selection is dominated by $t\bar{t}$, $W(\tau\nu)$+jets, and $Z(\tau\tau)$+jets events. The multi-jet and diboson backgrounds respectively contribute to about 0.2 and 2% of the total background in the 1τ channel, while their contribution in the 2τ channel amounts to 1 and 5%, respectively.

In the 1τ channel, three characteristic regions in the $(m_{\tilde{g}}, m_{\tilde{\chi}_1^0})$ parameter space of the simplified model are chosen as benchmark scenarios for the SR optimisation, with small (<100 GeV), medium (500–900 GeV) and large (>1200 GeV) mass splittings between the gluino and the LSP. In the following, the associated SRs are called Compressed, Medium-Mass and High-Mass SRs, respectively. The Compressed SR exploits topologies where a high-p_{T} jet from initial-state radiation (ISR) recoils against the pair of gluinos. In this situation, the soft visible particles produced in the gluino decay receive a transverse Lorentz boost. While tau leptons and jets from gluino decays typically have low p_{T}, such events have substantial $E_{\mathrm{T}}^{\mathrm{miss}}$ since both LSPs tend to be emitted oppositely to the ISR jet in the transverse plane. In the case of large mass splitting, high-p_{T} jets come mainly from gluino decays, and a high-p_{T} requirement on the first two leading jets is effective in rejecting background without inducing a large inefficiency for the signal. A requirement on the transverse mass m_{T}^{τ} is applied in the Medium-Mass and

Table 2 Selection criteria for the signal regions (SRs) of the 1τ channel (top) and the 2τ channel (bottom)

1τ channel	Compressed SR	Medium-Mass SR	High-Mass SR
Trigger plateau		$E_{\mathrm{T}}^{\mathrm{miss}} > 180$ GeV, $p_{\mathrm{T}}^{\mathrm{jet_1}} > 120$ GeV	
Tau leptons		$N_{\tau}^{\mathrm{loose}} = N_{\tau}^{\mathrm{medium}} = 1$, $p_{\mathrm{T}}^{\tau} > 20$ GeV	
Light leptons		$N_{\ell} = 0$	
Multi-jet rejection		$\Delta\phi(\mathrm{jet}_{1,2}, \vec{p}_{\mathrm{T}}^{\mathrm{miss}}) \geq 0.4$	
p_{T}^{τ}	<45 GeV	–	–
$p_{\mathrm{T}}^{\mathrm{jet_1}}$	>300 GeV	–	>220 GeV
$p_{\mathrm{T}}^{\mathrm{jet_2}}$	–	–	>220 GeV
N_{jet}	≥ 2	≥ 5	≥ 5
m_{T}^{τ}	>80 GeV	>200 GeV	>200 GeV
$E_{\mathrm{T}}^{\mathrm{miss}}$	>300 GeV	>300 GeV	–
H_{T}	–	>550 GeV	>550 GeV
2τ channel	Compressed SR	High-Mass SR	GMSB SR
Trigger plateau		$E_{\mathrm{T}}^{\mathrm{miss}} > 180$ GeV, $p_{\mathrm{T}}^{\mathrm{jet_1}} > 120$ GeV	
Tau leptons		$N_{\tau}^{\mathrm{loose}} \geq 2$, $p_{\mathrm{T}}^{\tau} > 20$ GeV	
Multi-jet rejection		$\Delta\phi(\mathrm{jet}_{1,2}, \vec{p}_{\mathrm{T}}^{\mathrm{miss}}) \geq 0.4$	
$m_{\mathrm{T}}^{\tau_1} + m_{\mathrm{T}}^{\tau_2}$	–	>350 GeV	>150 GeV
H_{T}	–	>800 GeV	>1700 GeV
N_{jet}	≥ 2	≥ 3	≥ 2
$m_{\mathrm{T2}}^{\tau\tau}$	>60 GeV	–	–
$m_{\mathrm{T}}^{\mathrm{sum}}$	>1400 GeV	–	–

High-Mass SRs to suppress $W(\tau\nu)$+jets events as well as semileptonic $t\bar{t}$ events with a tau lepton in the final state. The H_{T} variable is also used in these two SRs, as H_{T} increases for signal events with increasing mass splittings. No SR is defined for the GMSB model, as the expected sensitivity in the 1τ channel is significantly lower than that in the 2τ channel.

In the 2τ channel, two SRs are defined for the simplified model to cover small (<900 GeV) and large (>1200 GeV) mass-splitting scenarios. The Compressed SR imposes a requirement on $m_{\mathrm{T2}}^{\tau\tau}$ to exploit the fact that most of SM background contributions exhibit a kinematic endpoint around the W or Z boson mass, which is not the case for tau leptons produced in the cascade decay of gluinos. A requirement is also applied on $m_{\mathrm{T}}^{\mathrm{sum}}$ to take advantage of the large $E_{\mathrm{T}}^{\mathrm{miss}}$ and the large jet and tau lepton multiplicity that is expected for signal events. The High-Mass SR includes a requirement on H_{T}, which is efficient for High-Mass gluino signals. A requirement on $m_{\mathrm{T}}^{\tau_1} + m_{\mathrm{T}}^{\tau_2}$ is also applied. In $Z(\tau\tau)$+jets events, where $E_{\mathrm{T}}^{\mathrm{miss}}$ originates from neutrinos from tau lepton decays, the trigger plateau requirement selects events with a high-p_{T} Z boson recoiling against jets in the transverse plane. This topology leads to tau leptons with a small $\Delta\phi$ separation, which results in low values of $m_{\mathrm{T}}^{\tau_1} + m_{\mathrm{T}}^{\tau_2}$ given that tau neutrinos are themselves collimated with the visible decay products of tau leptons. For dileptonic $t\bar{t}$ events with two tau leptons and large genuine $E_{\mathrm{T}}^{\mathrm{miss}}$, and for $W(\tau\nu)$+jets events and semileptonic $t\bar{t}$ events with a high-p_{T} jet mis-identified as a tau lepton, $m_{\mathrm{T}}^{\tau_1} + m_{\mathrm{T}}^{\tau_2}$ can be larger, but even larger values are expected for High-Mass gluino signals. A signal region is also defined for the GMSB model, and targets more specifically squark–antisquark production rather than gluino pair production in the region $\Lambda \gtrsim 80$ TeV, not excluded by Run 1 searches. Among the distinctive features that give large discrimination power to H_{T}, decay chains are potentially longer than in the simplified model, and the almost-massless gravitino LSP leaves more phase space to other particles in the decay. Table 2 summarises the selection criteria for all the SRs of the 1τ and 2τ channels.

6 Background estimation

To predict the background contributions in the SRs, the normalisation of the dominant backgrounds is fitted to data in dedicated CRs. In each channel and for each SR, a simultaneous fit over the relevant CRs is performed using HistFitter [80] to extract these normalisation factors. Control regions are designed to have an enhanced contribution from a single background process, with contributions from other backgrounds as small as possible to reduce the uncertainties originating from correlations between CRs. Furthermore,

Table 3 Selection criteria defining the control and validation regions of the Compressed SR in the 1τ channel. The pre-selection criteria are also applied although not shown in the table. Unless mentioned, criteria apply to both the top quark and V+jets background regions. Symbols * indicate that criteria are only applied to regions targeting the top quark background, and symbols † denote criteria only applied to V+jets background regions

1τ channel	True-tau CR	True-tau VR	Fake-tau CR	Fake-tau VR
$E_{\mathrm{T}}^{\mathrm{miss}}$	$180 < E_{\mathrm{T}}^{\mathrm{miss}} < 300$ GeV	>300 GeV	$180 < E_{\mathrm{T}}^{\mathrm{miss}} < 250$ GeV	$250 < E_{\mathrm{T}}^{\mathrm{miss}} < 300$ GeV
m_{T}^{τ}	<100 GeV	<80 GeV	$100 < m_{\mathrm{T}}^{\tau} < 330$ GeV	$100 < m_{\mathrm{T}}^{\tau} < 330$ GeV
H_{T}	–	>400 GeV	$<550^*/400^\dagger$ GeV	$>550^*/400^\dagger$ GeV
p_{T}^{τ}	<45 GeV	<60 GeV	<45 GeV	<60 GeV
N_{jet}	–	$\geq 4^*$	–	$\geq 4^*$
$N_{b-\mathrm{jet}}$	$\geq 1^*/=0^\dagger$	$\geq 1^*/=0^\dagger$	$\geq 1^*/=0^\dagger$	$\geq 1^*/=0^\dagger$
$\Delta\phi(\mathrm{jet}_1, \vec{p}_{\mathrm{T}}^{\,\mathrm{miss}})$	$>1.8^\dagger$	–	$>2.0^*$	–
$\Delta\phi(\tau, \vec{p}_{\mathrm{T}}^{\,\mathrm{miss}})$	–	–	>1.0	>1.0
$E_{\mathrm{T}}^{\mathrm{miss}}/m_{\mathrm{eff}}$	–	–	$>0.2^*/0.3^\dagger$	$>0.2^*/0.3^\dagger$

CRs are defined in phase-space regions close to that of SRs, to avoid the extrapolation of the background normalisations over very different kinematic regimes.

A set of VRs is defined in intermediate phase-space regions between a SR and its associated CRs, where signal contributions are small. These VRs are not part of the fit; they are used to compare the fitted background predictions with the observed data in the vicinity of the SRs before unblinding those.

6.1 Vector-boson and top quark backgrounds

In both channels, the dominant backgrounds originate from SM processes involving the top quark or a massive vector boson and jets. These two backgrounds can be separated from each other by either requiring or vetoing the presence of a b-tagged jet in the event. In addition, a tau-lepton candidate can be either a genuine tau lepton (*true tau lepton*) from a $W(\tau\nu)$ decay or a jet mis-identified as a tau lepton (*fake tau lepton*), which leads to two types of CRs.

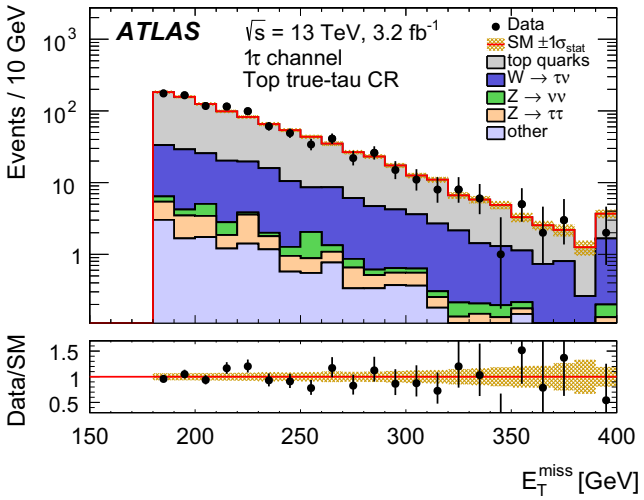
In CRs targeting true tau-lepton contributions, the normalisation factor is used to absorb the theoretical uncertainties in cross-section computations, the experimental uncertainties in the integrated luminosity, and potential differences in the tau-lepton reconstruction and identification efficiencies between data and simulation. In the case of fake tau-lepton contributions, the normalisation factor combines several effects: the quark/gluon composition of jets mis-identified as tau leptons, which is process-dependent, the parton shower and hadronisation models of the generator, and the modelling in the simulation of jet shower shapes in the calorimeter, which mainly depends on the GEANT4 hadronic interaction model and the modelling of the ATLAS detector. Other contributions affecting the background normalisation include the modelling of the kinematics and acceptance of background processes. These contributions are absorbed into the true and fake tau-lepton normalisation factors in the 1τ channel, while they are treated as a separate *kinematic* normalisation factor in the 2τ channel to avoid double-counting (true- or fake-tau normalisation factors are applied to each tau lepton, while the kinematic normalisation factor is applied once per event).

In the 1τ channel, four CRs are defined, with four associated normalisation factors. They target the top quark background (including $t\bar{t}$ and single-top-quark processes) with either a true or a fake tau lepton, and V+jets events with either a true or a fake tau lepton, respectively dominated by $W(\tau\nu)$+jets and $Z(\nu\nu)$+jets processes. The discrimination between true and fake tau-lepton contributions is achieved by a requirement on m_{T}^{τ}. A common set of four CRs is defined for the Medium-Mass and High-Mass SRs, due to the similarity of background compositions and event kinematics. These are separated from the SRs by an upper bound on m_{T}^{τ}. Another set of four CRs is defined for the Compressed SR, to study more specifically the background modelling for low-p_{T} tau leptons. These CRs are separated from the SR by an upper bound on $E_{\mathrm{T}}^{\mathrm{miss}}$. The selection criteria defining these CRs are summarised in Tables 3 and 4. Figure 3 illustrates the good modelling of the background in the various CRs after the fit.

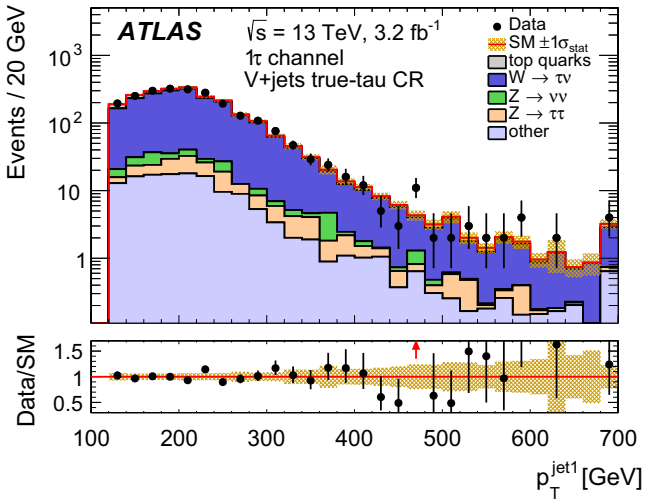
Three types of VRs are used in the 1τ channel for the Medium- and High-Mass SRs, to validate the background extrapolation from low-H_{T} to high-H_{T} for selections based on true tau leptons, and the extrapolations along H_{T} and m_{T}^{τ} for selections based on fake tau leptons. The separation of the VRs from the SRs is achieved by inverting the selections on m_{T}^{τ} or H_{T}. For the Compressed SR, four VRs are used to validate the extrapolation of V+jets and top quark background predictions along $E_{\mathrm{T}}^{\mathrm{miss}}$, for both the true and fake tau-lepton selections. The separation of the VRs from the SRs is achieved by an inverted requirement on m_{T}^{τ} and $E_{\mathrm{T}}^{\mathrm{miss}}$, for true and fake tau-lepton VRs, respectively. The selection criteria defining all the VRs in the 1τ channel are listed in Tables 3 and 4.

Table 4 Selection criteria defining the control and validation regions of the Medium-Mass and High-Mass SRs in the 1τ channel. The preselection criteria are also applied although not shown in the table. Unless mentioned, criteria apply to both the top quark and V+jets background regions. Symbols* indicate that criteria are only applied to regions targeting the top quark background, and symbols† denote criteria only applied to V+jets background regions

1τ channel	True-tau CR	True-tau VR	Fake-tau CR	Fake-tau VR1	Fake-tau VR2
$E_{\mathrm{T}}^{\mathrm{miss}}$	–	–	–	$<400^{\dagger}$ GeV	–
m_{T}	<100 GeV	<100 GeV	$100 < m_{\mathrm{T}} < 200$ GeV	$100 < m_{\mathrm{T}} < 200$ GeV	$200 < m_{\mathrm{T}} < 330$ GeV
H_{T}	<550 GeV	>550 GeV	$<550^{*}/400^{\dagger}$ GeV	$>550^{*}$ GeV	<550 GeV
	–	–	–	$400 < H_{\mathrm{T}} < 700^{\dagger}$ GeV	–
p_{T}^{τ}	–	>45 GeV	–	–	–
N_{jet}	≥ 4	≥ 4	–	$\geq 4^{*}$	$\geq 4^{*}$
$N_{b\text{-jet}}$	$\geq 1^{*}/=0^{\dagger}$	$\geq 1^{*}/=0^{\dagger}$	$\geq 1^{*}/=0^{\dagger}$	$\geq 1^{*}/=0^{\dagger}$	$\geq 1^{*}/=0^{\dagger}$
$p_{\mathrm{T}}^{\mathrm{jet_1}}$	–	–	–	$<500^{\dagger}$ GeV	–
$\Delta\phi(\mathrm{jet_1}, \vec{p}_{\mathrm{T}}^{\mathrm{miss}})$	–	–	>2.0	–	–
$\Delta\phi(\tau, \vec{p}_{\mathrm{T}}^{\mathrm{miss}})$	–	–	>1.0	>1.0	>1.0
$E_{\mathrm{T}}^{\mathrm{miss}}/m_{\mathrm{eff}}$	–	–	$>0.2^{*}/0.3^{\dagger}$	$>0.2^{*}/0.3^{\dagger}$	$>0.2^{*}/0.3^{\dagger}$



(a) top true-tau CR of the Medium- and High-Mass SRs



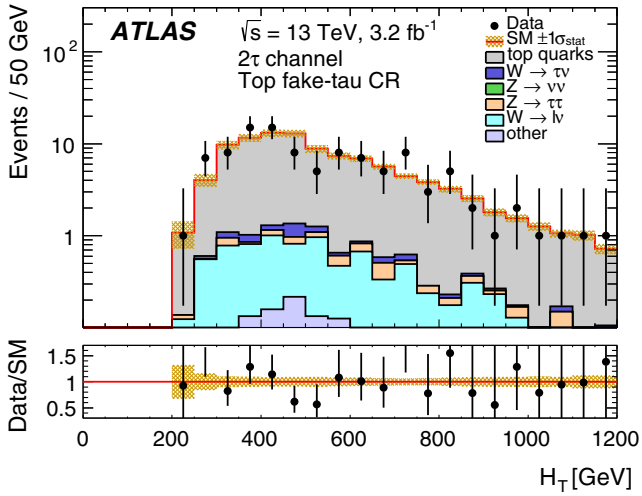
(b) V+jets true-tau CR of the Compressed SR

Fig. 3 Missing transverse momentum and leading-jet p_{T} distributions in two different control regions of the 1τ channel after the fit, illustrating the overall background modelling in the CRs. By construction, the total fitted background is equal to the number of observed events in each CR. The last bin includes overflow events. The *shaded bands* indicate the statistical uncertainties in the background predictions. *Red arrows* in the data/SM ratio indicate bins where the corresponding entry falls outside the plotted range

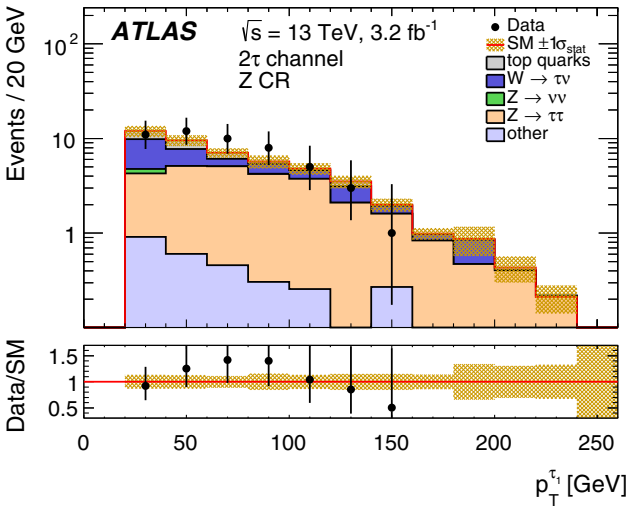
In the 2τ channel, the dominant backgrounds are $Z(\tau\tau)$+jets and dileptonic top quark contributions (including $t\bar{t}$ and single-top quark processes) with two true tau leptons, $W(\tau\nu)$+jets and semileptonic top quark contributions with one true and one fake tau lepton, and $W(\ell\nu)$+jets and top quark contributions with two fake tau leptons. Control regions are defined for W+jets and top quark backgrounds to extract normalisation factors related to the modelling of the process kinematics, and the modelling of real and fake tau leptons in the simulation. These CRs are separated from the SRs by replacing the requirement on the two tau leptons with requirements on different final-state objects, which stand in for true or fake tau leptons. To be independent from tau-lepton considerations, kinematic CRs are based on events with one muon, jets, $E_{\mathrm{T}}^{\mathrm{miss}}$, and without or with b-jets, to select $W(\mu\nu)$+jets and semileptonic top quark events with a final-state muon, respectively. The fake tau-lepton CRs use the same baseline selections as the kinematic CRs, but in addition, the presence of a loose tau-lepton candidate is required. Events with large m_{T}^{μ} values are discarded to suppress the dileptonic top quark background with a muon and a true tau lepton. The true tau-lepton CRs, which tar-

Table 5 Overview of the control regions used in the 2τ channel

2τ channel	Kinematic CR		Fake tau CR		True tau CR		
	W+jets	Top	W+jets	Top	W+jets	Top	Z+jets
Trigger plateau	$E_{\mathrm{T}}^{\mathrm{miss}} > 180$ GeV, $p_{\mathrm{T}}^{\mathrm{jet}_1} > 120$ GeV						
Tau leptons	$N_\tau^{\mathrm{loose}} = 0$		$N_\tau^{\mathrm{loose}} = 1$				$N_\tau^{\mathrm{loose}} = 2$, opposite charge
Light leptons	$N_\mu = 1$				$N_\mu = 0$		–
N_{jet}	≥ 3		≥ 2		≥ 3		≥ 2
$N_{b-\mathrm{jet}}$	$= 0$	≥ 1	$= 0$	≥ 1	$= 0$	≥ 1	$= 0$
Multi-jet rejection	$0.4 < \Delta\phi(\mathrm{jet}_{1,2}, \vec{p}_{\mathrm{T}}^{\,\mathrm{miss}}) < 2.9$						$\Delta\phi(\mathrm{jet}_{1,2}, \vec{p}_{\mathrm{T}}^{\,\mathrm{miss}}) > 0.4$
CR selection	$H_{\mathrm{T}} < 1\,200$ GeV						$H_{\mathrm{T}} < 800$ GeV
	–		$m_{\mathrm{T}}^{\mu} < 100$ GeV		$m_{\mathrm{T}}^{\tau} < 80$ GeV		$m_{\mathrm{T}}^{\tau_1} + m_{\mathrm{T}}^{\tau_2} < 150$ GeV



(a) top quark fake-tau CR



(b) $Z(\tau\tau)$+jets CR

Fig. 4 H_{T} distribution in the top quark fake-tau CR and transverse momentum of the leading tau lepton in the $Z(\tau\tau)$+jets CR of the 2τ channel after the fit, illustrating the overall background modelling in the control regions. By construction, the total fitted background is equal to the number of observed events in each CR. The last bin includes overflow events. The *shaded bands* indicate the statistical uncertainties in the background predictions

Table 6 Overview of the validation regions defined in the 2τ channel

2τ channel	VR W+jets	VR Top	VR Z+jets
Trigger plateau	$E_{\mathrm{T}}^{\mathrm{miss}} > 180$ GeV, $p_{\mathrm{T}}^{\mathrm{jet}_1} > 120$ GeV		
Tau leptons	$N_\tau^{\mathrm{loose}} \geq 2$		
N_{jet}	≥ 2		
$N_{b-\mathrm{jet}}$	$= 0$	≥ 1	$= 0$
Multi-jet rejection	$\Delta\phi(\mathrm{jet}_{1,2}, \vec{p}_{\mathrm{T}}^{\,\mathrm{miss}}) \geq 0.4$		
VR selection	$H_{\mathrm{T}} < 800$ GeV $m_{\mathrm{T}}^{\tau_1} + m_{\mathrm{T}}^{\tau_2} > 150$ GeV $m_{\mathrm{T2}}^{\tau\tau} < 60$ GeV		$H_{\mathrm{T}} > 800$ GeV $m_{\mathrm{T}}^{\tau_1} + m_{\mathrm{T}}^{\tau_2} < 150$ GeV –

get $W(\tau\nu)$+jets and semileptonic top quark processes with a true tau lepton, are based on events with a loose tau lepton, jets and $E_{\mathrm{T}}^{\mathrm{miss}}$, without or with b-jets. Similarly, contributions from fake tau leptons are suppressed by a requirement on m_{T}^{τ}. A separate CR is designed to study $Z(\tau\tau)$+jets events by inverting the $m_{\mathrm{T}}^{\tau_1} + m_{\mathrm{T}}^{\tau_2}$ and H_{T} requirements from the SRs. This selection requires two loose tau leptons of opposite electric charge. The selection criteria defining the various CRs are summarised in Table 5. Figure 4 illustrates the good background modelling in the CRs after the fit.

The VRs of the 2τ channel are presented in Table 6. For the $Z(\tau\tau)$+jets background, the validation of the background extrapolation is performed from low-H_{T} to high-H_{T}, while keeping the upper bound on $m_{\mathrm{T}}^{\tau_1} + m_{\mathrm{T}}^{\tau_2}$ which is effective in selecting $Z(\tau\tau)$+jets events. The validity of the top quark and $W(\tau\nu)$+jets background predictions obtained with alternative object selections are checked for selections with two reconstructed tau leptons. High values of $m_{\mathrm{T}}^{\tau_1} + m_{\mathrm{T}}^{\tau_2}$ are required to suppress $Z(\tau\tau)$+jets events as in the SRs, while upper bounds on m_{T2} and H_{T} ensure there is no overlap

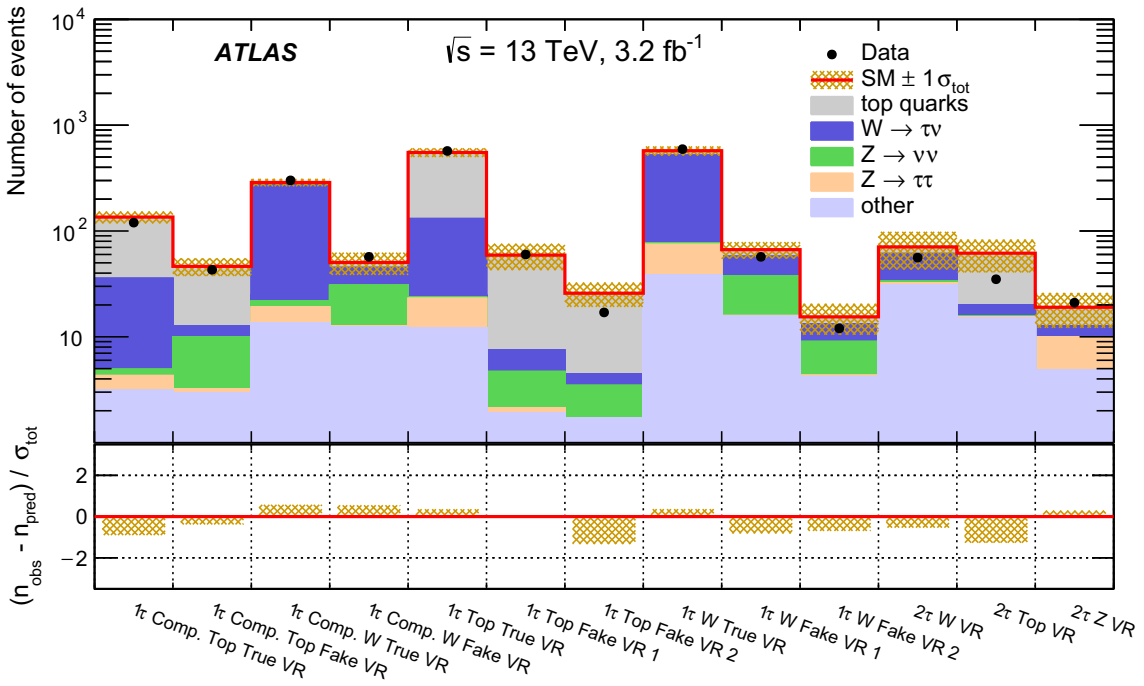


Fig. 5 Number of observed events, n_{obs}, and predicted background yields after the fit, n_{pred}, in the validation regions of the 1τ and 2τ channels. The background predictions are scaled using normalisation factors derived in the control regions. The *shaded bands* indicate the statistical uncertainties in the background predictions, and correspond to the σ_{tot} uncertainties used in the *lower part* of the figure

between SRs and VRs. The same set of CRs and VRs is used for the three SRs of the 2τ channel.

The resulting normalisation factors for both channels do not deviate from 1 by more than 25%, except for $t\bar{t}$ events with fake tau leptons in the 1τ channel, where the normalisation factor reaches 2 within large statistical uncertainty. The typical level of agreement between data and background distributions in the CRs after the fit can be seen in Figs. 3 and 4. Good modelling of kinematic distributions is observed in all CRs. The comparison between the number of observed events and the predicted background yields in the VRs is displayed in Fig. 5. Agreement within approximately one standard deviation is observed.

6.2 Multi-jet background

The multi-jet background contributes to the selection when two conditions are simultaneously fulfilled: jets have to be mis-identified as tau leptons, and large missing transverse momentum must arise from jet energy mis-measurement. This background is estimated from data, because final-state objects arising from mis-measurements are much more challenging to simulate than the reconstruction and identification of genuine objects. Moreover, the very large multi-jet production cross section at the LHC would imply simulating a prohibitively large number of multi-jet events.

The *jet smearing* method [81] employed in the 1τ channel proceeds in two steps. First, multi-jet events with well-measured jets are selected in a data sample collected by single-jet triggers. This is achieved by requiring $E_{\text{T}}^{\text{miss}}/(\sum E_{\text{T}})^{1/3} < 5\ \text{GeV}^{2/3}$, where the objects entering the $\sum E_{\text{T}}$ term are those entering the $E_{\text{T}}^{\text{miss}}$ calculation. Selected events are required to have at least two jets, no light lepton and exactly one tau candidate satisfying the medium identification criteria. The selection is dominated by multi-jet production, such that most tau candidates are jets mis-identified as tau leptons. In a second step, jet energies are smeared according to the p_{T}-dependent jet energy resolution extracted from simulation. The smearing is performed multiple times for each event, leading to a large pseudo-data set where $E_{\text{T}}^{\text{miss}}$ originates from resolution effects and which includes an adequate fraction of jets mis-identified as tau leptons.

This method cannot be used in the 2τ channel because of the limited number of events with well-measured jets that contain at least two loose tau candidates. Instead, a *fake rate* approach is adopted. The probability for jets to be mis-identified as tau leptons or muons, obtained from simulated dijet events, is applied to jets from an inclusive data sample collected by single-jet triggers and dominated by multi-jet events.

Table 7 Dominant systematic uncertainties in the total background predictions, in percent, for the signal regions of the 1τ (top) and 2τ (bottom) channels. The total systematic uncertainty accounts for other minor contributions not listed in this table, as well as correlations between the uncertainties

Source of uncertainty	1τ Compressed SR	1τ Medium-Mass SR	1τ High-Mass SR
Top generator modelling	8.1	6.5	12
V+jets generator modelling	1.5	6.4	6.3
Jet energy scale	2.0	6.7	0.4
Jet energy resolution	0.6	0.2	0.7
b-tagging efficiencies	1.9	3.2	7.7
Tau energy scale	1.8	2.8	5.5
Total	13	16	21
Source of uncertainty	2τ Compressed SR	2τ High-Mass SR	2τ GMSB SR
Top generator modelling	60	23	22
V+jets generator modelling	4.2	6.3	4.3
Jet energy scale	14	2.0	6.0
Jet energy resolution	8.1	1.2	4.3
b-tagging efficiencies	8.8	5.1	7.7
Tau energy scale	19	13	8.5
Total	72	36	35

7 Systematic uncertainties

For all simulated processes, theoretical and experimental systematic uncertainties are considered. The former includes cross-section uncertainties, which are not relevant for the dominant backgrounds normalised to data, and generator modelling uncertainties. The latter refers to all the uncertainties related to the reconstruction, identification, calibration and corrections applied to jets, tau leptons, electrons, muons and missing transverse momentum. Specific uncertainties are evaluated for the multi-jet background, which is estimated from data.

Theoretical uncertainties are evaluated for all simulated samples. For backgrounds that are normalised in CRs, the uncertainty in the transfer factors, i.e. the ratio of the expected event yields in a SR or VR over the respective CR, is evaluated for all SRs and VRs. The difference between the nominal simulation and the systematically varied sample is used as an additional uncertainty. For backgrounds that are evaluated from simulation alone, i.e. the diboson background, a global normalisation uncertainty is added. Uncertainties for V+jets samples generated with SHERPA are estimated by up and down variations by factors of two and one-half in the renormalisation and factorisation scales, resummation scale (maximum scale of the additional emission to be resummed by the parton shower) and CKKW matching scale (matching between matrix elements and parton shower). The effect of scale variations is parameterised at generator level as a function of the vector boson p_{T} and the number of particle jets. For the top quark background, the nominal predictions from POWHEG- BOX + PYTHIA6 are compared with predictions from alternative generators, and the differences are taken as systematic uncertainties. The MG5_AMC@NLO + HERWIG++ generators are used to evaluate uncertainties in the modelling of the hard scattering, parton shower and hadronisation. The POWHEG- BOX + HERWIG++ generators are used to compute a specific uncertainty in the parton shower and hadronisation models. An uncertainty in the ISR modelling is also assessed by varying the POWHEG- BOX parameter which controls the transverse momentum of the first additional parton emission beyond the Born configuration. In the case of the diboson background, a 6% uncertainty in the cross section due to scale and PDF uncertainties is considered. Uncertainties in signal cross sections are obtained by using different PDF sets and factorisation and renormalisation scales, as discussed in Sect. 3.

Systematic uncertainties affecting jets arise from the jet energy scale and jet energy resolution [66], as well as efficiency corrections for jet-vertex-tagging [68] and b-tagging [82]. A set of p_{T}- and η-dependent uncertainties in the jet energy scale and resolution is estimated by varying the conditions used in the simulation. Another set of uncertainties accounts for the modelling of the residual pile-up dependence. Additional uncertainties account for the jet flavour composition of samples that are used to derive in-situ energy scale corrections, where jets are calibrated against well-measured objects. A punch-through uncertainty for jets not entirely contained in the calorimeters, as well as a single-hadron response uncertainty, are also included for high-p_{T} jets. An overall uncertainty in the jet energy resolution is

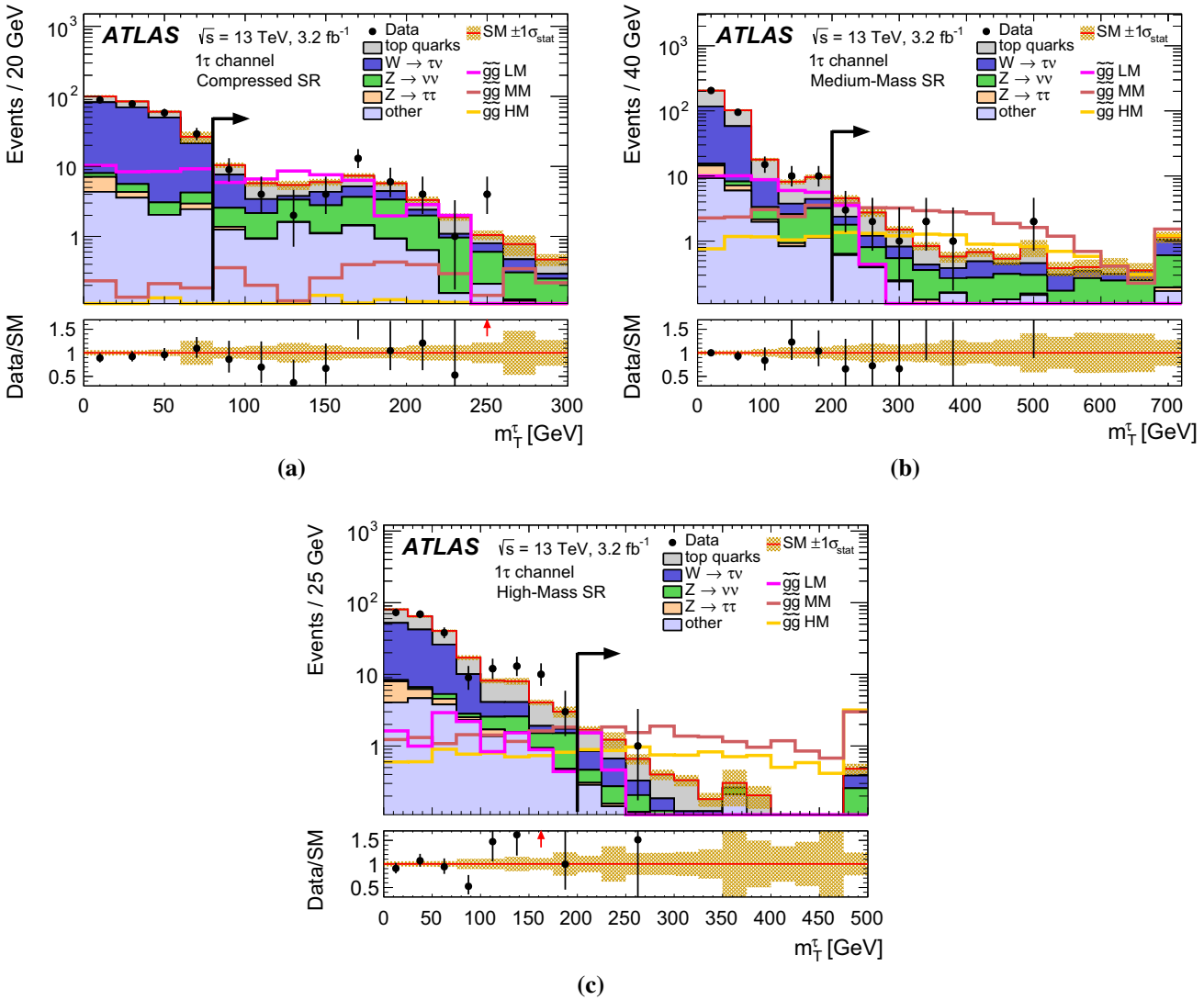


Fig. 6 m_{T}^{τ} distributions for "extended SR selections" of the 1τ channel, for **a** the Compressed SR selection without the $m_{\mathrm{T}}^{\tau} > 80$ GeV requirement, **b** the Medium-Mass SR selection without the $m_{\mathrm{T}}^{\tau} > 200$ GeV requirement, and **c** the High-Mass SR selection without the $m_{\mathrm{T}}^{\tau} > 200$ GeV requirement. The last bin includes overflow events. The *shaded bands* indicate the statistical uncertainties in the background predictions. *Red arrows* in the data/SM ratio indicate bins where the corresponding entry falls outside the plotted range. The signal region is indicated by the *black arrow*. Signal predictions are overlaid for several benchmark models, normalised to their predicted cross sections. For the simplified model, *LM* low mass splitting, or compressed scenario, with $m_{\tilde{g}} = 665$ GeV and $m_{\tilde{\chi}_1^0} = 585$ GeV; *MM* medium mass splitting, with $m_{\tilde{g}} = 1145$ GeV and $m_{\tilde{\chi}_1^0} = 265$ GeV; *HM* high mass splitting scenario, with $m_{\tilde{g}} = 1305$ GeV and $m_{\tilde{\chi}_1^0} = 105$ GeV

applied to jets in the simulation as a Gaussian energy smearing.

Systematic uncertainties affecting correctly identified tau leptons arise from the reconstruction, identification and tau-electron overlap-removal efficiencies, and the energy scale calibration [75]. Most of the uncertainties are estimated by varying nominal parameters in the simulation: detector material, underlying event, hadronic shower model, pile-up and noise in the calorimeters. The uncertainty in the energy scale also includes non-closure of the calibration found in simulation, a single-pion response uncertainty, and an uncertainty in the in-situ energy calibration of data with respect to simulation derived in $Z(\tau\tau)$ events with a hadronically decaying tau lepton and a muon in the final state. In the case of signal samples, which undergo fast calorimeter simulation, a dedicated uncertainty takes into account the difference in performance between full and fast simulation. The effect of mis-identified tau leptons is largely constrained by the background estimation approaches. Uncertainties arise due to the extrapolation from the CRs to the VRs and SRs. These are considered as part of the theory uncertainties, which account for the impact of hadronisation on the mis-identification of jets as tau leptons.

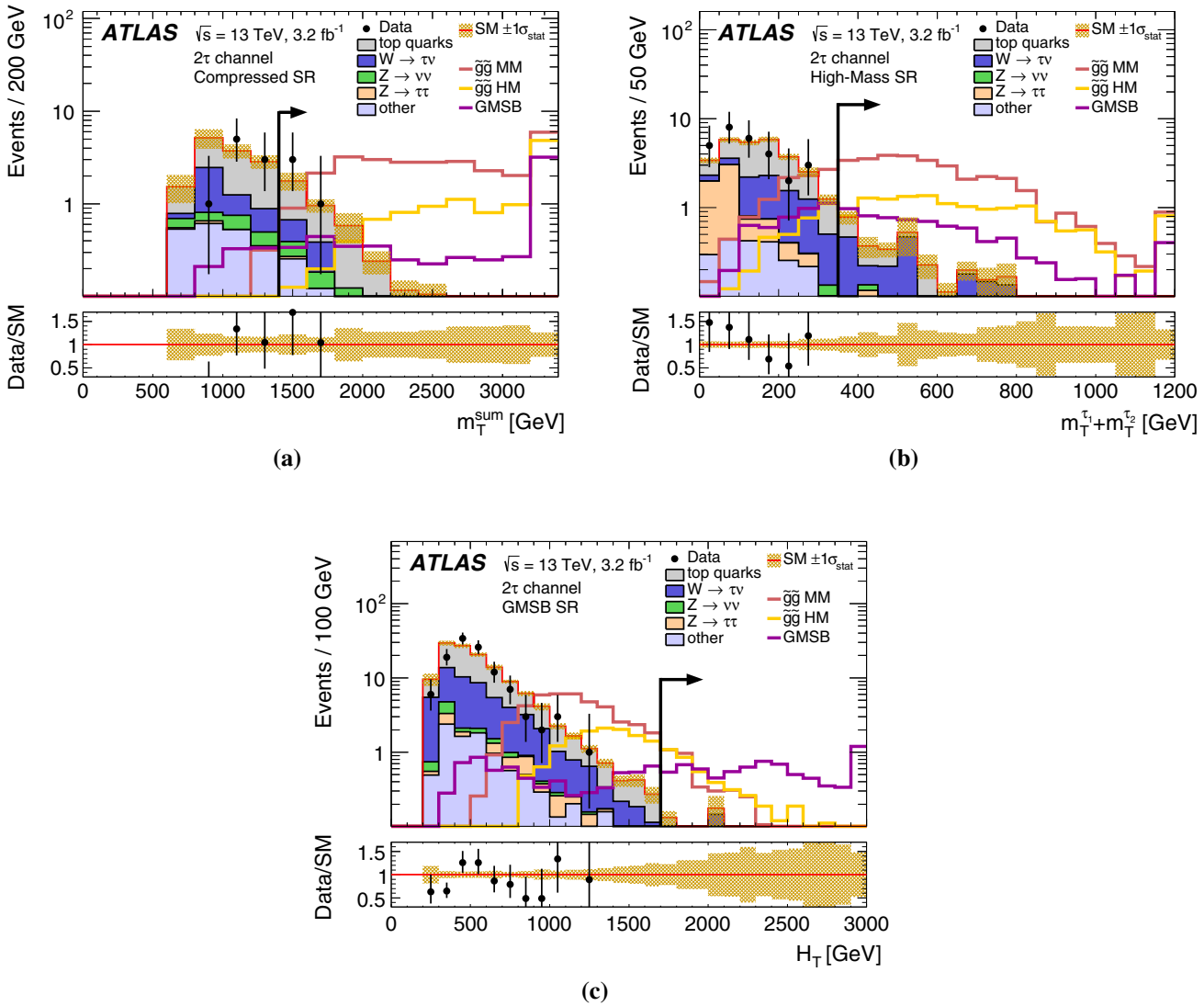


Fig. 7 Kinematic distributions for "extended SR selections" of the 2τ channel, for **a** $m_{\mathrm{T}}^{\mathrm{sum}}$ in the Compressed SR selection without the $m_{\mathrm{T}}^{\mathrm{sum}} > 1400$ GeV requirement, **b** $m_{\mathrm{T}}^{\tau_1} + m_{\mathrm{T}}^{\tau_2}$ in the High-Mass SR selection without the $m_{\mathrm{T}}^{\tau_1} + m_{\mathrm{T}}^{\tau_2} > 350$ GeV requirement, and **c** H_{T} in the GMSB SR selection without the $H_{\mathrm{T}} > 1700$ GeV requirement. The last bin includes overflow events. The *shaded bands* indicate the statistical uncertainties in the background predictions. The signal region is indicated by the *black arrow*. Signal predictions are overlaid for several benchmark models, normalised to their predicted cross sections. For the simplified model, *MM* medium mass splitting, with $m_{\tilde{g}} = 1145$ GeV and $m_{\tilde{\chi}_1^0} = 265$ GeV; *HM* high mass splitting scenario, with $m_{\tilde{g}} = 1305$ GeV and $m_{\tilde{\chi}_1^0} = 105$ GeV. The GMSB benchmark model corresponds to $\Lambda = 90$ TeV and $\tan\beta = 40$

Systematic uncertainties affecting electrons and muons are related to the energy or momentum calibration, as well as efficiency corrections for the reconstruction, identification and isolation requirements. These uncertainties have a negligible impact on the background predictions.

Systematic uncertainties in the missing transverse momentum originate from uncertainties in the energy or momentum calibration of jets, tau leptons, electrons, and muons, which are propagated to the $E_{\mathrm{T}}^{\mathrm{miss}}$ calculation. Additional uncertainties are related to the calculation of the track-based soft-term. These uncertainties are derived by studying the p_{T} balance in $Z(\mu\mu)$ events between the soft-term and the hard-term composed of all reconstructed objects. Soft-term uncertainties include scale uncertainties along the hard-term axis, and resolution uncertainties along and perpendicular to the hard-term axis [83].

A systematic uncertainty of the pile-up modelling is estimated by varying the distribution of the average number of interactions per bunch crossing in the simulation. The range of the variation is determined by studying the correlation in data and simulation between the average number of interactions and the number of reconstructed primary vertices. This uncertainty ranges from a few percent in the 1τ channel to about 15% in the poorly populated SRs of the 2τ channel.

Table 8 Number of observed events and predicted background yields in the three signal regions of the 1τ channel. The background prediction is scaled using normalisation factors derived in the control regions. All systematic and statistical uncertainties are included in the quoted uncertainties. The bottom part of the table shows the observed and expected model-independent upper limits at the 95% CL on the number of signal events, S^{95}_{obs} and S^{95}_{exp}, respectively, the corresponding observed upper limit on the visible cross section, $\langle\sigma_{\text{vis}}\rangle^{95}_{\text{obs}}$, and the CL_b value, i.e. the confidence level observed for the background-only hypothesis

1τ channel	Compressed SR	Medium-Mass SR	High-Mass SR
Data	47	11	1
Total background	49.2 ± 6.2	15.0 ± 2.4	5.7 ± 1.2
Top	14.3 ± 4.5	6.0 ± 1.3	2.49 ± 0.87
$W(\tau\nu)$+jets	12.1 ± 1.3	2.78 ± 0.62	1.17 ± 0.33
$Z(\nu\nu)$+jets	13.9 ± 2.3	3.8 ± 1.1	0.83 ± 0.21
V+jets, other	6.24 ± 0.90	1.44 ± 0.32	0.75 ± 0.23
Diboson	1.85 ± 0.23	0.76 ± 0.16	0.20 ± 0.03
Multi-jet	0.74 ± 0.54	0.19 ± 0.18	0.24 ± 0.17
S^{95}_{obs} (S^{95}_{exp})	16.7 ($18.4^{+6.9}_{-5.0}$)	7.5 ($9.7^{+3.5}_{-2.5}$)	3.8 ($6.1^{+2.1}_{-1.5}$)
$\langle\sigma_{\text{vis}}\rangle^{95}_{\text{obs}}$ (fb)	5.19	2.34	1.17
CL_b	0.41	0.23	0.02

Table 9 Number of observed events and predicted background yields in the three signal regions of the 2τ channel. The background prediction is scaled using normalisation factors derived in the control regions. All systematic and statistical uncertainties are included in the quoted uncertainties. The bottom part of the table shows the observed and expected model-independent upper limits at the 95% CL on the number of signal events, S^{95}_{obs} and S^{95}_{exp}, respectively, the corresponding observed upper limit on the visible cross section, $\langle\sigma_{\text{vis}}\rangle^{95}_{\text{obs}}$, and the CL_b value, i.e. the confidence level observed for the background-only hypothesis

2τ channel	Compressed SR	High-Mass SR	GMSB SR
Data	4	0	0
Total background	4.2 ± 3.0	3.2 ± 1.2	0.69 ± 0.24
Top	$2.5^{+2.9}_{-2.5}$	0.87 ± 0.78	0.20 ± 0.20
$W(\tau\nu)$+jets	0.51 ± 0.38	1.75 ± 0.65	0.31 ± 0.14
$Z(\tau\tau)$+jets	0.04 ± 0.02	0.13 ± 0.06	0.04 ± 0.02
$Z(\nu\nu)$+jets	0.28 ± 0.12	0.07 ± 0.03	0.02 ± 0.01
$W(\ell\nu)$+jets	0.37 ± 0.34	0.12 ± 0.07	0.02 ± 0.01
Diboson	0.25 ± 0.10	0.21 ± 0.08	0.06 ± 0.02
Multi-jet	0.21 ± 0.21	0.07 ± 0.07	0.06 ± 0.06
S^{95}_{obs} (S^{95}_{exp})	8.2 ($8.0^{+2.1}_{-2.0}$)	3.4 ($4.8^{+1.4}_{-1.0}$)	3.4 ($3.7^{+0.5}_{-0.2}$)
$\langle\sigma_{\text{vis}}\rangle^{95}_{\text{obs}}$ (fb)	2.55	1.07	1.07
CL_b	0.53	0.12	0.53

The uncertainty in the integrated luminosity is ±2.1%. It is derived, following a methodology similar to that detailed in Ref. [84], from a calibration of the luminosity scale using x–y beam-separation scans performed in August 2015. This uncertainty only affects the diboson background prediction and the signal yields, as other backgrounds are normalised to the data.

The systematic uncertainty in the small multi-jet background contribution is estimated by considering alternative normalisation regions and different jet smearing parameters in the case of the 1τ channel. An uncertainty of the order of 70% is found for the 1τ channel, and a 100% uncertainty is assigned in the 2τ channel.

The influence of the main systematic uncertainties in the total background predictions in the SRs of the 1τ and 2τ channels are summarised in Table 7. The uncertainties reported in the table are derived assuming that no signal is present in the CRs.

The total uncertainties range between 13 and 72%. For all SRs, the largest uncertainties, between 7 and 60%, originate from the MC generator modelling of top quark events. The larger uncertainty found for the Compressed SR of the 2τ channel is explained by the larger statistical uncertainty in the predictions from alternative generators. Energy scale uncertainties affecting tau leptons and jets contribute significantly in all regions as well. Other uncertainties, e.g. in the b-tagging efficiency and the jet energy resolution, do not play a large role in most of the SRs.

8 Results

Kinematic distributions for *extended SR selections* of the 1τ and 2τ channels are shown in Figs. 6 and 7, respectively. These regions are defined by the same set of selection criteria as for the SRs, except that the criterion corresponding to the plotted variable is not applied. Data and background predictions, fitted to data in the control regions, are compared, and signal predictions are also shown for several benchmark models. Variables providing the most discrimination between signal and background are displayed: m_{T}^{τ} distributions for the 1τ channel, and $m_{\text{T}}^{\text{sum}}$, $m_{\text{T}}^{\tau_1} + m_{\text{T}}^{\tau_2}$ and H_{T} distributions for the 2τ channel. Reasonable agreement between data and background distributions is observed, given the low event yields remaining in data after these selections. The numbers of observed events and expected background events in all SRs are reported in Tables 8 and 9 for the 1τ and 2τ channels, respectively.

No significant excess is observed in data over the SM predictions. Therefore, upper limits are set at the 95% confidence level (CL) on the number of hypothetical signal events, or equivalently, on the signal cross section. The one-sided profile-likelihood-ratio test statistic is used to assess the compatibility of the observed data with the background-only and signal-plus-background hypotheses. Systematic uncertainties are included in the likelihood function as nuisance parameters with Gaussian probability densities. Following

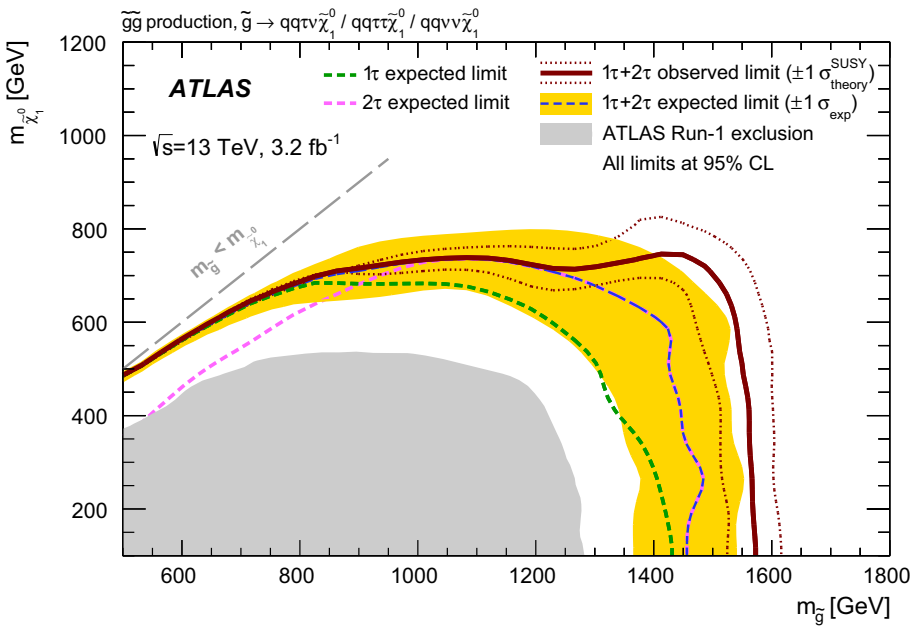


Fig. 8 Exclusion contours at the 95% confidence level for the simplified model of gluino pair production, based on results from the 1τ and 2τ channels. The *red solid line* and the *blue dashed line* correspond to the observed and median expected limits, respectively, for the combination of the two channels. The *yellow band* shows the one-standard-deviation spread of expected limits around the median. The effect of the signal cross-section uncertainty in the observed limits is shown as *red dotted lines*. Additionally, expected limits are shown for the 1τ and 2τ channels individually as *dashed green* and *magenta lines*, respectively. The previous ATLAS result [19] obtained with 20.3 fb^{-1} of 8 TeV data is shown as the *grey filled area*

the standards used for LHC analyses, p-values are computed according to the CL_s prescription [85].

Model-independent upper limits are calculated for each SR, assuming no signal contribution in the CRs. The results are derived using profile-likelihood-ratio distributions obtained from pseudo-experiments. Upper limits on signal yields are converted into limits on the visible cross section (σ_{vis}) of BSM processes by dividing by the integrated luminosity of the data. The visible cross section is defined as the product of production cross section, acceptance and selection efficiency. Results are summarised at the bottom of Tables 8 and 9. The most stringent observed upper limits on the visible cross section are 1.17 fb for the High-Mass SR of the 1τ channel and 1.07 fb for the High-Mass and GMSB SRs of the 2τ channel.

The results are interpreted in the context of the simplified model of gluino pair production and the GMSB model. In the case of model-dependent interpretations, the signal contribution in the control regions is included in the calculation of upper limits, and asymptotic properties of test-statistic distributions are used [86]. Exclusion contours at the 95% CL are derived in the $(m_{\tilde{g}}, m_{\tilde{\chi}_1^0})$ plane for the simplified model and in the $(\Lambda, \tan\beta)$ plane for the GMSB model. Results are shown in Figs. 8 and 9. The solid lines and the dashed lines correspond to the observed and median expected limits, respectively. The band shows the one-standard-deviation spread of the expected limits around the median, which originates from statistical and systematic uncertainties in the background and signal. The theoretical uncertainty in the signal cross section is not included in the band. Its effect on the observed limits is shown separately as the dotted lines. For the simplified model, exclusion contours are shown for the 1τ and 2τ channels and their combination. The combination is performed by selecting, for each signal scenario, the SR with the lowest expected CL_s value. The combination retains the Compressed SR of the 1τ channel in the region where the LSP mass is close to the gluino mass, and favours the High-Mass SR of the 2τ channel when the mass splitting is large. For the GMSB model, limits are shown for the GMSB SR of the 2τ channel. The stronger limits at high values of $\tan\beta$ are explained by the nature of the NSLP, which is the lightest scalar tau in this region. For both models, the exclusion limits obtained with 3.2 fb^{-1} of collision data at $\sqrt{s} = 13$ TeV significantly improve upon the previous ATLAS results [14,19] established with 20.3 fb^{-1} of 8 TeV data.

9 Summary

A search for squarks and gluinos has been performed in events with hadronically decaying tau leptons, jets and missing transverse momentum, using 3.2 fb^{-1} of pp collision

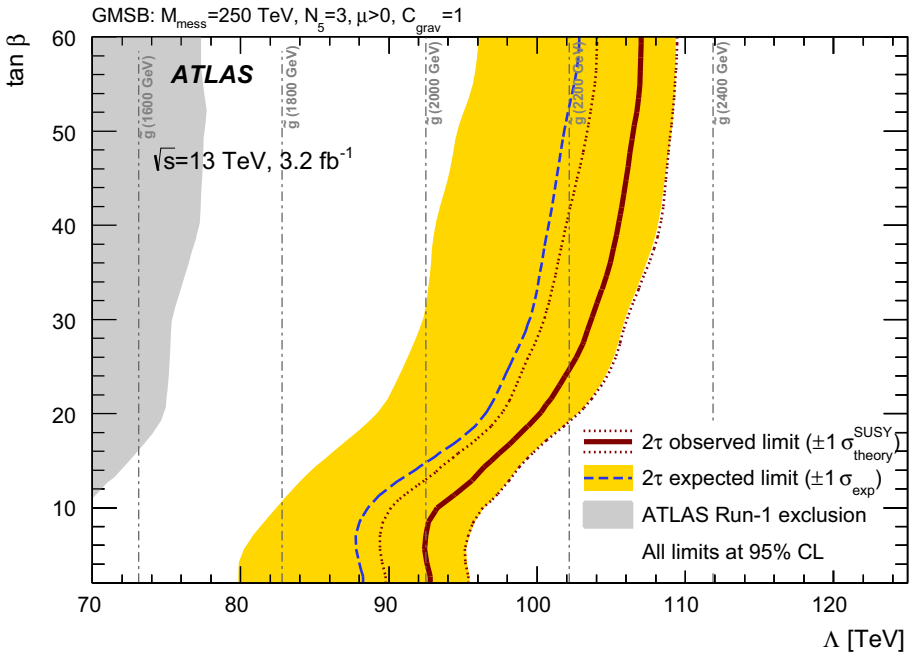


Fig. 9 Exclusion contours at the 95% confidence level for the gauge-mediated supersymmetry-breaking model, based on results from the 2τ channel. The *red solid line* and the *blue dashed line* correspond to the observed and median expected limits, respectively. The *yellow band* shows the one-standard-deviation spread of expected limits around the median. The effect of the signal cross-section uncertainty in the observed limits is shown as *red dotted lines*. The previous ATLAS result [14] obtained with 20.3 fb^{-1} of 8 TeV data is shown as the *grey filled area*

data at $\sqrt{s} = 13$ TeV recorded by the ATLAS detector at the LHC in 2015. Two channels, with either one tau lepton or at least two tau leptons, are separately optimised. The numbers of observed events in the different signal regions are in agreement with the Standard Model predictions. Results are interpreted in the context of a gauge-mediated supersymmetry breaking model and a simplified model of gluino pair production with tau-rich cascade decay. In the GMSB model, limits are set on the SUSY-breaking scale Λ as a function of $\tan\beta$. Values of Λ below 92 TeV are excluded at the 95% CL, corresponding to gluino masses below 2000 GeV. A stronger exclusion is achieved for large values of $\tan\beta$, where Λ and gluino mass values are excluded up to 107 TeV and 2300 GeV, respectively. In the simplified model, gluino masses are excluded up to 1570 GeV for neutralino masses around 100 GeV, neutralino masses below 700 GeV are excluded for all gluino masses between 800 and 1500 GeV, while the strongest neutralino-mass exclusion of 750 GeV is achieved for gluino masses around 1450 GeV. A dedicated signal region provides good sensitivity to scenarios with a small mass difference between the gluino and the neutralino LSP.

Acknowledgements We thank CERN for the very successful operation of the LHC, as well as the support staff from our institutions without whom ATLAS could not be operated efficiently. We acknowledge the support of ANPCyT, Argentina; YerPhI, Armenia; ARC, Australia; BMWFW and FWF, Austria; ANAS, Azerbaijan; SSTC, Belarus; CNPq and FAPESP, Brazil; NSERC, NRC and CFI, Canada; CERN; CONICYT, Chile; CAS, MOST and NSFC, China; COLCIENCIAS, Colombia; MSMT CR, MPO CR and VSC CR, Czech Republic; DNRF and DNSRC, Denmark; IN2P3-CNRS, CEA-DSM/IRFU, France; GNSF, Georgia; BMBF, HGF, and MPG, Germany; GSRT, Greece; RGC, Hong Kong SAR, China; ISF, I-CORE and Benoziyo Center, Israel; INFN, Italy; MEXT and JSPS, Japan; CNRST, Morocco; FOM and NWO, Netherlands; RCN, Norway; MNiSW and NCN, Poland; FCT, Portugal; MNE/IFA, Romania; MES of Russia and NRC KI, Russian Federation; JINR; MESTD, Serbia; MSSR, Slovakia; ARRS and MIZŠ, Slovenia; DST/NRF, South Africa; MINECO, Spain; SRC and Wallenberg Foundation, Sweden; SERI, SNSF and Cantons of Bern and Geneva, Switzerland; MOST, Taiwan; TAEK, Turkey; STFC, United Kingdom; DOE and NSF, United States of America. In addition, individual groups and members have received support from BCKDF, the Canada Council, CANARIE, CRC, Compute Canada, FQRNT, and the Ontario Innovation Trust, Canada; EPLANET, ERC, FP7, Horizon 2020 and Marie Skłodowska-Curie Actions, European Union; Investissements d'Avenir Labex and Idex, ANR, Région Auvergne and Fondation Partager le Savoir, France; DFG and AvH Foundation, Germany; Herakleitos, Thales and Aristeia programmes co-financed by EU-ESF and the Greek NSRF; BSF, GIF and Minerva, Israel; BRF, Norway; Generalitat de Catalunya, Generalitat Valenciana, Spain; the Royal Society and Leverhulme Trust, United Kingdom. The crucial computing support from all WLCG partners is acknowledged gratefully, in particular from CERN, the ATLAS Tier-1 facilities at TRIUMF (Canada), NDGF (Denmark, Norway, Sweden), CC-IN2P3 (France), KIT/GridKA (Germany), INFN-CNAF (Italy), NL-T1 (Netherlands), PIC (Spain), ASGC (Taiwan), RAL (UK) and BNL (USA), the Tier-2 facilities worldwide and large non-WLCG resource providers. Major contributors of computing resources are listed in Ref. [87].

Open Access This article is distributed under the terms of the Creative Commons Attribution 4.0 International License (http://creativecommons.org/licenses/by/4.0/), which permits unrestricted use, distribution, and reproduction in any medium, provided you give appropriate credit to the original author(s) and the source, provide a link to the Creative Commons license, and indicate if changes were made.
Funded by SCOAP[3].

References

1. Y.A. Golfand, E.P. Likhtman, Extension of the algebra of poincare group generators and violation of p invariance. JETP Lett. **13**, 323 (1971)
2. D.V. Volkov, V.P. Akulov, Is the neutrino a goldstone particle? Phys. Lett. B **46**, 109 (1973). doi:10.1016/0370-2693(73)90490-5
3. J. Wess, B. Zumino, Supergauge transformations in four-dimensions. Nucl. Phys. B **70**, 39 (1974). doi:10.1016/0550-3213(74)90355-1
4. J. Wess, B. Zumino, Supergauge invariant extension of quantum electrodynamics. Nucl. Phys. B **78**, 1 (1974). doi:10.1016/0550-3213(74)90112-6
5. S. Ferrara, B. Zumino, Supergauge invariant Yang–Mills theories. Nucl. Phys. B **79**, 413 (1974). doi:10.1016/0550-3213(74)90559-8
6. A. Salam, J.A. Strathdee, Supersymmetry and nonabelian gauges. Phys. Lett. B **51**, 353 (1974). doi:10.1016/0370-2693(74)90226-3
7. P. Fayet, Supersymmetry and weak, electromagnetic and strong interactions. Phys. Lett. B **64**, 159 (1976). doi:10.1016/0370-2693(76)90319-1
8. P. Fayet, Spontaneously broken supersymmetric theories of weak, electromagnetic and strong interactions. Phys. Lett. B **69**, 489 (1977). doi:10.1016/0370-2693(77)90852-8
9. G.R. Farrar, P. Fayet, Phenomenology of the production, decay, and detection of new hadronic states associated with supersymmetry. Phys. Lett. B **76**, 575 (1978). doi:10.1016/0370-2693(78)90858-4
10. P. Fayet, Relations between the masses of the superpartners of leptons and quarks, the goldstino couplings and the neutral currents. Phys. Lett. B **84**, 416 (1979). doi:10.1016/0370-2693(79)91229-2
11. S. Dimopoulos, H. Georgi, Softly broken supersymmetry and SU(5). Nucl. Phys. B **193**, 150 (1981). doi:10.1016/0550-3213(81)90522-8
12. D. Albornoz Vásquez, G. Bélanger, C. Bœhm, Revisiting light neutralino scenarios in the MSSM, Phys. Rev. D **84**, 095015 (2011). http://dx.doi.org/10.1103/PhysRevD.84.095015. arXiv:1108.1338 [hep-ph]
13. ATLAS Collaboration, Search for supersymmetry in events with large missing transverse momentum, jets, and at least one tau lepton in 7 TeV proton–proton collision data with the ATLAS detector, Eur. Phys. J. C **72**, 2215 (2012). http://dx.doi.org/10.1140/epjc/s10052-012-2215-7. arXiv:1210.1314 [hep-ex]
14. ATLAS Collaboration, Search for supersymmetry in events with large missing transverse momentum, jets, and at least one tau lepton in 20 fb^{-1} of $\sqrt{s} = 8$ TeV proton–proton collision data with the ATLAS detector, JHEP **1409**, 103 (2014). http://dx.doi.org/10.1007/JHEP09(2014)103. arXiv:1407.0603 [hep-ex]
15. CMS Collaboration, Search for physics beyond the standard model in events with τ leptons, jets, and large transverse momentum imbalance in pp collisions at $\sqrt{s} = 7$ TeV. Eur. Phys. J. C **73**, 2493 (2013). doi:10.1140/epjc/s10052-013-2493-8. arXiv:1301.3792 [hep-ex]
16. M. Dine, W. Fischler, A phenomenological model of particle physics based on supersymmetry. Phys. Lett. B **110**, 227 (1982). doi:10.1016/0370-2693(82)91241-2
17. L. Alvarez-Gaume, M. Claudson, M.B. Wise, Low-energy supersymmetry. Nucl. Phys. B **207**, 96 (1982). doi:10.1016/0550-3213(82)90138-9
18. C.R. Nappi, B.A. Ovrut, Supersymmetric extension of the SU(3) x SU(2) x U(1) model. Phys. Lett. B **113**, 175 (1982). doi:10.1016/0370-2693(82)90418-X
19. ATLAS Collaboration, Summary of the searches for squarks and gluinos using $\sqrt{s} = 8$ TeV pp collisions with the ATLAS experiment at the LHC, JHEP **1510**, 054 (2015). http://dx.doi.org/10.1007/JHEP10(2015)054. arXiv:1507.05525 [hep-ex]
20. MSSM Working Group Collaboration, A. Djouadi et al., The minimal supersymmetric standard model: group summary report. In: GDR (Groupement De Recherche)—Supersymetrie Montpellier, France (1998). arXiv:hep-ph/9901246
21. C.F. Berger, J.S. Gainer, J.L. Hewett, T.G. Rizzo, Supersymmetry without prejudice. JHEP **0902**, 023 (2009). doi:10.1088/1126-6708/2009/02/023. arXiv:0812.0980 [hep-ph]
22. ATLAS Collaboration, The ATLAS experiment at the CERN large hadron collider, JINST **3**, S08003 (2008). http://dx.doi.org/10.1088/1748-0221/3/08/S08003
23. ATLAS Collaboration, ATLAS insertable B-layer technical design report, ATLAS-TDR-19, 2010. http://cds.cern.ch/record/1291633, ATLAS Insertable B-Layer Technical Design Report Addendum, ATLAS-TDR-19-ADD-1 (2012). http://cds.cern.ch/record/1451888
24. ATLAS Collaboration, 2015 start-up trigger menu and initial performance assessment of the ATLAS trigger using Run-2 data, ATL-DAQ-PUB-2016-001 (2016). https://cds.cern.ch/record/2136007/
25. T. Sjöstrand, S. Ask, J.R. Christiansen, R. Corke, N. Desai, P. Ilten, S. Mrenna, S. Prestel, C.O. Rasmussen, P.Z. Skands, An introduction to PYTHIA 8.2. Comput. Phys. Commun. **191**, 159 (2015). doi:10.1016/j.cpc.2015.01.024. arXiv:1410.3012 [hep-ph]
26. ATLAS Collaboration, Summary of ATLAS Pythia 8 tunes, ATL-PHYS-PUB-2012-003 (2012). http://cds.cern.ch/record/1474107
27. A.D. Martin, W.J. Stirling, R.S. Thorne, G. Watt, Parton distributions for the LHC. Eur. Phys. J. C **63**, 189 (2009). doi:10.1140/epjc/s10052-009-1072-5. arXiv:0901.0002 [hep-ph]
28. ATLAS Collaboration, The ATLAS simulation infrastructure, Eur. Phys. J. C **70**, 823 (2010). http://dx.doi.org/10.1140/epjc/s10052-010-1429-9. arXiv:1005.4568 [hep-ex]
29. GEANT4 Collaboration, S. Agostinelli et al., GEANT4: a simulation toolkit, Nucl. Instrum. Meth. A **506**, 250 (2003). http://dx.doi.org/10.1016/S0168-9002(03)01368-8
30. ATLAS Collaboration, Performance of the fast ATLAS tracking simulation (FATRAS) and the ATLAS fast calorimeter simulation (FastCaloSim) with single particles, ATL-SOFT-PUB-2014-01 (2014). http://cdsweb.cern.ch/record/1669341
31. T. Gleisberg, S. Höche, F. Krauss, M. Schönherr, S. Schumann et al., Event generation with SHERPA 1.1, JHEP **0902**, 007 (2009). http://dx.doi.org/10.1088/1126-6708/2009/02/007. arXiv:0811.4622 [hep-ph]
32. F. Cascioli, P. Maierhofer, S. Pozzorini, Scattering amplitudes with open loops. Phys. Rev. Lett. **108**, 111601 (2012). doi:10.1103/PhysRevLett.108.111601. arXiv:1111.5206 [hep-ph]
33. T. Gleisberg, S. Höche, Comix, a new matrix element generator. JHEP **0812**, 039 (2008). doi:10.1088/1126-6708/2008/12/039. arXiv:0808.3674 [hep-ph]
34. Z. Czyczula, T. Przedzinski, Z. Was, TauSpinner program for studies on spin effect in tau production at the LHC. Eur. Phys. J. C **72**, 1988 (2012). doi:10.1140/epjc/s10052-012-1988-z. arXiv:1201.0117 [hep-ph]
35. S. Schumann, F. Krauss, A parton shower algorithm based on Catani–Seymour dipole factorisation. JHEP **0803**, 038 (2008). doi:10.1088/1126-6708/2008/03/038. arXiv:0709.1027 [hep-ph]

36. S. Höche, F. Krauss, M. Schönherr, F. Siegert, QCD matrix elements + parton showers: the NLO case. JHEP **1304**, 027 (2013). doi:10.1007/JHEP04(2013)027. arXiv:1207.5030 [hep-ph]
37. H.-L. Lai, M. Guzzi, J. Huston, Z. Li, P.M. Nadolsky, J. Pumplin, C.P. Yuan, New parton distributions for collider physics. Phys. Rev. D **82**, 074024 (2010). doi:10.1103/PhysRevD.82.074024. arXiv:1007.2241 [hep-ph]
38. S. Catani, L. Cieri, G. Ferrera, D. de Florian, M. Grazzini, Vector boson production at hadron colliders: a fully exclusive QCD calculation at NNLO. Phys. Rev. Lett. **103**, 082001 (2009). doi:10.1103/PhysRevLett.103.082001. arXiv:0903.2120 [hep-ph]
39. C. Anastasiou, L.J. Dixon, K. Melnikov, F. Petriello, High precision QCD at hadron colliders: electroweak gauge boson rapidity distributions at NNLO. Phys. Rev. D **69**, 094008 (2004). doi:10.1103/PhysRevD.69.094008. arXiv:hep-ph/0312266
40. S. Alioli, P. Nason, C. Oleari, E. Re, A general framework for implementing NLO calculations in shower Monte Carlo programs: the POWHEG BOX. JHEP **1006**, 043 (2010). doi:10.1007/JHEP06(2010)043. arXiv:1002.2581 [hep-ph]
41. P. Artoisenet, R. Frederix, O. Mattelaer, R. Rietkerk, Automatic spin-entangled decays of heavy resonances in Monte Carlo simulations. JHEP **1303**, 015 (2013). doi:10.1007/JHEP03(2013)015. arXiv:1212.3460 [hep-ph]
42. T. Sjöstrand, S. Mrenna, P.Z. Skands, PYTHIA 6.4 Physics and Manual, JHEP **0605**, 026 (2006). http://dx.doi.org/10.1088/1126-6708/2006/05/026. arXiv:hep-ph/0603175
43. J. Pumplin, D.R. Stump, J. Huston, H.L. Lai, P.M. Nadolsky, W.K. Tung, New generation of parton distributions with uncertainties from global QCD analysis. JHEP **0207**, 012 (2002). doi:10.1088/1126-6708/2002/07/012. arXiv:hep-ph/0201195
44. P.Z. Skands, Tuning monte carlo generators: the perugia tunes. Phys. Rev. D **82**, 074018 (2010). doi:10.1103/PhysRevD.82.074018. arXiv:1005.3457 [hep-ph]
45. M. Czakon, A. Mitov, Top++: a program for the calculation of the top-pair cross-section at hadron colliders. Comput. Phys. Commun. **185**, 2930 (2014). doi:10.1016/j.cpc.2014.06.021. arXiv:1112.5675 [hep-ph]
46. J. Alwall, R. Frederix, S. Frixione, V. Hirschi, F. Maltoni et al., The automated computation of tree-level and next-to-leading order differential cross sections, and their matching to parton shower simulations. JHEP **1407**, 079 (2014). doi:10.1007/JHEP07(2014)079. arXiv:1405.0301 [hep-ph]
47. ATLAS Collaboration, ATLAS Pythia 8 tunes to 7 TeV data, ATL-PHYS-PUB-2014-021 (2014). http://cdsweb.cern.ch/record/1966419
48. NNPDF Collaboration, R.D. Ball, V. Bertone, S. Carrazza, L. Del Debbio, S. Forte, A. Guffanti, N.P. Hartland, J. Rojo, Parton distributions with QED corrections, Nucl. Phys. B **877**, 290 (2013). http://dx.doi.org/10.1016/j.nuclphysb.2013.10.010. arXiv:1308.0598 [hep-ph]
49. L. Lonnblad, Correcting the color dipole cascade model with fixed order matrix elements. JHEP **0205**, 046 (2002). doi:10.1088/1126-6708/2002/05/046. arXiv:hep-ph/0112284
50. M. Bahr et al., Herwig++ physics and manual. Eur. Phys. J. C **58**, 639 (2008). doi:10.1140/epjc/s10052-008-0798-9. arXiv:0803.0883 [hep-ph]
51. S. Gieseke, C. Rohr, A. Siodmok, Colour reconnections in Herwig++. Eur. Phys. J. C **72**, 2225 (2012). doi:10.1140/epjc/s10052-012-2225-5. arXiv:1206.0041 [hep-ph]
52. W. Porod, F. Staub, SPheno 3.1: extensions including flavour, CP-phases and models beyond the MSSM. Comput. Phys. Commun. **183**, 2458 (2012). doi:10.1016/j.cpc.2012.05.021. arXiv:1104.1573 [hep-ph]
53. G. Marchesini, B.R. Webber, Simulation of QCD jets including soft gluon interference. Nucl. Phys. B **238**, 1 (1984). doi:10.1016/0550-3213(84)90463-2
54. G. Marchesini, B.R. Webber, Monte carlo simulation of general hard processes with coherent QCD radiation. Nucl. Phys. B **310**, 461 (1988). doi:10.1016/0550-3213(88)90089-2
55. S. Gieseke, P. Stephens, B. Webber, New formalism for QCD parton showers. JHEP **0312**, 045 (2003). doi:10.1088/1126-6708/2003/12/045. arXiv:hep-ph/0310083
56. W. Beenakker, R. Hopker, M. Spira, P. Zerwas, Squark and gluino production at hadron colliders. Nucl. Phys. B **492**, 51 (1997). doi:10.1016/S0550-3213(97)00084-9. arXiv:hep-ph/9610490
57. A. Kulesza, L. Motyka, Threshold resummation for squark–antisquark and gluino-pair production at the LHC. Phys. Rev. Lett. **102**, 111802 (2009). doi:10.1103/PhysRevLett.102.111802. arXiv:0807.2405 [hep-ph]
58. A. Kulesza, L. Motyka, Soft gluon resummation for the production of gluino–gluino and squark–antisquark pairs at the LHC. Phys. Rev. D **80**, 095004 (2009). doi:10.1103/PhysRevD.80.095004. arXiv:0905.4749 [hep-ph]
59. W. Beenakker, S. Brensing, M. Kramer, A. Kulesza, E. Laenen et al., Soft-gluon resummation for squark and gluino hadroproduction. JHEP **0912**, 041 (2009). doi:10.1088/1126-6708/2009/12/041. arXiv:0909.4418 [hep-ph]
60. W. Beenakker et al., Squark and gluino hadroproduction. Int. J. Mod. Phys. A **26**, 2637 (2011). doi:10.1142/S0217751X11053560. arXiv:1105.1110 [hep-ph]
61. M. Kramer, A. Kulesza, R. van der Leeuw, M. Mangano, S. Padhi, et al., Supersymmetry production cross sections in pp collisions at $\sqrt{s} = 7$ TeV. arXiv:1206.2892 [hep-ph]
62. ATLAS Collaboration, Vertex Reconstruction Performance of the ATLAS Detector at $\sqrt{s} = 13\ TeV$. ATL-PHYS-PUB-2015-026 (2015). http://cdsweb.cern.ch/record/2037717
63. M. Cacciari, G.P. Salam, G. Soyez, The anti-k_t jet clustering algorithm. JHEP **0804**, 063 (2008). doi:10.1088/1126-6708/2008/04/063. arXiv:0802.1189 [hep-ph]
64. ATLAS Collaboration, Topological cell clustering in the ATLAS calorimeters and its performance in LHC Run 1. arXiv:1603.02934 [hep-ex]
65. ATLAS Collaboration, Jet global sequential corrections with the ATLAS detector in proton–proton collisions at $\sqrt{s} = 8\ TeV$, ATLAS-CONF-2015-002 (2015). http://cdsweb.cern.ch/record/2001682
66. ATLAS Collaboration, Jet calibration and systematic uncertainties for jets reconstructed in the ATLAS detector at $\sqrt{s} = 13\ TeV$, ATL-PHYS-PUB-2015-015 (2015). https://cds.cern.ch/record/2037613
67. ATLAS Collaboration, Performance of pile-up mitigation techniques for jets in pp collisions at $\sqrt{s} = 8\ TeV$ using the ATLAS detector. arXiv:1510.03823 [hep-ex]
68. ATLAS Collaboration, Tagging and suppression of pileup jets with the ATLAS detector, ATLAS-CONF-2014-018 (2014). http://cdsweb.cern.ch/record/1700870
69. ATLAS Collaboration, Selection of jets produced in 13 TeV proton–proton collisions with the ATLAS detector, ATLAS-CONF-2015-029 (2015). http://cdsweb.cern.ch/record/2037702
70. ATLAS Collaboration, Expected performance of the ATLAS b-tagging algorithms in Run-2, ATL-PHYS-PUB-2015-022 (2015). http://cdsweb.cern.ch/record/2037697
71. ATLAS Collaboration, Commissioning of the ATLAS b-tagging algorithms using $t\bar{t}$ events in early Run 2 data, ATL-PHYS-PUB-2015-039 (2015). http://cdsweb.cern.ch/record/2047871
72. ATLAS Collaboration, Electron and photon energy calibration with the ATLAS detector using LHC Run 1 data, Eur. Phys. J. C **74**, 3071 (2014). http://dx.doi.org/10.1140/epjc/s10052-014-3071-4. arXiv:1407.5063 [hep-ex]

73. ATLAS Collaboration, Electron identification measurements in ATLAS using $\sqrt{s} = 13\ TeV$ data with 50 ns bunch spacing, ATL-PHYS-PUB-2015-041 (2015). http://cdsweb.cern.ch/record/2048202
74. ATLAS Collaboration, Muon reconstruction performance of the ATLAS detector in proton–proton collision data at $\sqrt{s}$ =13 TeV, Eur. Phys. J. C **76**, 292 (2016). http://dx.doi.org/10.1140/epjc/s10052-016-4120-y. arXiv:1603.05598 [hep-ex]
75. ATLAS Collaboration, Reconstruction, energy calibration, and identification of hadronically decaying tau leptons in the ATLAS experiment for Run-2 of the LHC, ATL-PHYS-PUB-2015-045 (2015). https://cds.cern.ch/record/2064383/
76. ATLAS Collaboration, Jet energy measurement with the ATLAS detector in proton–proton collisions at $\sqrt{s} = 7\ TeV$, Eur. Phys. J. C **73**, 2304 (2013). http://dx.doi.org/10.1140/epjc/s10052-013-2304-2. arXiv:1112.6426 [hep-ex]
77. ATLAS Collaboration, Performance of missing transverse momentum reconstruction with the ATLAS detector in the first proton–proton collisions at $\sqrt{s} = 13\ TeV$, ATL-PHYS-PUB-2015-027 (2015). http://cdsweb.cern.ch/record/2037904
78. C.G. Lester, D.J. Summers, Measuring masses of semiinvisibly decaying particles pair produced at hadron colliders. Phys. Lett. B **463**, 99 (1999). doi:10.1016/S0370-2693(99)00945-4. arXiv:hep-ph/9906349
79. C.G. Lester, B. Nachman, Bisection-based asymmetric M_{T2} computation: a higher precision calculator than existing symmetric methods. JHEP **1503**, 100 (2015). doi:10.1007/JHEP03(2015)100. arXiv:1411.4312 [hep-ph]
80. M. Baak, G.J. Besjes, D. Côte, A. Koutsman, J. Lorenz, D. Short, HistFitter software framework for statistical data analysis, Eur. Phys. J. C **75**, 153 (2015). doi:10.1140/epjc/s10052-015-3327-7. arXiv:1410.1280 [hep-ex]
81. ATLAS Collaboration, Search for squarks and gluinos with the ATLAS detector in final states with jets and missing transverse momentum using 4.7 fb^{-1} of $\sqrt{s} = 7$ TeV proton–proton collision data, Phys. Rev. D **87**, 012008 (2013). http://dx.doi.org/10.1103/PhysRevD.87.012008. arXiv:1208.0949 [hep-ex]
82. ATLAS Collaboration, Calibration of the performance of b-tagging for c and light-flavour jets in the 2012 ATLAS data, ATLAS-CONF-2014-046 (2014). http://cdsweb.cern.ch/record/1741020
83. ATLAS Collaboration, Expected performance of missing transverse momentum reconstruction for the ATLAS detector at $\sqrt{s} = 13\ TeV$, ATL-PHYS-PUB-2015-023 (2015). http://cdsweb.cern.ch/record/2037700
84. ATLAS Collaboration, Improved luminosity determination in pp collisions at $\sqrt{s} = 7\ TeV$ using the ATLAS detector at the LHC, Eur. Phys. J. C **73**, 2518 (2013). http://dx.doi.org/10.1140/epjc/s10052-013-2518-3. arXiv:1302.4393 [hep-ex]
85. A.L. Read, Presentation of search results: the CLs technique. J. Phys. G **28**, 2693 (2002). doi:10.1088/0954-3899/28/10/313
86. G. Cowan, K. Cranmer, E. Gross, O. Vitells, Asymptotic formulae for likelihood-based tests of new physics. Eur. Phys. J. C **71**, 1554 (2011). doi:10.1140/epjc/s10052-011-1554-0. doi:10.1140/epjc/s10052-013-2501-z. arXiv:1007.1727 [physics.data-an]. **(Erratum: Eur. Phys. J. C 73, 2501 (2013))**
87. ATLAS Collaboration, ATLAS Computing Acknowledgements 2016–2017, ATL-GEN-PUB-2016-002. http://cds.cern.ch/record/2202407

ATLAS Collaboration

M. Aaboud[136d], G. Aad[87], B. Abbott[114], J. Abdallah[65], O. Abdinov[12], B. Abeloos[118], R. Aben[108], O. S. AbouZeid[138], N. L. Abraham[152], H. Abramowicz[156], H. Abreu[155], R. Abreu[117], Y. Abulaiti[149a,149b], B. S. Acharya[168a,168b,a], L. Adamczyk[40a], D. L. Adams[27], J. Adelman[109], S. Adomeit[101], T. Adye[132], A. A. Affolder[76], T. Agatonovic-Jovin[14], J. Agricola[56], J. A. Aguilar-Saavedra[127a,127f], S. P. Ahlen[24], F. Ahmadov[67,b], G. Aielli[134a,134b], H. Akerstedt[149a,149b], T. P. A. Åkesson[83], A. V. Akimov[97], G. L. Alberghi[22a,22b], J. Albert[173], S. Albrand[57], M. J. Alconada Verzini[73], M. Aleksa[32], I. N. Aleksandrov[67], C. Alexa[28b], G. Alexander[156], T. Alexopoulos[10], M. Alhroob[114], B. Ali[129], M. Aliev[75a,75b], G. Alimonti[93a], J. Alison[33], S. P. Alkire[37], B. M. M. Allbrooke[152], B. W. Allen[117], P. P. Allport[19], A. Aloisio[105a,105b], A. Alonso[38], F. Alonso[73], C. Alpigiani[139], A. A. Alshehri[55], M. Alstaty[87], B. Alvarez Gonzalez[32], D. Álvarez Piqueras[171], M. G. Alviggi[105a,105b], B. T. Amadio[16], K. Amako[68], Y. Amaral Coutinho[26a], C. Amelung[25], D. Amidei[91], S. P. Amor Dos Santos[127a,127c], A. Amorim[127a,127b], S. Amoroso[32], G. Amundsen[25], C. Anastopoulos[142], L. S. Ancu[51], N. Andari[19], T. Andeen[11], C. F. Anders[60b], G. Anders[32], J. K. Anders[76], K. J. Anderson[33], A. Andreazza[93a,93b], V. Andrei[60a], S. Angelidakis[9], I. Angelozzi[108], P. Anger[46], A. Angerami[37], F. Anghinolfi[32], A. V. Anisenkov[110,c], N. Anjos[13], A. Annovi[125a,125b], C. Antel[60a], M. Antonelli[49], A. Antonov[99,*], F. Anulli[133a], M. Aoki[68], L. Aperio Bella[19], G. Arabidze[92], Y. Arai[68], J. P. Araque[127a], A. T. H. Arce[47], F. A. Arduh[73], J-F. Arguin[96], S. Argyropoulos[65], M. Arik[20a], A. J. Armbruster[146], L. J. Armitage[78], O. Arnaez[32], H. Arnold[50], M. Arratia[30], O. Arslan[23], A. Artamonov[98], G. Artoni[121], S. Artz[85], S. Asai[158], N. Asbah[44], A. Ashkenazi[156], B. Åsman[149a,149b], L. Asquith[152], K. Assamagan[27], R. Astalos[147a], M. Atkinson[170], N. B. Atlay[144], K. Augsten[129], G. Avolio[32], B. Axen[16], M. K. Ayoub[118], G. Azuelos[96,d], M. A. Baak[32], A. E. Baas[60a], M. J. Baca[19], H. Bachacou[137], K. Bachas[75a,75b], M. Backes[121], M. Backhaus[32], P. Bagiacchi[133a,133b], P. Bagnaia[133a,133b], Y. Bai[35a], J. T. Baines[132], O. K. Baker[180], E. M. Baldin[110,c], P. Balek[176], T. Balestri[151], F. Balli[137], W. K. Balunas[123], E. Banas[41], Sw. Banerjee[177,e], A. A. E. Bannoura[179], L. Barak[32], E. L. Barberio[90], D. Barberis[52a,52b], M. Barbero[87], T. Barillari[102], M-S Barisits[32], T. Barklow[146], N. Barlow[30], S. L. Barnes[86], B. M. Barnett[132], R. M. Barnett[16], Z. Barnovska-Blenessy[5], A. Baroncelli[135a], G. Barone[25], A. J. Barr[121], L. Barranco Navarro[171], F. Barreiro[84], J. Barreiro Guimarães da Costa[35a], R. Bartoldus[146], A. E. Barton[74], P. Bartos[147a], A. Basalaev[124], A. Bassalat[118,f], R. L. Bates[55], S. J. Batista[162], J. R. Batley[30], M. Battaglia[138], M. Bauce[133a,133b],

F. Bauer[137], H. S. Bawa[146,g], J. B. Beacham[112], M. D. Beattie[74], T. Beau[82], P. H. Beauchemin[166], P. Bechtle[23], H. P. Beck[18,h], K. Becker[121], M. Becker[85], M. Beckingham[174], C. Becot[111], A. J. Beddall[20d], A. Beddall[20b], V. A. Bednyakov[67], M. Bedognetti[108], C. P. Bee[151], L. J. Beemster[108], T. A. Beermann[32], M. Begel[27], J. K. Behr[44], C. Belanger-Champagne[89], A. S. Bell[80], G. Bella[156], L. Bellagamba[22a], A. Bellerive[31], M. Bellomo[88], K. Belotskiy[99], O. Beltramello[32], N. L. Belyaev[99], O. Benary[156,*], D. Benchekroun[136a], M. Bender[101], K. Bendtz[149a,149b], N. Benekos[10], Y. Benhammou[156], E. Benhar Noccioli[180], J. Benitez[65], D. P. Benjamin[47], J. R. Bensinger[25], S. Bentvelsen[108], L. Beresford[121], M. Beretta[49], D. Berge[108], E. Bergeaas Kuutmann[169], N. Berger[5], J. Beringer[16], S. Berlendis[57], N. R. Bernard[88], C. Bernius[111], F. U. Bernlochner[23], T. Berry[79], P. Berta[130], C. Bertella[85], G. Bertoli[149a,149b], F. Bertolucci[125a,125b], I. A. Bertram[74], C. Bertsche[44], D. Bertsche[114], G. J. Besjes[38], O. Bessidskaia Bylund[149a,149b], M. Bessner[44], N. Besson[137], C. Betancourt[50], A. Bethani[57], S. Bethke[102], A. J. Bevan[78], R. M. Bianchi[126], L. Bianchini[25], M. Bianco[32], O. Biebel[101], D. Biedermann[17], R. Bielski[86], N. V. Biesuz[125a,125b], M. Biglietti[135a], J. Bilbao De Mendizabal[51], T. R. V. Billoud[96], H. Bilokon[49], M. Bindi[56], S. Binet[118], A. Bingul[20b], C. Bini[133a,133b], S. Biondi[22a,22b], T. Bisanz[56], D. M. Bjergaard[47], C. W. Black[153], J. E. Black[146], K. M. Black[24], D. Blackburn[139], R. E. Blair[6], J. -B. Blanchard[137], T. Blazek[147a], I. Bloch[44], C. Blocker[25], A. Blue[55], W. Blum[85,*], U. Blumenschein[56], S. Blunier[34a], G. J. Bobbink[108], V. S. Bobrovnikov[110,c], S. S. Bocchetta[83], A. Bocci[47], C. Bock[101], M. Boehler[50], D. Boerner[179], J. A. Bogaerts[32], D. Bogavac[14], A. G. Bogdanchikov[110], C. Bohm[149a], V. Boisvert[79], P. Bokan[14], T. Bold[40a], A. S. Boldyrev[168a,168c], M. Bomben[82], M. Bona[78], M. Boonekamp[137], A. Borisov[131], G. Borissov[74], J. Bortfeldt[32], D. Bortoletto[121], V. Bortolotto[62a,62b,62c], K. Bos[108], D. Boscherini[22a], M. Bosman[13], J. D. Bossio Sola[29], J. Boudreau[126], J. Bouffard[2], E. V. Bouhova-Thacker[74], D. Boumediene[36], C. Bourdarios[118], S. K. Boutle[55], A. Boveia[32], J. Boyd[32], I. R. Boyko[67], J. Bracinik[19], A. Brandt[8], G. Brandt[56], O. Brandt[60a], U. Bratzler[159], B. Brau[88], J. E. Brau[117], H. M. Braun[179,*], W. D. Breaden Madden[55], K. Brendlinger[123], A. J. Brennan[90], L. Brenner[108], R. Brenner[169], S. Bressler[176], T. M. Bristow[48], D. Britton[55], D. Britzger[44], F. M. Brochu[30], I. Brock[23], R. Brock[92], G. Brooijmans[37], T. Brooks[79], W. K. Brooks[34b], J. Brosamer[16], E. Brost[109], J. H Broughton[19], P. A. Bruckman de Renstrom[41], D. Bruncko[147b], R. Bruneliere[50], A. Bruni[22a], G. Bruni[22a], L. S. Bruni[108], BH Brunt[30], M. Bruschi[22a], N. Bruscino[23], P. Bryant[33], L. Bryngemark[83], T. Buanes[15], Q. Buat[145], P. Buchholz[144], A. G. Buckley[55], I. A. Budagov[67], F. Buehrer[50], M. K. Bugge[120], O. Bulekov[99], D. Bullock[8], H. Burckhart[32], S. Burdin[76], C. D. Burgard[50], B. Burghgrave[109], K. Burka[41], S. Burke[132], I. Burmeister[45], J. T. P. Burr[121], E. Busato[36], D. Büscher[50], V. Büscher[85], P. Bussey[55], J. M. Butler[24], C. M. Buttar[55], J. M. Butterworth[80], P. Butti[108], W. Buttinger[27], A. Buzatu[55], A. R. Buzykaev[110,c], S. Cabrera Urbán[171], D. Caforio[129], V. M. Cairo[39a,39b], O. Cakir[4a], N. Calace[51], P. Calafiura[16], A. Calandri[87], G. Calderini[82], P. Calfayan[101], G. Callea[39a,39b], L. P. Caloba[26a], S. Calvente Lopez[84], D. Calvet[36], S. Calvet[36], T. P. Calvet[87], R. Camacho Toro[33], S. Camarda[32], P. Camarri[134a,134b], D. Cameron[120], R. Caminal Armadans[170], C. Camincher[57], S. Campana[32], M. Campanelli[80], A. Camplani[93a,93b], A. Campoverde[144], V. Canale[105a,105b], A. Canepa[164a], M. Cano Bret[141], J. Cantero[115], T. Cao[42], M. D. M. Capeans Garrido[32], I. Caprini[28b], M. Caprini[28b], M. Capua[39a,39b], R. M. Carbone[37], R. Cardarelli[134a], F. Cardillo[50], I. Carli[130], T. Carli[32], G. Carlino[105a], L. Carminati[93a,93b], S. Caron[107], E. Carquin[34b], G. D. Carrillo-Montoya[32], J. R. Carter[30], J. Carvalho[127a,127c], D. Casadei[19], M. P. Casado[13,i], M. Casolino[13], D. W. Casper[167], E. Castaneda-Miranda[148a], R. Castelijn[108], A. Castelli[108], V. Castillo Gimenez[171], N. F. Castro[127a,j], A. Catinaccio[32], J. R. Catmore[120], A. Cattai[32], J. Caudron[23], V. Cavaliere[170], E. Cavallaro[13], D. Cavalli[93a], M. Cavalli-Sforza[13], V. Cavasinni[125a,125b], F. Ceradini[135a,135b], L. Cerda Alberich[171], B. C. Cerio[47], A. S. Cerqueira[26b], A. Cerri[152], L. Cerrito[134a,134b], F. Cerutti[16], M. Cerv[32], A. Cervelli[18], S. A. Cetin[20c], A. Chafaq[136a], D. Chakraborty[109], S. K. Chan[58], Y. L. Chan[62a], P. Chang[170], J. D. Chapman[30], D. G. Charlton[19], A. Chatterjee[51], C. C. Chau[162], C. A. Chavez Barajas[152], S. Che[112], S. Cheatham[168a,168c], A. Chegwidden[92], S. Chekanov[6], S. V. Chekulaev[164a], G. A. Chelkov[67,k], M. A. Chelstowska[91], C. Chen[66], H. Chen[27], K. Chen[151], S. Chen[35b], S. Chen[158], X. Chen[35c], Y. Chen[69], H. C. Cheng[91], H. J Cheng[35a], Y. Cheng[33], A. Cheplakov[67], E. Cheremushkina[131], R. Cherkaoui El Moursli[136e], V. Chernyatin[27,*], E. Cheu[7], L. Chevalier[137], V. Chiarella[49], G. Chiarelli[125a,125b], G. Chiodini[75a], A. S. Chisholm[32], A. Chitan[28b], M. V. Chizhov[67], K. Choi[63], A. R. Chomont[36], S. Chouridou[9], B. K. B. Chow[101], V. Christodoulou[80], D. Chromek-Burckhart[32], J. Chudoba[128], A. J. Chuinard[89], J. J. Chwastowski[41], L. Chytka[116], G. Ciapetti[133a,133b], A. K. Ciftci[4a], D. Cinca[45], V. Cindro[77], I. A. Cioara[23], C. Ciocca[22a,22b], A. Ciocio[16], F. Cirotto[105a,105b], Z. H. Citron[176], M. Citterio[93a], M. Ciubancan[28b], A. Clark[51], B. L. Clark[58], M. R. Clark[37], P. J. Clark[48], R. N. Clarke[16], C. Clement[149a,149b], Y. Coadou[87], M. Cobal[168a,168c], A. Coccaro[51], J. Cochran[66], L. Colasurdo[107], B. Cole[37], A. P. Colijn[108], J. Collot[57], T. Colombo[167], G. Compostella[102], P. Conde Muiño[127a,127b], E. Coniavitis[50], S. H. Connell[148b], I. A. Connelly[79], V. Consorti[50], S. Constantinescu[28b], G. Conti[32], F. Conventi[105a,l], M. Cooke[16], B. D. Cooper[80], A. M. Cooper-Sarkar[121], K. J. R. Cormier[162], T. Cornelissen[179], M. Corradi[133a,133b], F. Corriveau[89,m], A. Corso-Radu[167], A. Cortes-Gonzalez[32], G. Cortiana[102], G. Costa[93a], M. J. Costa[171], D. Costanzo[142], G. Cottin[30], G. Cowan[79],

B. E. Cox[86], K. Cranmer[111], S. J. Crawley[55], G. Cree[31], S. Crépé-Renaudin[57], F. Crescioli[82], W. A. Cribbs[149a,149b], M. Crispin Ortuzar[121], M. Cristinziani[23], V. Croft[107], G. Crosetti[39a,39b], A. Cueto[84], T. Cuhadar Donszelmann[142], J. Cummings[180], M. Curatolo[49], J. Cúth[85], H. Czirr[144], P. Czodrowski[3], G. D'amen[22a,22b], S. D'Auria[55], M. D'Onofrio[76], M. J. Da Cunha Sargedas De Sousa[127a,127b], C. Da Via[86], W. Dabrowski[40a], T. Dado[147a], T. Dai[91], O. Dale[15], F. Dallaire[96], C. Dallapiccola[88], M. Dam[38], J. R. Dandoy[33], N. P. Dang[50], A. C. Daniells[19], N. S. Dann[86], M. Danninger[172], M. Dano Hoffmann[137], V. Dao[50], G. Darbo[52a], S. Darmora[8], J. Dassoulas[3], A. Dattagupta[117], W. Davey[23], C. David[173], T. Davidek[130], M. Davies[156], P. Davison[80], E. Dawe[90], I. Dawson[142], K. De[8], R. de Asmundis[105a], A. De Benedetti[114], S. De Castro[22a,22b], S. De Cecco[82], N. De Groot[107], P. de Jong[108], H. De la Torre[92], F. De Lorenzi[66], A. De Maria[56], D. De Pedis[133a], A. De Salvo[133a], U. De Sanctis[152], A. De Santo[152], J. B. De Vivie De Regie[118], W. J. Dearnaley[74], R. Debbe[27], C. Debenedetti[138], D. V. Dedovich[67], N. Dehghanian[3], I. Deigaard[108], M. Del Gaudio[39a,39b], J. Del Peso[84], T. Del Prete[125a,125b], D. Delgove[118], F. Deliot[137], C. M. Delitzsch[51], A. Dell'Acqua[32], L. Dell'Asta[24], M. Dell'Orso[125a,125b], M. Della Pietra[105a,l], D. della Volpe[51], M. Delmastro[5], P. A. Delsart[57], D. A. DeMarco[162], S. Demers[180], M. Demichev[67], A. Demilly[82], S. P. Denisov[131], D. Denysiuk[137], D. Derendarz[41], J. E. Derkaoui[136d], F. Derue[82], P. Dervan[76], K. Desch[23], C. Deterre[44], K. Dette[45], P. O. Deviveiros[32], A. Dewhurst[132], S. Dhaliwal[25], A. Di Ciaccio[134a,134b], L. Di Ciaccio[5], W. K. Di Clemente[123], C. Di Donato[133a,133b], A. Di Girolamo[32], B. Di Girolamo[32], B. Di Micco[135a,135b], R. Di Nardo[32], A. Di Simone[50], R. Di Sipio[162], D. Di Valentino[31], C. Diaconu[87], M. Diamond[162], F. A. Dias[48], M. A. Diaz[34a], E. B. Diehl[91], J. Dietrich[17], S. Díez Cornell[44], A. Dimitrievska[14], J. Dingfelder[23], P. Dita[28b], S. Dita[28b], F. Dittus[32], F. Djama[87], T. Djobava[53b], J. I. Djuvsland[60a], M. A. B. do Vale[26c], D. Dobos[32], M. Dobre[28b], C. Doglioni[83], J. Dolejsi[130], Z. Dolezal[130], M. Donadelli[26d], S. Donati[125a,125b], P. Dondero[122a,122b], J. Donini[36], J. Dopke[132], A. Doria[105a], M. T. Dova[73] , A. T. Doyle[55], E. Drechsler[56], M. Dris[10], Y. Du[140], J. Duarte-Campderros[156], E. Duchovni[176], G. Duckeck[101], O. A. Ducu[96,n], D. Duda[108], A. Dudarev[32], A. Chr. Dudder[85], E. M. Duffield[16], L. Duflot[118], M. Dührssen[32], M. Dumancic[176], M. Dunford[60a], H. Duran Yildiz[4a], M. Düren[54], A. Durglishvili[53b], D. Duschinger[46], B. Dutta[44], M. Dyndal[44], C. Eckardt[44], K. M. Ecker[102], R. C. Edgar[91], N. C. Edwards[48], T. Eifert[32], G. Eigen[15], K. Einsweiler[16], T. Ekelof[169], M. El Kacimi[136c], V. Ellajosyula[87], M. Ellert[169], S. Elles[5], F. Ellinghaus[179], A. A. Elliot[173], N. Ellis[32], J. Elmsheuser[27], M. Elsing[32], D. Emeliyanov[132], Y. Enari[158], O. C. Endner[85], J. S. Ennis[174], J. Erdmann[45], A. Ereditato[18], G. Ernis[179], J. Ernst[2], M. Ernst[27], S. Errede[170], E. Ertel[85], M. Escalier[118], H. Esch[45], C. Escobar[126], B. Esposito[49], A. I. Etienvre[137], E. Etzion[156], H. Evans[63], A. Ezhilov[124], F. Fabbri[22a,22b], L. Fabbri[22a,22b], G. Facini[33], R. M. Fakhrutdinov[131], S. Falciano[133a], R. J. Falla[80], J. Faltova[32], Y. Fang[35a], M. Fanti[93a,93b], A. Farbin[8], A. Farilla[135a], C. Farina[126], E. M. Farina[122a,122b], T. Farooque[13], S. Farrell[16], S. M. Farrington[174], P. Farthouat[32] , F. Fassi[136e], P. Fassnacht[32], D. Fassouliotis[9], M. Faucci Giannelli[79], A. Favareto[52a,52b], W. J. Fawcett[121], L. Fayard[118], O. L. Fedin[124,o], W. Fedorko[172], S. Feigl[120], L. Feligioni[87], C. Feng[140], E. J. Feng[32], H. Feng[91], A. B. Fenyuk[131], L. Feremenga[8], P. Fernandez Martinez[171], S. Fernandez Perez[13], J. Ferrando[44], A. Ferrari[169], P. Ferrari[108], R. Ferrari[122a], D. E. Ferreira de Lima[60b], A. Ferrer[171], D. Ferrere[51], C. Ferretti[91], A. Ferretto Parodi[52a,52b], F. Fiedler[85], A. Filipčič[77], M. Filipuzzi[44], F. Filthaut[107], M. Fincke-Keeler[173], K. D. Finelli[153], M. C. N. Fiolhais[127a,127c], L. Fiorini[171], A. Firan[42], A. Fischer[2], C. Fischer[13], J. Fischer[179], W. C. Fisher[92], N. Flaschel[44], I. Fleck[144], P. Fleischmann[91], G. T. Fletcher[142], R. R. M. Fletcher[123], T. Flick[179], L. R. Flores Castillo[62a], M. J. Flowerdew[102], G. T. Forcolin[86], A. Formica[137], A. Forti[86], A. G. Foster[19], D. Fournier[118], H. Fox[74], S. Fracchia[13], P. Francavilla[82], M. Franchini[22a,22b], D. Francis[32], L. Franconi[120], M. Franklin[58], M. Frate[167], M. Fraternali[122a,122b], D. Freeborn[80], S. M. Fressard-Batraneanu[32], F. Friedrich[46], D. Froidevaux[32], J. A. Frost[121], C. Fukunaga[159], E. Fullana Torregrosa[85], T. Fusayasu[103], J. Fuster[171], C. Gabaldon[57], O. Gabizon[179], A. Gabrielli[22a,22b], A. Gabrielli[16], G. P. Gach[40a], S. Gadatsch[32], S. Gadomski[79], G. Gagliardi[52a,52b], L. G. Gagnon[96], P. Gagnon[63], C. Galea[107], B. Galhardo[127a,127c], E. J. Gallas[121], B. J. Gallop[132], P. Gallus[129], G. Galster[38], K. K. Gan[112], J. Gao[59], Y. Gao[48], Y. S. Gao[146,g], F. M. Garay Walls[48], C. García[171], J. E. García Navarro[171], M. Garcia-Sciveres[16], R. W. Gardner[33], N. Garelli[146], V. Garonne[120], A. Gascon Bravo[44], K. Gasnikova[44], C. Gatti[49], A. Gaudiello[52a,52b], G. Gaudio[122a], L. Gauthier[96], I. L. Gavrilenko[97], C. Gay[172], G. Gaycken[23], E. N. Gazis[10], Z. Gecse[172], C. N. P. Gee[132], Ch. Geich-Gimbel[23], M. Geisen[85], M. P. Geisler[60a], K. Gellerstedt[149a,149b], C. Gemme[52a], M. H. Genest[57], C. Geng[59,p], S. Gentile[133a,133b], C. Gentsos[157], S. George[79], D. Gerbaudo[13], A. Gershon[156], S. Ghasemi[144], M. Ghneimat[23], B. Giacobbe[22a], S. Giagu[133a,133b], P. Giannetti[125a,125b], B. Gibbard[27], S. M. Gibson[79], M. Gignac[172], M. Gilchriese[16], T. P. S. Gillam[30], D. Gillberg[31], G. Gilles[179], D. M. Gingrich[3,d], N. Giokaris[9], M. P. Giordani[168a,168c], F. M. Giorgi[22a], F. M. Giorgi[17], P. F. Giraud[137], P. Giromini[58], D. Giugni[93a], F. Giuli[121], C. Giuliani[102], M. Giulini[60b], B. K. Gjelsten[120], S. Gkaitatzis[157], I. Gkialas[157], E. L. Gkougkousis[118], L. K. Gladilin[100], C. Glasman[84], J. Glatzer[50], P. C. F. Glaysher[48], A. Glazov[44], M. Goblirsch-Kolb[25], J. Godlewski[41], S. Goldfarb[90], T. Golling[51], D. Golubkov[131], A. Gomes[127a,127b,127d], R. Gonçalo[127a], J. Goncalves Pinto Firmino Da Costa[137], G. Gonella[50], L. Gonella[19], A. Gongadze[67], S. González de la Hoz[171], G. Gonzalez Parra[13], S. Gonzalez-Sevilla[51],

L. Goossens[32], P. A. Gorbounov[98], H. A. Gordon[27], I. Gorelov[106], B. Gorini[32], E. Gorini[75a,75b], A. Gorišek[77], E. Gornicki[41], A. T. Goshaw[47], C. Gössling[45], M. I. Gostkin[67], C. R. Goudet[118], D. Goujdami[136c], A. G. Goussiou[139], N. Govender[148b,q], E. Gozani[155], L. Graber[56], I. Grabowska-Bold[40a], P. O. J. Gradin[57], P. Grafström[22a,22b], J. Gramling[51], E. Gramstad[120], S. Grancagnolo[17], V. Gratchev[124], P. M. Gravila[28e], H. M. Gray[32], E. Graziani[135a], Z. D. Greenwood[81,r], C. Grefe[23], K. Gregersen[80], I. M. Gregor[44], P. Grenier[146], K. Grevtsov[5], J. Griffiths[8], A. A. Grillo[138], K. Grimm[74], S. Grinstein[13,s], Ph. Gris[36], J.-F. Grivaz[118], S. Groh[85], J. P. Grohs[46], E. Gross[176], J. Grosse-Knetter[56], G. C. Grossi[81], Z. J. Grout[80], L. Guan[91], W. Guan[177], J. Guenther[64], F. Guescini[51], D. Guest[167], O. Gueta[156], E. Guido[52a,52b], T. Guillemin[5], S. Guindon[2], U. Gul[55], C. Gumpert[32], J. Guo[141], Y. Guo[59,p], R. Gupta[42], S. Gupta[121], G. Gustavino[133a,133b], P. Gutierrez[114], N. G. Gutierrez Ortiz[80], C. Gutschow[46], C. Guyot[137], C. Gwenlan[121], C. B. Gwilliam[76], A. Haas[111], C. Haber[16], H. K. Hadavand[8], N. Haddad[136e], A. Hadef[87], S. Hageböck[23], Z. Hajduk[41], H. Hakobyan[181,*], M. Haleem[44], J. Haley[115], G. Halladjian[92], G. D. Hallewell[87], K. Hamacher[179], P. Hamal[116], K. Hamano[173], A. Hamilton[148a], G. N. Hamity[142], P. G. Hamnett[44], L. Han[59], K. Hanagaki[68,t], K. Hanawa[158], M. Hance[138], B. Haney[123], P. Hanke[60a], R. Hanna[137], J. B. Hansen[38], J. D. Hansen[38], M. C. Hansen[23], P. H. Hansen[38], K. Hara[165], A. S. Hard[177], T. Harenberg[179], F. Hariri[118], S. Harkusha[94], R. D. Harrington[48], P. F. Harrison[174], F. Hartjes[108], N. M. Hartmann[101], M. Hasegawa[69], Y. Hasegawa[143], A. Hasib[114], S. Hassani[137], S. Haug[18], R. Hauser[92], L. Hauswald[46], M. Havranek[128], C. M. Hawkes[19], R. J. Hawkings[32], D. Hayakawa[160], D. Hayden[92], C. P. Hays[121], J. M. Hays[78], H. S. Hayward[76], S. J. Haywood[132], S. J. Head[19], T. Heck[85], V. Hedberg[83], L. Heelan[8], S. Heim[123], T. Heim[16], B. Heinemann[16], J. J. Heinrich[101], L. Heinrich[111], C. Heinz[54], J. Hejbal[128], L. Helary[32], S. Hellman[149a,149b], C. Helsens[32], J. Henderson[121], R. C. W. Henderson[74], Y. Heng[177], S. Henkelmann[172], A. M. Henriques Correia[32], S. Henrot-Versille[118], G. H. Herbert[17], H. Herde[25], V. Herget[178], Y. Hernández Jiménez[171], G. Herten[50], R. Hertenberger[101], L. Hervas[32], G. G. Hesketh[80], N. P. Hessey[108], J. W. Hetherly[42], R. Hickling[78], E. Higón-Rodriguez[171], E. Hill[173], J. C. Hill[30], K. H. Hiller[44], S. J. Hillier[19], I. Hinchliffe[16], E. Hines[123], R. R. Hinman[16], M. Hirose[50], D. Hirschbuehl[179], J. Hobbs[151], N. Hod[164a], M. C. Hodgkinson[142], P. Hodgson[142], A. Hoecker[32], M. R. Hoeferkamp[106], F. Hoenig[101], D. Hohn[23], T. R. Holmes[16], M. Homann[45], T. Honda[68], T. M. Hong[126], B. H. Hooberman[170], W. H. Hopkins[117], Y. Horii[104], A. J. Horton[145], J-Y. Hostachy[57], S. Hou[154], A. Hoummada[136a], J. Howarth[44], J. Hoya[73], M. Hrabovsky[116], I. Hristova[17], J. Hrivnac[118], T. Hryn'ova[5], A. Hrynevich[95], C. Hsu[148c], P. J. Hsu[154,u], S.-C. Hsu[139], D. Hu[37], Q. Hu[59], S. Hu[141], Y. Huang[44], Z. Hubacek[129], F. Hubaut[87], F. Huegging[23], T. B. Huffman[121], E. W. Hughes[37], G. Hughes[74], M. Huhtinen[32], P. Huo[151], N. Huseynov[67,b], J. Huston[92], J. Huth[58], G. Iacobucci[51], G. Iakovidis[27], I. Ibragimov[144], L. Iconomidou-Fayard[118], E. Ideal[180], Z. Idrissi[136e], P. Iengo[32], O. Igonkina[108,v], T. Iizawa[175], Y. Ikegami[68], M. Ikeno[68], Y. Ilchenko[11,w], D. Iliadis[157], N. Ilic[146], T. Ince[102], G. Introzzi[122a,122b], P. Ioannou[9,*], M. Iodice[135a], K. Iordanidou[37], V. Ippolito[58], N. Ishijima[119], M. Ishino[158], M. Ishitsuka[160], R. Ishmukhametov[112], C. Issever[121], S. Istin[20a], F. Ito[165], J. M. Iturbe Ponce[86], R. Iuppa[163a,163b], W. Iwanski[64], H. Iwasaki[68], J. M. Izen[43], V. Izzo[105a], S. Jabbar[3], B. Jackson[123], P. Jackson[1], V. Jain[2], K. B. Jakobi[85], K. Jakobs[50], S. Jakobsen[32], T. Jakoubek[128], D. O. Jamin[115], D. K. Jana[81], R. Jansky[64], J. Janssen[23], M. Janus[56], G. Jarlskog[83], N. Javadov[67,b], T. Javůrek[50], F. Jeanneau[137], L. Jeanty[16], G.-Y. Jeng[153], D. Jennens[90], P. Jenni[50,x], C. Jeske[174], S. Jézéquel[5], H. Ji[177], J. Jia[151], H. Jiang[66], Y. Jiang[59], S. Jiggins[80], J. Jimenez Pena[171], S. Jin[35a], A. Jinaru[28b], O. Jinnouchi[160], H. Jivan[148c], P. Johansson[142], K. A. Johns[7], W. J. Johnson[139], K. Jon-And[149a,149b], G. Jones[174], R. W. L. Jones[74], S. Jones[7], T. J. Jones[76], J. Jongmanns[60a], P. M. Jorge[127a,127b], J. Jovicevic[164a], X. Ju[177], A. Juste Rozas[13,s], M. K. Köhler[176], A. Kaczmarska[41], M. Kado[118], H. Kagan[112], M. Kagan[146], S. J. Kahn[87], T. Kaji[175], E. Kajomovitz[47], C. W. Kalderon[121], A. Kaluza[85], S. Kama[42], A. Kamenshchikov[131], N. Kanaya[158], S. Kaneti[30], L. Kanjir[77], V. A. Kantserov[99], J. Kanzaki[68], B. Kaplan[111], L. S. Kaplan[177], A. Kapliy[33], D. Kar[148c], K. Karakostas[10], A. Karamaoun[3], N. Karastathis[10], M. J. Kareem[56], E. Karentzos[10], M. Karnevskiy[85], S. N. Karpov[67], Z. M. Karpova[67], K. Karthik[111], V. Kartvelishvili[74], A. N. Karyukhin[131], K. Kasahara[165], L. Kashif[177], R. D. Kass[112], A. Kastanas[15], Y. Kataoka[158], C. Kato[158], A. Katre[51], J. Katzy[44], K. Kawade[104], K. Kawagoe[72], T. Kawamoto[158], G. Kawamura[56], V. F. Kazanin[110,c], R. Keeler[173], R. Kehoe[42], J. S. Keller[44], J. J. Kempster[79], H. Keoshkerian[162], O. Kepka[128], B. P. Kerševan[77], S. Kersten[179], R. A. Keyes[89], M. Khader[170], F. Khalil-zada[12], A. Khanov[115], A. G. Kharlamov[110,c], T. Kharlamova[110], T. J. Khoo[51], V. Khovanskiy[98], E. Khramov[67], J. Khubua[53b,y], S. Kido[69], C. R. Kilby[79], H. Y. Kim[8], S. H. Kim[165], Y. K. Kim[33], N. Kimura[157], O. M. Kind[17], B. T. King[76], M. King[171], J. Kirk[132], A. E. Kiryunin[102], T. Kishimoto[158], D. Kisielewska[40a], F. Kiss[50], K. Kiuchi[165], O. Kivernyk[137], E. Kladiva[147b], M. H. Klein[37], M. Klein[76], U. Klein[76], K. Kleinknecht[85], P. Klimek[109], A. Klimentov[27], R. Klingenberg[45], J. A. Klinger[142], T. Klioutchnikova[32], E. -E. Kluge[60a], P. Kluit[108], S. Kluth[102], J. Knapik[41], E. Kneringer[64], E. B. F. G. Knoops[87], A. Knue[55], A. Kobayashi[158], D. Kobayashi[160], T. Kobayashi[158], M. Kobel[46], M. Kocian[146], P. Kodys[130], N. M. Koehler[102], T. Koffas[31], E. Koffeman[108], T. Koi[146], H. Kolanoski[17], M. Kolb[60b], I. Koletsou[5], A. A. Komar[97,*], Y. Komori[158], T. Kondo[68], N. Kondrashova[44], K. Köneke[50], A. C. König[107], T. Kono[68,z], R. Konoplich[111,aa], N. Konstantinidis[80], R. Kopeliansky[63], S. Koperny[40a],

L. Köpke[85], A. K. Kopp[50], K. Korcyl[41], K. Kordas[157], A. Korn[80], A. A. Korol[110,c], I. Korolkov[13], E. V. Korolkova[142], O. Kortner[102], S. Kortner[102], T. Kosek[130], V. V. Kostyukhin[23], A. Kotwal[47], A. Kourkoumeli-Charalampidi[122a,122b], C. Kourkoumelis[9], V. Kouskoura[27], A. B. Kowalewska[41], R. Kowalewski[173], T. Z. Kowalski[40a], C. Kozakai[158], W. Kozanecki[137], A. S. Kozhin[131], V. A. Kramarenko[100], G. Kramberger[77], D. Krasnopevtsev[99], M. W. Krasny[82], A. Krasznahorkay[32], A. Kravchenko[27], M. Kretz[60c], J. Kretzschmar[76], K. Kreutzfeldt[54], P. Krieger[162], K. Krizka[33], K. Kroeninger[45], H. Kroha[102], J. Kroll[123], J. Kroseberg[23], J. Krstic[14], U. Kruchonak[67], H. Krüger[23], N. Krumnack[66], A. Kruse[177], M. C. Kruse[47], M. Kruskal[24], T. Kubota[90], H. Kucuk[80], S. Kuday[4b], J. T. Kuechler[179], S. Kuehn[50], A. Kugel[60c], F. Kuger[178], A. Kuhl[138], T. Kuhl[44], V. Kukhtin[67], R. Kukla[137], Y. Kulchitsky[94], S. Kuleshov[34b], M. Kuna[133a,133b], T. Kunigo[70], A. Kupco[128], H. Kurashige[69], Y. A. Kurochkin[94], V. Kus[128], E. S. Kuwertz[173], M. Kuze[160], J. Kvita[116], T. Kwan[173], D. Kyriazopoulos[142], A. La Rosa[102], J. L. La Rosa Navarro[26d], L. La Rotonda[39a,39b], C. Lacasta[171], F. Lacava[133a,133b], J. Lacey[31], H. Lacker[17], D. Lacour[82], V. R. Lacuesta[171], E. Ladygin[67], R. Lafaye[5], B. Laforge[82], T. Lagouri[180], S. Lai[56], S. Lammers[63], W. Lampl[7], E. Lançon[137], U. Landgraf[50], M. P. J. Landon[78], M. C. Lanfermann[51], V. S. Lang[60a], J. C. Lange[13], A. J. Lankford[167], F. Lanni[27], K. Lantzsch[23], A. Lanza[122a], S. Laplace[82], C. Lapoire[32], J. F. Laporte[137], T. Lari[93a], F. Lasagni Manghi[22a,22b], M. Lassnig[32], P. Laurelli[49], W. Lavrijsen[16], A. T. Law[138], P. Laycock[76], T. Lazovich[58], M. Lazzaroni[93a,93b], B. Le[90], O. Le Dortz[82], E. Le Guirriec[87], E. P. Le Quilleuc[137], M. LeBlanc[173], T. LeCompte[6], F. Ledroit-Guillon[57], C. A. Lee[27], S. C. Lee[154], L. Lee[1], B. Lefebvre[89], G. Lefebvre[82], M. Lefebvre[173], F. Legger[101], C. Leggett[16], A. Lehan[76], G. Lehmann Miotto[32], X. Lei[7], W. A. Leight[31], A. Leisos[157,ab], A. G. Leister[180], M. A. L. Leite[26d], R. Leitner[130], D. Lellouch[176], B. Lemmer[56], K. J. C. Leney[80], T. Lenz[23], B. Lenzi[32], R. Leone[7], S. Leone[125a,125b], C. Leonidopoulos[48], S. Leontsinis[10], G. Lerner[152], C. Leroy[96], A. A. J. Lesage[137], C. G. Lester[30], M. Levchenko[124], J. Levêque[5], D. Levin[91], L. J. Levinson[176], M. Levy[19], D. Lewis[78], A. M. Leyko[23], M. Leyton[43], B. Li[59,p], C. Li[59], H. Li[151], H. L. Li[33], L. Li[47], L. Li[141], Q. Li[35a], S. Li[47], X. Li[86], Y. Li[144], Z. Liang[35a], B. Liberti[134a], A. Liblong[162], P. Lichard[32], K. Lie[170], J. Liebal[23], W. Liebig[15], A. Limosani[153], S. C. Lin[154,ac], T. H. Lin[85], B. E. Lindquist[151], A. E. Lionti[51], E. Lipeles[123], A. Lipniacka[15], M. Lisovyi[60b], T. M. Liss[170], A. Lister[172], A. M. Litke[138], B. Liu[154,ad], D. Liu[154], H. Liu[91], H. Liu[27], J. Liu[87], J. B. Liu[59], K. Liu[87], L. Liu[170], M. Liu[47], M. Liu[59], Y. L. Liu[59], Y. Liu[59], M. Livan[122a,122b], A. Lleres[57], J. Llorente Merino[35a], S. L. Lloyd[78], F. Lo Sterzo[154], E. M. Lobodzinska[44], P. Loch[7], W. S. Lockman[138], F. K. Loebinger[86], A. E. Loevschall-Jensen[38], K. M. Loew[25], A. Loginov[180,*], T. Lohse[17], K. Lohwasser[44], M. Lokajicek[128], B. A. Long[24], J. D. Long[170], R. E. Long[74], L. Longo[75a,75b], K. A. Looper[112], D. Lopez Mateos[58], B. Lopez Paredes[142], I. Lopez Paz[13], A. Lopez Solis[82], J. Lorenz[101], N. Lorenzo Martinez[63], M. Losada[21], P. J. Lösel[101], X. Lou[35a], A. Lounis[118], J. Love[6], P. A. Love[74], H. Lu[62a], N. Lu[91], H. J. Lubatti[139], C. Luci[133a,133b], A. Lucotte[57], C. Luedtke[50], F. Luehring[63], W. Lukas[64], L. Luminari[133a], O. Lundberg[149a,149b], B. Lund-Jensen[150], P. M. Luzi[82], D. Lynn[27], R. Lysak[128], E. Lytken[83], V. Lyubushkin[67], H. Ma[27], L. L. Ma[140], Y. Ma[140], G. Maccarrone[49], A. Macchiolo[102], C. M. Macdonald[142], B. Maček[77], J. Machado Miguens[123,127b], D. Madaffari[87], R. Madar[36], H. J. Maddocks[169], W. F. Mader[46], A. Madsen[44], J. Maeda[69], S. Maeland[15], T. Maeno[27], A. Maevskiy[100], E. Magradze[56], J. Mahlstedt[108], C. Maiani[118], C. Maidantchik[26a], A. A. Maier[102], T. Maier[101], A. Maio[127a,127b,127d], S. Majewski[117], Y. Makida[68], N. Makovec[118], B. Malaescu[82], Pa. Malecki[41], V. P. Maleev[124], F. Malek[57], U. Mallik[65], D. Malon[6], C. Malone[146], C. Malone[30], S. Maltezos[10], S. Malyukov[32], J. Mamuzic[171], G. Mancini[49], L. Mandelli[93a], I. Mandić[77], J. Maneira[127a,127b], L. Manhaes de Andrade Filho[26b], J. Manjarres Ramos[164b], A. Mann[101], A. Manousos[32], B. Mansoulie[137], J. D. Mansour[35a], R. Mantifel[89], M. Mantoani[56], S. Manzoni[93a,93b], L. Mapelli[32], G. Marceca[29], L. March[51], G. Marchiori[82], M. Marcisovsky[128], M. Marjanovic[14], D. E. Marley[91], F. Marroquim[26a], S. P. Marsden[86], Z. Marshall[16], S. Marti-Garcia[171], B. Martin[92], T. A. Martin[174], V. J. Martin[48], B. Martin dit Latour[15], M. Martinez[13,s], V. I. Martinez Outschoorn[170], S. Martin-Haugh[132], V. S. Martoiu[28b], A. C. Martyniuk[80], M. Marx[139], A. Marzin[32], L. Masetti[85], T. Mashimo[158], R. Mashinistov[97], J. Masik[86], A. L. Maslennikov[110,c], I. Massa[22a,22b], L. Massa[22a,22b], P. Mastrandrea[5], A. Mastroberardino[39a,39b], T. Masubuchi[158], P. Mättig[179], J. Mattmann[85], J. Maurer[28b], S. J. Maxfield[76], D. A. Maximov[110,c], R. Mazini[154], S. M. Mazza[93a,93b], N. C. Mc Fadden[106], G. Mc Goldrick[162], S. P. Mc Kee[91], A. McCarn[91], R. L. McCarthy[151], T. G. McCarthy[102], L. I. McClymont[80], E. F. McDonald[90], J. A. Mcfayden[80], G. Mchedlidze[56], S. J. McMahon[132], R. A. McPherson[173,m], M. Medinnis[44], S. Meehan[139], S. Mehlhase[101], A. Mehta[76], K. Meier[60a], C. Meineck[101], B. Meirose[43], D. Melini[171], B. R. Mellado Garcia[148c], M. Melo[147a], F. Meloni[18], A. Mengarelli[22a,22b], S. Menke[102], E. Meoni[166], S. Mergelmeyer[17], P. Mermod[51], L. Merola[105a,105b], C. Meroni[93a], F. S. Merritt[33], A. Messina[133a,133b], J. Metcalfe[6], A. S. Mete[167], C. Meyer[85], C. Meyer[123], J.-P. Meyer[137], J. Meyer[108], H. Meyer Zu Theenhausen[60a], F. Miano[152], R. P. Middleton[132], S. Miglioranzi[52a,52b], L. Mijović[48], G. Mikenberg[176], M. Mikestikova[128], M. Mikuž[77], M. Milesi[90], A. Milic[64], D. W. Miller[33], C. Mills[48], A. Milov[176], D. A. Milstead[149a,149b], A. A. Minaenko[131], Y. Minami[158], I. A. Minashvili[67], A. I. Mincer[111], B. Mindur[40a], M. Mineev[67], Y. Minegishi[158], Y. Ming[177], L. M. Mir[13], K. P. Mistry[123], T. Mitani[175],

J. Mitrevski[101], V. A. Mitsou[171], A. Miucci[18], P. S. Miyagawa[142], J. U. Mjörnmark[83], M. Mlynarikova[130], T. Moa[149a,149b], K. Mochizuki[96], S. Mohapatra[37], S. Molander[149a,149b], R. Moles-Valls[23], R. Monden[70], M. C. Mondragon[92], K. Mönig[44], J. Monk[38], E. Monnier[87], A. Montalbano[151], J. Montejo Berlingen[32], F. Monticelli[73], S. Monzani[93a,93b], R. W. Moore[3], N. Morange[118], D. Moreno[21], M. Moreno Llácer[56], P. Morettini[52a], S. Morgenstern[32], D. Mori[145], T. Mori[158], M. Morii[58], M. Morinaga[158], V. Morisbak[120], S. Moritz[85], A. K. Morley[153], G. Mornacchi[32], J. D. Morris[78], S. S. Mortensen[38], L. Morvaj[151], M. Mosidze[53b], J. Moss[146,ae], K. Motohashi[160], R. Mount[146], E. Mountricha[27], E. J. W. Moyse[88], S. Muanza[87], R. D. Mudd[19], F. Mueller[102], J. Mueller[126], R. S. P. Mueller[101], T. Mueller[30], D. Muenstermann[74], P. Mullen[55], G. A. Mullier[18], F. J. Munoz Sanchez[86], J. A. Murillo Quijada[19], W. J. Murray[174,132], H. Musheghyan[56], M. Muškinja[77], A. G. Myagkov[131,af], M. Myska[129], B. P. Nachman[146], O. Nackenhorst[51], K. Nagai[121], R. Nagai[68,z], K. Nagano[68], Y. Nagasaka[61], K. Nagata[165], M. Nagel[50], E. Nagy[87], A. M. Nairz[32], Y. Nakahama[104], K. Nakamura[68], T. Nakamura[158], I. Nakano[113], H. Namasivayam[43], R. F. Naranjo Garcia[44], R. Narayan[11], D. I. Narrias Villar[60a], I. Naryshkin[124], T. Naumann[44], G. Navarro[21], R. Nayyar[7], H. A. Neal[91], P. Yu. Nechaeva[97], T. J. Neep[86], A. Negri[122a,122b], M. Negrini[22a], S. Nektarijevic[107], C. Nellist[118], A. Nelson[167], S. Nemecek[128], P. Nemethy[111], A. A. Nepomuceno[26a], M. Nessi[32,ag], M. S. Neubauer[170], M. Neumann[179], R. M. Neves[111], P. Nevski[27], P. R. Newman[19], D. H. Nguyen[6], T. Nguyen Manh[96], R. B. Nickerson[121], R. Nicolaidou[137], J. Nielsen[138], A. Nikiforov[17], V. Nikolaenko[131,af], I. Nikolic-Audit[82], K. Nikolopoulos[19], J. K. Nilsen[120], P. Nilsson[27], Y. Ninomiya[158], A. Nisati[133a], R. Nisius[102], T. Nobe[158], M. Nomachi[119], I. Nomidis[31], T. Nooney[78], S. Norberg[114], M. Nordberg[32], N. Norjoharuddeen[121], O. Novgorodova[46], S. Nowak[102], M. Nozaki[68], L. Nozka[116], K. Ntekas[167], E. Nurse[80], F. Nuti[90], F. O'grady[7], D. C. O'Neil[145], A. A. O'Rourke[44], V. O'Shea[55], F. G. Oakham[31,d], H. Oberlack[102], T. Obermann[23], J. Ocariz[82], A. Ochi[69], I. Ochoa[37], J. P. Ochoa-Ricoux[34a], S. Oda[72], S. Odaka[68], H. Ogren[63], A. Oh[86], S. H. Oh[47], C. C. Ohm[16], H. Ohman[169], H. Oide[32], H. Okawa[165], Y. Okumura[158], T. Okuyama[68], A. Olariu[28b], L. F. Oleiro Seabra[127a], S. A. Olivares Pino[48], D. Oliveira Damazio[27], A. Olszewski[41], J. Olszowska[41], A. Onofre[127a,127e], K. Onogi[104], P. U. E. Onyisi[11,w], M. J. Oreglia[33], Y. Oren[156], D. Orestano[135a,135b], N. Orlando[62b], R. S. Orr[162], B. Osculati[52a,52b,*], R. Ospanov[86], G. Otero y Garzon[29], H. Otono[72], M. Ouchrif[136d], F. Ould-Saada[120], A. Ouraou[137], K. P. Oussoren[108], Q. Ouyang[35a], M. Owen[55], R. E. Owen[19], V. E. Ozcan[20a], N. Ozturk[8], K. Pachal[145], A. Pacheco Pages[13], L. Pacheco Rodriguez[137], C. Padilla Aranda[13], M. Pagáčová[50], S. Pagan Griso[16], M. Paganini[180], F. Paige[27], P. Pais[88], K. Pajchel[120], G. Palacino[164b], S. Palazzo[39a,39b], S. Palestini[32], M. Palka[40b], D. Pallin[36], E. St. Panagiotopoulou[10], C. E. Pandini[82], J. G. Panduro Vazquez[79], P. Pani[149a,149b], S. Panitkin[27], D. Pantea[28b], L. Paolozzi[51], Th. D. Papadopoulou[10], K. Papageorgiou[157], A. Paramonov[6], D. Paredes Hernandez[180], A. J. Parker[74], M. A. Parker[30], K. A. Parker[142], F. Parodi[52a,52b], J. A. Parsons[37], U. Parzefall[50], V. R. Pascuzzi[162], E. Pasqualucci[133a], S. Passaggio[52a], Fr. Pastore[79], G. Pásztor[31,ah], S. Pataraia[179], J. R. Pater[86], T. Pauly[32], J. Pearce[173], B. Pearson[114], L. E. Pedersen[38], M. Pedersen[120], S. Pedraza Lopez[171], R. Pedro[127a,127b], S. V. Peleganchuk[110,c], O. Penc[128], C. Peng[35a], H. Peng[59], J. Penwell[63], B. S. Peralva[26b], M. M. Perego[137], D. V. Perepelitsa[27], E. Perez Codina[164a], L. Perini[93a,93b], H. Pernegger[32], S. Perrella[105a,105b], R. Peschke[44], V. D. Peshekhonov[67], K. Peters[44], R. F. Y. Peters[86], B. A. Petersen[32], T. C. Petersen[38], E. Petit[57], A. Petridis[1], C. Petridou[157], P. Petroff[118], E. Petrolo[133a], M. Petrov[121], F. Petrucci[135a,135b], N. E. Pettersson[88], A. Peyaud[137], R. Pezoa[34b], P. W. Phillips[132], G. Piacquadio[146,ai], E. Pianori[174], A. Picazio[88], E. Piccaro[78], M. Piccinini[22a,22b], M. A. Pickering[121], R. Piegaia[29], J. E. Pilcher[33], A. D. Pilkington[86], A. W. J. Pin[86], M. Pinamonti[168a168c,aj], J. L. Pinfold[3], A. Pingel[38], S. Pires[82], H. Pirumov[44], M. Pitt[176], L. Plazak[147a], M.-A. Pleier[27], V. Pleskot[85], E. Plotnikova[67], P. Plucinski[92], D. Pluth[66], R. Poettgen[149a,149b], L. Poggioli[118], D. Pohl[23], G. Polesello[122a], A. Poley[44], A. Policicchio[39a,39b], R. Polifka[162], A. Polini[22a], C. S. Pollard[55], V. Polychronakos[27], K. Pommès[32], L. Pontecorvo[133a], B. G. Pope[92], G. A. Popeneciu[28c], A. Poppleton[32], S. Pospisil[129], K. Potamianos[16], I. N. Potrap[67], C. J. Potter[30], C. T. Potter[117], G. Poulard[32], J. Poveda[32], V. Pozdnyakov[67], M. E. Pozo Astigarraga[32], P. Pralavorio[87], A. Pranko[16], S. Prell[66], D. Price[86], L. E. Price[6], M. Primavera[75a], S. Prince[89], K. Prokofiev[62c], F. Prokoshin[34b], S. Protopopescu[27], J. Proudfoot[6], M. Przybycien[40a], D. Puddu[135a,135b], M. Purohit[27,ak], P. Puzo[118], J. Qian[91], G. Qin[55], Y. Qin[86], A. Quadt[56], W. B. Quayle[168a,168b], M. Queitsch-Maitland[86], D. Quilty[55], S. Raddum[120], V. Radeka[27], V. Radescu[121], S. K. Radhakrishnan[151], P. Radloff[117], P. Rados[90], F. Ragusa[93a,93b], G. Rahal[182], J. A. Raine[86], S. Rajagopalan[27], M. Rammensee[32], C. Rangel-Smith[169], M. G. Ratti[93a,93b], F. Rauscher[101], S. Rave[85], T. Ravenscroft[55], I. Ravinovich[176], M. Raymond[32], A. L. Read[120], N. P. Readioff[76], M. Reale[75a,75b], D. M. Rebuzzi[122a,122b], A. Redelbach[178], G. Redlinger[27], R. Reece[138], K. Reeves[43], L. Rehnisch[17], J. Reichert[123], A. Reiss[85], C. Rembser[32], H. Ren[35a], M. Rescigno[133a], S. Resconi[93a], O. L. Rezanova[110,c], P. Reznicek[130], R. Rezvani[96], R. Richter[102], S. Richter[80], E. Richter-Was[40b], O. Ricken[23], M. Ridel[82], P. Rieck[17], C. J. Riegel[179], J. Rieger[56], O. Rifki[114], M. Rijssenbeek[151], A. Rimoldi[122a,122b], M. Rimoldi[18], L. Rinaldi[22a], B. Ristić[51], E. Ritsch[32], I. Riu[13], F. Rizatdinova[115], E. Rizvi[78], C. Rizzi[13], S. H. Robertson[89,m], A. Robichaud-Veronneau[89], D. Robinson[30], J. E. M. Robinson[44], A. Robson[55],

C. Roda[125a,125b], Y. Rodina[87], A. Rodriguez Perez[13], D. Rodriguez Rodriguez[171], S. Roe[32], C. S. Rogan[58], O. Røhne[120], A. Romaniouk[99], M. Romano[22a,22b], S. M. Romano Saez[36], E. Romero Adam[171], N. Rompotis[139], M. Ronzani[50], L. Roos[82], E. Ros[171], S. Rosati[133a], K. Rosbach[50], P. Rose[138], N.-A. Rosien[56], V. Rossetti[149a,149b], E. Rossi[105a,105b], L. P. Rossi[52a], J. H. N. Rosten[30], R. Rosten[139], M. Rotaru[28b], I. Roth[176], J. Rothberg[139], D. Rousseau[118], A. Rozanov[87], Y. Rozen[155], X. Ruan[148c], F. Rubbo[146], M. S. Rudolph[162], F. Rühr[50], A. Ruiz-Martinez[31], Z. Rurikova[50], N. A. Rusakovich[67], A. Ruschke[101], H. L. Russell[139], J. P. Rutherfoord[7], N. Ruthmann[32], Y. F. Ryabov[124], M. Rybar[170], G. Rybkin[118], S. Ryu[6], A. Ryzhov[131], G. F. Rzehorz[56], A. F. Saavedra[153], G. Sabato[108], S. Sacerdoti[29], H. F-W. Sadrozinski[138], R. Sadykov[67], F. Safai Tehrani[133a], P. Saha[109], M. Sahinsoy[60a], M. Saimpert[137], T. Saito[158], H. Sakamoto[158], Y. Sakurai[175], G. Salamanna[135a,135b], A. Salamon[134a,134b], J. E. Salazar Loyola[34b], D. Salek[108], P. H. Sales De Bruin[139], D. Salihagic[102], A. Salnikov[146], J. Salt[171], D. Salvatore[39a,39b], F. Salvatore[152], A. Salvucci[62a,62b,62c], A. Salzburger[32], D. Sammel[50], D. Sampsonidis[157], A. Sanchez[105a,105b], J. Sánchez[171], V. Sanchez Martinez[171], H. Sandaker[120], R. L. Sandbach[78], H. G. Sander[85], M. Sandhoff[179], C. Sandoval[21], D. P. C. Sankey[132], M. Sannino[52a,52b], A. Sansoni[49], C. Santoni[36], R. Santonico[134a,134b], H. Santos[127a], I. Santoyo Castillo[152], K. Sapp[126], A. Sapronov[67], J. G. Saraiva[127a,127d], B. Sarrazin[23], O. Sasaki[68], K. Sato[165], E. Sauvan[5], G. Savage[79], P. Savard[162,d], N. Savic[102], C. Sawyer[132], L. Sawyer[81,r], J. Saxon[33], C. Sbarra[22a], A. Sbrizzi[22a,22b], T. Scanlon[80], D. A. Scannicchio[167], M. Scarcella[153], V. Scarfone[39a,39b], J. Schaarschmidt[176], P. Schacht[102], B. M. Schachtner[101], D. Schaefer[32], L. Schaefer[123], R. Schaefer[44], J. Schaeffer[85], S. Schaepe[23], S. Schaetzel[60b], U. Schäfer[85], A. C. Schaffer[118], D. Schaile[101], R. D. Schamberger[151], V. Scharf[60a], V. A. Schegelsky[124], D. Scheirich[130], M. Schernau[167], C. Schiavi[52a,52b], S. Schier[138], C. Schillo[50], M. Schioppa[39a,39b], S. Schlenker[32], K. R. Schmidt-Sommerfeld[102], K. Schmieden[32], C. Schmitt[85], S. Schmitt[44], S. Schmitz[85], B. Schneider[164a], U. Schnoor[50], L. Schoeffel[137], A. Schoening[60b], B. D. Schoenrock[92], E. Schopf[23], M. Schott[85], J. F. P. Schouwenberg[107], J. Schovancova[8], S. Schramm[51], M. Schreyer[178], N. Schuh[85], A. Schulte[85], M. J. Schultens[23], H.-C. Schultz-Coulon[60a], H. Schulz[17], M. Schumacher[50], B. A. Schumm[138], Ph. Schune[137], A. Schwartzman[146], T. A. Schwarz[91], H. Schweiger[86], Ph. Schwemling[137], R. Schwienhorst[92], J. Schwindling[137], T. Schwindt[23], G. Sciolla[25], F. Scuri[125a,125b], F. Scutti[90], J. Searcy[91], P. Seema[23], S. C. Seidel[106], A. Seiden[138], F. Seifert[129], J. M. Seixas[26a], G. Sekhniaidze[105a], K. Sekhon[91], S. J. Sekula[42], D. M. Seliverstov[124,*], N. Semprini-Cesari[22a,22b], C. Serfon[120], L. Serin[118], L. Serkin[168a,168b], M. Sessa[135a,135b], R. Seuster[173], H. Severini[114], T. Sfiligoj[77], F. Sforza[32], A. Sfyrla[51], E. Shabalina[56], N. W. Shaikh[149a,149b], L. Y. Shan[35a], R. Shang[170], J. T. Shank[24], M. Shapiro[16], P. B. Shatalov[98], K. Shaw[168a,168b], S. M. Shaw[86], A. Shcherbakova[149a,149b], C. Y. Shehu[152], P. Sherwood[80], L. Shi[154,al], S. Shimizu[69], C. O. Shimmin[167], M. Shimojima[103], S. Shirabe[72], M. Shiyakova[67,am], A. Shmeleva[97], D. Shoaleh Saadi[96], M. J. Shochet[33], S. Shojaii[93a,93b], D. R. Shope[114], S. Shrestha[112], E. Shulga[99], M. A. Shupe[7], P. Sicho[128], A. M. Sickles[170], P. E. Sidebo[150], O. Sidiropoulou[178], D. Sidorov[115], A. Sidoti[22a,22b], F. Siegert[46], Dj. Sijacki[14], J. Silva[127a,127d], S. B. Silverstein[149a], V. Simak[129], Lj. Simic[14], S. Simion[118], E. Simioni[85], B. Simmons[80], D. Simon[36], M. Simon[85], P. Sinervo[162], N. B. Sinev[117], M. Sioli[22a,22b], G. Siragusa[178], S. Yu. Sivoklokov[100], J. Sjölin[149a,149b], M. B. Skinner[74], H. P. Skottowe[58], P. Skubic[114], M. Slater[19], T. Slavicek[129], M. Slawinska[108], K. Sliwa[166], R. Slovak[130], V. Smakhtin[176], B. H. Smart[5], L. Smestad[15], J. Smiesko[147a], S. Yu. Smirnov[99], Y. Smirnov[99], L. N. Smirnova[100,an], O. Smirnova[83], M. N. K. Smith[37], R. W. Smith[37], M. Smizanska[74], K. Smolek[129], A. A. Snesarev[97], I. M. Snyder[117], S. Snyder[27], R. Sobie[173,m], F. Socher[46], A. Soffer[156], D. A. Soh[154], G. Sokhrannyi[77], C. A. Solans Sanchez[32], M. Solar[129], E. Yu. Soldatov[99], U. Soldevila[171], A. A. Solodkov[131], A. Soloshenko[67], O. V. Solovyanov[131], V. Solovyev[124], P. Sommer[50], H. Son[166], H. Y. Song[59,ao], A. Sood[16], A. Sopczak[129], V. Sopko[129], V. Sorin[13], D. Sosa[60b], C. L. Sotiropoulou[125a,125b], R. Soualah[168a,168c], A. M. Soukharev[110,c], D. South[44], B. C. Sowden[79], S. Spagnolo[75a,75b], M. Spalla[125a,125b], M. Spangenberg[174], F. Spanò[79], D. Sperlich[17], F. Spettel[102], R. Spighi[22a], G. Spigo[32], L. A. Spiller[90], M. Spousta[130], R. D. St. Denis[55,*], A. Stabile[93a], R. Stamen[60a], S. Stamm[17], E. Stanecka[41], R. W. Stanek[6], C. Stanescu[135a], M. Stanescu-Bellu[44], M. M. Stanitzki[44], S. Stapnes[120], E. A. Starchenko[131], G. H. Stark[33], J. Stark[57], P. Staroba[128], P. Starovoitov[60a], S. Stärz[32], R. Staszewski[41], P. Steinberg[27], B. Stelzer[145], H. J. Stelzer[32], O. Stelzer-Chilton[164a], H. Stenzel[54], G. A. Stewart[55], J. A. Stillings[23], M. C. Stockton[89], M. Stoebe[89], G. Stoicea[28b], P. Stolte[56], S. Stonjek[102], A. R. Stradling[8], A. Straessner[46], M. E. Stramaglia[18], J. Strandberg[150], S. Strandberg[149a,149b], A. Strandlie[120], M. Strauss[114], P. Strizenec[147b], R. Ströhmer[178], D. M. Strom[117], R. Stroynowski[42], A. Strubig[107], S. A. Stucci[27], B. Stugu[15], N. A. Styles[44], D. Su[146], J. Su[126], S. Suchek[60a], Y. Sugaya[119], M. Suk[129], V. V. Sulin[97], S. Sultansoy[4c], T. Sumida[70], S. Sun[58], X. Sun[35a], J. E. Sundermann[50], K. Suruliz[152], G. Susinno[39a,39b], M. R. Sutton[152], S. Suzuki[68], M. Svatos[128], M. Swiatlowski[33], I. Sykora[147a], T. Sykora[130], D. Ta[50], C. Taccini[135a,135b], K. Tackmann[44], J. Taenzer[162], A. Taffard[167], R. Tafirout[164a], N. Taiblum[156], H. Takai[27], R. Takashima[71], T. Takeshita[143], Y. Takubo[68], M. Talby[87], A. A. Talyshev[110,c], K. G. Tan[90], J. Tanaka[158], M. Tanaka[160], R. Tanaka[118], S. Tanaka[68], R. Tanioka[69], B. B. Tannenwald[112], S. Tapia Araya[34b], S. Tapprogge[85], S. Tarem[155], G. F. Tartarelli[93a], P. Tas[130], M. Tasevsky[128], T. Tashiro[70], E. Tassi[39a,39b], A. Tavares Delgado[127a,127b], Y. Tayalati[136e], A. C. Taylor[106], G. N. Taylor[90],

P. T. E. Taylor[90], W. Taylor[164b], F. A. Teischinger[32], P. Teixeira-Dias[79], K. K. Temming[50], D. Temple[145], H. Ten Kate[32], P. K. Teng[154], J. J. Teoh[119], F. Tepel[179], S. Terada[68], K. Terashi[158], J. Terron[84], S. Terzo[13], M. Testa[49], R. J. Teuscher[162,m], T. Theveneaux-Pelzer[87], J. P. Thomas[19], J. Thomas-Wilsker[79], E. N. Thompson[37], P. D. Thompson[19], A. S. Thompson[55], L. A. Thomsen[180], E. Thomson[123], M. Thomson[30], M. J. Tibbetts[16], R. E. Ticse Torres[87], V. O. Tikhomirov[97,ap], Yu. A. Tikhonov[110,c], S. Timoshenko[99], P. Tipton[180], S. Tisserant[87], K. Todome[160], T. Todorov[5,*], S. Todorova-Nova[130], J. Tojo[72], S. Tokár[147a], K. Tokushuku[68], E. Tolley[58], L. Tomlinson[86], M. Tomoto[104], L. Tompkins[146,aq], K. Toms[106], B. Tong[58], P. Tornambe[50], E. Torrence[117], H. Torres[145], E. Torró Pastor[139], J. Toth[87,ar], F. Touchard[87], D. R. Tovey[142], T. Trefzger[178], A. Tricoli[27], I. M. Trigger[164a], S. Trincaz-Duvoid[82], M. F. Tripiana[13], W. Trischuk[162], B. Trocmé[57], A. Trofymov[44], C. Troncon[93a], M. Trottier-McDonald[16], M. Trovatelli[173], L. Truong[168a,168c], M. Trzebinski[41], A. Trzupek[41], J. C-L. Tseng[121], P. V. Tsiareshka[94], G. Tsipolitis[10], N. Tsirintanis[9], S. Tsiskaridze[13], V. Tsiskaridze[50], E. G. Tskhadadze[53a], K. M. Tsui[62a], I. I. Tsukerman[98], V. Tsulaia[16], S. Tsuno[68], D. Tsybychev[151], Y. Tu[62b], A. Tudorache[28b], V. Tudorache[28b], A. N. Tuna[58], S. A. Tupputi[22a,22b], S. Turchikhin[67], D. Turecek[129], D. Turgeman[176], R. Turra[93a,93b], P. M. Tuts[37], M. Tyndel[132], G. Ucchielli[22a,22b], I. Ueda[158], M. Ughetto[149a,149b], F. Ukegawa[165], G. Unal[32], A. Undrus[27], G. Unel[167], F. C. Ungaro[90], Y. Unno[68], C. Unverdorben[101], J. Urban[147b], P. Urquijo[90], P. Urrejola[85], G. Usai[8], L. Vacavant[87], V. Vacek[129], B. Vachon[89], C. Valderanis[101], E. Valdes Santurio[149a,149b], N. Valencic[108], S. Valentinetti[22a,22b], A. Valero[171], L. Valery[13], S. Valkar[130], J. A. Valls Ferrer[171], W. Van Den Wollenberg[108], P. C. Van Der Deijl[108], H. van der Graaf[108], N. van Eldik[155], P. van Gemmeren[6], J. Van Nieuwkoop[145], I. van Vulpen[108], M. C. van Woerden[32], M. Vanadia[133a,133b], W. Vandelli[32], R. Vanguri[123], A. Vaniachine[161], P. Vankov[108], G. Vardanyan[181], R. Vari[133a], E. W. Varnes[7], T. Varol[42], D. Varouchas[82], A. Vartapetian[8], K. E. Varvell[153], J. G. Vasquez[180], G. A. Vasquez[34b], F. Vazeille[36], T. Vazquez Schroeder[89], J. Veatch[56], V. Veeraraghavan[7], L. M. Veloce[162], F. Veloso[127a,127c], S. Veneziano[133a], A. Ventura[75a,75b], M. Venturi[173], N. Venturi[162], A. Venturini[25], V. Vercesi[122a], M. Verducci[133a,133b], W. Verkerke[108], J. C. Vermeulen[108], A. Vest[46,as], M. C. Vetterli[145,d], O. Viazlo[83], I. Vichou[170,*], T. Vickey[142], O. E. Vickey Boeriu[142], G. H. A. Viehhauser[121], S. Viel[16], L. Vigani[121], M. Villa[22a,22b], M. Villaplana Perez[93a,93b], E. Vilucchi[49], M. G. Vincter[31], V. B. Vinogradov[67], C. Vittori[22a,22b], I. Vivarelli[152], S. Vlachos[10], M. Vlasak[129], M. Vogel[179], P. Vokac[129], G. Volpi[125a,125b], M. Volpi[90], H. von der Schmitt[102], E. von Toerne[23], V. Vorobel[130], K. Vorobev[99], M. Vos[171], R. Voss[32], J. H. Vossebeld[76], N. Vranjes[14], M. Vranjes Milosavljevic[14], V. Vrba[128], M. Vreeswijk[108], R. Vuillermet[32], I. Vukotic[33], Z. Vykydal[129], P. Wagner[23], W. Wagner[179], H. Wahlberg[73], S. Wahrmund[46], J. Wakabayashi[104], J. Walder[74], R. Walker[101], W. Walkowiak[144], V. Wallangen[149a,149b], C. Wang[35b], C. Wang[140,87], F. Wang[177], H. Wang[16], H. Wang[42], J. Wang[44], J. Wang[153], K. Wang[89], R. Wang[6], S. M. Wang[154], T. Wang[23], T. Wang[37], W. Wang[59], X. Wang[180], C. Wanotayaroj[117], A. Warburton[89], C. P. Ward[30], D. R. Wardrope[80], A. Washbrook[48], P. M. Watkins[19], A. T. Watson[19], M. F. Watson[19], G. Watts[139], S. Watts[86], B. M. Waugh[80], S. Webb[85], M. S. Weber[18], S. W. Weber[178], S. A. Weber[31], J. S. Webster[6], A. R. Weidberg[121], B. Weinert[63], J. Weingarten[56], C. Weiser[50], H. Weits[108], P. S. Wells[32], T. Wenaus[27], T. Wengler[32], S. Wenig[32], N. Wermes[23], M. Werner[50], M. D. Werner[66], P. Werner[32], M. Wessels[60a], J. Wetter[166], K. Whalen[117], N. L. Whallon[139], A. M. Wharton[74], A. White[8], M. J. White[1], R. White[34b], D. Whiteson[167], F. J. Wickens[132], W. Wiedenmann[177], M. Wielers[132], C. Wiglesworth[38], L. A. M. Wiik-Fuchs[23], A. Wildauer[102], F. Wilk[86], H. G. Wilkens[32], H. H. Williams[123], S. Williams[108], C. Willis[92], S. Willocq[88], J. A. Wilson[19], I. Wingerter-Seez[5], F. Winklmeier[117], O. J. Winston[152], B. T. Winter[23], M. Wittgen[146], J. Wittkowski[101], T. M. H. Wolf[108], M. W. Wolter[41], H. Wolters[127a,127c], S. D. Worm[132], B. K. Wosiek[41], J. Wotschack[32], M. J. Woudstra[86], K. W. Wozniak[41], M. Wu[57], M. Wu[33], S. L. Wu[177], X. Wu[51], Y. Wu[91], T. R. Wyatt[86], B. M. Wynne[48], S. Xella[38], D. Xu[35a], L. Xu[27], B. Yabsley[153], S. Yacoob[148a], D. Yamaguchi[160], Y. Yamaguchi[119], A. Yamamoto[68], S. Yamamoto[158], T. Yamanaka[158], K. Yamauchi[104], Y. Yamazaki[69], Z. Yan[24], H. Yang[141], H. Yang[177], Y. Yang[154], Z. Yang[15], W-M. Yao[16], Y. C. Yap[82], Y. Yasu[68], E. Yatsenko[5], K. H. Yau Wong[23], J. Ye[42], S. Ye[27], I. Yeletskikh[67], A. L. Yen[58], E. Yildirim[85], K. Yorita[175], R. Yoshida[6], K. Yoshihara[123], C. Young[146], C. J. S. Young[32], S. Youssef[24], D. R. Yu[16], J. Yu[8], J. M. Yu[91], J. Yu[66], L. Yuan[69], S. P. Y. Yuen[23], I. Yusuff[30,at], B. Zabinski[41], R. Zaidan[65], A. M. Zaitsev[131,af], N. Zakharchuk[44], J. Zalieckas[15], A. Zaman[151], S. Zambito[58], L. Zanello[133a,133b], D. Zanzi[90], C. Zeitnitz[179], M. Zeman[129], A. Zemla[40a], J. C. Zeng[170], Q. Zeng[146], K. Zengel[25], O. Zenin[131], T. Ženiš[147a], D. Zerwas[118], D. Zhang[91], F. Zhang[177], G. Zhang[59,ao], H. Zhang[35b], J. Zhang[6], L. Zhang[50], R. Zhang[23], R. Zhang[59,au], X. Zhang[140], Z. Zhang[118], X. Zhao[42], Y. Zhao[140], Z. Zhao[59], A. Zhemchugov[67], J. Zhong[121], B. Zhou[91], C. Zhou[47], L. Zhou[37], L. Zhou[42], M. Zhou[151], N. Zhou[35c], C. G. Zhu[140], H. Zhu[35a], J. Zhu[91], Y. Zhu[59], X. Zhuang[35a], K. Zhukov[97], A. Zibell[178], D. Zieminska[63], N. I. Zimine[67], C. Zimmermann[85], S. Zimmermann[50], Z. Zinonos[56], M. Zinser[85], M. Ziolkowski[144], L. Živković[14], G. Zobernig[177], A. Zoccoli[22a,22b], M. zur Nedden[17], L. Zwalinski[32]

[1] Department of Physics, University of Adelaide, Adelaide, Australia
[2] Physics Department, SUNY Albany, Albany, NY, USA
[3] Department of Physics, University of Alberta, Edmonton, AB, Canada
[4] [(a)]Department of Physics, Ankara University, Ankara, Turkey; [(b)]Istanbul Aydin University, Istanbul, Turkey; [(c)]Division of Physics, TOBB University of Economics and Technology, Ankara, Turkey
[5] LAPP, CNRS/IN2P3 and Université Savoie Mont Blanc, Annecy-le-Vieux, France
[6] High Energy Physics Division, Argonne National Laboratory, Argonne, IL, USA
[7] Department of Physics, University of Arizona, Tucson, AZ, USA
[8] Department of Physics, The University of Texas at Arlington, Arlington, TX, USA
[9] Physics Department, University of Athens, Athens, Greece
[10] Physics Department, National Technical University of Athens, Zografou, Greece
[11] Department of Physics, The University of Texas at Austin, Austin, TX, USA
[12] Institute of Physics, Azerbaijan Academy of Sciences, Baku, Azerbaijan
[13] Institut de Física d'Altes Energies (IFAE), The Barcelona Institute of Science and Technology, Barcelona, Spain
[14] Institute of Physics, University of Belgrade, Belgrade, Serbia
[15] Department for Physics and Technology, University of Bergen, Bergen, Norway
[16] Physics Division, Lawrence Berkeley National Laboratory and University of California, Berkeley, CA, USA
[17] Department of Physics, Humboldt University, Berlin, Germany
[18] Albert Einstein Center for Fundamental Physics and Laboratory for High Energy Physics, University of Bern, Bern, Switzerland
[19] School of Physics and Astronomy, University of Birmingham, Birmingham, UK
[20] [(a)]Department of Physics, Bogazici University, Istanbul, Turkey; [(b)]Department of Physics Engineering, Gaziantep University, Gaziantep, Turkey; [(c)]Faculty of Engineering and Natural Sciences, Istanbul Bilgi University, Istanbul, Turkey; [(d)]Faculty of Engineering and Natural Sciences, Bahcesehir University, Istanbul, Turkey
[21] Centro de Investigaciones, Universidad Antonio Narino, Bogotá, Colombia
[22] [(a)]INFN Sezione di Bologna, Bologna, Italy; [(b)]Dipartimento di Fisica e Astronomia, Università di Bologna, Bologna, Italy
[23] Physikalisches Institut, University of Bonn, Bonn, Germany
[24] Department of Physics, Boston University, Boston, MA, USA
[25] Department of Physics, Brandeis University, Waltham, MA, USA
[26] [(a)]Universidade Federal do Rio De Janeiro COPPE/EE/IF, Rio de Janeiro, Brazil; [(b)]Electrical Circuits Department, Federal University of Juiz de Fora (UFJF), Juiz de Fora, Brazil; [(c)]Federal University of Sao Joao del Rei (UFSJ), Sao Joao del Rei, Brazil; [(d)]Instituto de Fisica, Universidade de Sao Paulo, Sao Paulo, Brazil
[27] Physics Department, Brookhaven National Laboratory, Upton, NY, USA
[28] [(a)]Transilvania University of Brasov, Brasov, Romania; [(b)]National Institute of Physics and Nuclear Engineering, Bucharest, Romania; [(c)]Physics Department, National Institute for Research and Development of Isotopic and Molecular Technologies, Cluj Napoca, Romania; [(d)]University Politehnica Bucharest, Bucharest, Romania; [(e)]West University in Timisoara, Timisoara, Romania
[29] Departamento de Física, Universidad de Buenos Aires, Buenos Aires, Argentina
[30] Cavendish Laboratory, University of Cambridge, Cambridge, UK
[31] Department of Physics, Carleton University, Ottawa, ON, Canada
[32] CERN, Geneva, Switzerland
[33] Enrico Fermi Institute, University of Chicago, Chicago, IL, USA
[34] [(a)]Departamento de Física, Pontificia Universidad Católica de Chile, Santiago, Chile; [(b)]Departamento de Física, Universidad Técnica Federico Santa María, Valparaiso, Chile
[35] [(a)]Institute of High Energy Physics, Chinese Academy of Sciences, Beijing, China; [(b)]Department of Physics, Nanjing University, Jiangsu, China; [(c)]Physics Department, Tsinghua University, Beijing 100084, China
[36] Laboratoire de Physique Corpusculaire, Clermont Université and Université Blaise Pascal and CNRS/IN2P3, Clermont-Ferrand, France
[37] Nevis Laboratory, Columbia University, Irvington, NY, USA
[38] Niels Bohr Institute, University of Copenhagen, Kobenhavn, Denmark
[39] [(a)]INFN Gruppo Collegato di Cosenza, Laboratori Nazionali di Frascati, Frascati, Italy; [(b)]Dipartimento di Fisica, Università della Calabria, Rende, Italy

[40] [(a)]Faculty of Physics and Applied Computer Science, AGH University of Science and Technology, Kraków, Poland; [(b)]Marian Smoluchowski Institute of Physics, Jagiellonian University, Kraków, Poland
[41] Institute of Nuclear Physics, Polish Academy of Sciences, Kraków, Poland
[42] Physics Department, Southern Methodist University, Dallas, TX, USA
[43] Physics Department, University of Texas at Dallas, Richardson, TX, USA
[44] DESY, Hamburg and Zeuthen, Germany
[45] Lehrstuhl für Experimentelle Physik IV, Technische Universität Dortmund, Dortmund, Germany
[46] Institut für Kern- und Teilchenphysik, Technische Universität Dresden, Dresden, Germany
[47] Department of Physics, Duke University, Durham, NC, USA
[48] SUPA-School of Physics and Astronomy, University of Edinburgh, Edinburgh, UK
[49] INFN Laboratori Nazionali di Frascati, Frascati, Italy
[50] Fakultät für Mathematik und Physik, Albert-Ludwigs-Universität, Freiburg, Germany
[51] Section de Physique, Université de Genève, Geneva, Switzerland
[52] [(a)]INFN Sezione di Genova, Genoa, Italy; [(b)]Dipartimento di Fisica, Università di Genova, Genoa, Italy
[53] [(a)]E. Andronikashvili Institute of Physics, Iv. Javakhishvili Tbilisi State University, Tbilisi, Georgia; [(b)]High Energy Physics Institute, Tbilisi State University, Tbilisi, Georgia
[54] II Physikalisches Institut, Justus-Liebig-Universität Giessen, Giessen, Germany
[55] SUPA-School of Physics and Astronomy, University of Glasgow, Glasgow, UK
[56] II Physikalisches Institut, Georg-August-Universität, Göttingen, Germany
[57] Laboratoire de Physique Subatomique et de Cosmologie, Université Grenoble-Alpes, CNRS/IN2P3, Grenoble, France
[58] Laboratory for Particle Physics and Cosmology, Harvard University, Cambridge, MA, USA
[59] Department of Modern Physics, University of Science and Technology of China, Anhui, China
[60] [(a)]Kirchhoff-Institut für Physik, Ruprecht-Karls-Universität Heidelberg, Heidelberg, Germany; [(b)]Physikalisches Institut, Ruprecht-Karls-Universität Heidelberg, Heidelberg, Germany; [(c)]ZITI Institut für technische Informatik, Ruprecht-Karls-Universität Heidelberg, Mannheim, Germany
[61] Faculty of Applied Information Science, Hiroshima Institute of Technology, Hiroshima, Japan
[62] [(a)]Department of Physics, The Chinese University of Hong Kong, Shatin, NT, Hong Kong; [(b)]Department of Physics, The University of Hong Kong, Pokfulam Road, Pokfulam, Hong Kong; [(c)]Department of Physics, The Hong Kong University of Science and Technology, Clear Water Bay, Kowloon, Hong Kong, China
[63] Department of Physics, Indiana University, Bloomington, IL, USA
[64] Institut für Astro- und Teilchenphysik, Leopold-Franzens-Universität, Innsbruck, Austria
[65] University of Iowa, Iowa City, IA, USA
[66] Department of Physics and Astronomy, Iowa State University, Ames, IA, USA
[67] Joint Institute for Nuclear Research, JINR Dubna, Dubna, Russia
[68] KEK, High Energy Accelerator Research Organization, Tsukuba, Japan
[69] Graduate School of Science, Kobe University, Kobe, Japan
[70] Faculty of Science, Kyoto University, Kyoto, Japan
[71] Kyoto University of Education, Kyoto, Japan
[72] Department of Physics, Kyushu University, Fukuoka, Japan
[73] Instituto de Física La Plata, Universidad Nacional de La Plata and CONICET, La Plata, Argentina
[74] Physics Department, Lancaster University, Lancaster, UK
[75] [(a)]INFN Sezione di Lecce, Lecce, Italy; [(b)]Dipartimento di Matematica e Fisica, Università del Salento, Lecce, Italy
[76] Oliver Lodge Laboratory, University of Liverpool, Liverpool, UK
[77] Department of Physics, Jožef Stefan Institute and University of Ljubljana, Ljubljana, Slovenia
[78] School of Physics and Astronomy, Queen Mary University of London, London, UK
[79] Department of Physics, Royal Holloway University of London, Surrey, UK
[80] Department of Physics and Astronomy, University College London, London, UK
[81] Louisiana Tech University, Ruston, LA, USA
[82] Laboratoire de Physique Nucléaire et de Hautes Energies, UPMC and Université Paris-Diderot and CNRS/IN2P3, Paris, France
[83] Fysiska institutionen, Lunds universitet, Lund, Sweden
[84] Departamento de Fisica Teorica C-15, Universidad Autonoma de Madrid, Madrid, Spain
[85] Institut für Physik, Universität Mainz, Mainz, Germany

[86] School of Physics and Astronomy, University of Manchester, Manchester, UK
[87] CPPM, Aix-Marseille Université and CNRS/IN2P3, Marseille, France
[88] Department of Physics, University of Massachusetts, Amherst, MA, USA
[89] Department of Physics, McGill University, Montreal, QC, Canada
[90] School of Physics, University of Melbourne, Melbourne, VIC, Australia
[91] Department of Physics, The University of Michigan, Ann Arbor, MI, USA
[92] Department of Physics and Astronomy, Michigan State University, East Lansing, MI, USA
[93] [(a)]INFN Sezione di Milano, Milan, Italy; [(b)]Dipartimento di Fisica, Università di Milano, Milan, Italy
[94] B.I. Stepanov Institute of Physics, National Academy of Sciences of Belarus, Minsk, Republic of Belarus
[95] National Scientific and Educational Centre for Particle and High Energy Physics, Minsk, Republic of Belarus
[96] Group of Particle Physics, University of Montreal, Montreal, QC, Canada
[97] P.N. Lebedev Physical Institute of the Russian Academy of Sciences, Moscow, Russia
[98] Institute for Theoretical and Experimental Physics (ITEP), Moscow, Russia
[99] National Research Nuclear University MEPhI, Moscow, Russia
[100] D.V. Skobeltsyn Institute of Nuclear Physics, M.V. Lomonosov Moscow State University, Moscow, Russia
[101] Fakultät für Physik, Ludwig-Maximilians-Universität München, Munich, Germany
[102] Max-Planck-Institut für Physik (Werner-Heisenberg-Institut), Munich, Germany
[103] Nagasaki Institute of Applied Science, Nagasaki, Japan
[104] Graduate School of Science and Kobayashi-Maskawa Institute, Nagoya University, Nagoya, Japan
[105] [(a)]INFN Sezione di Napoli, Naples, Italy; [(b)]Dipartimento di Fisica, Università di Napoli, Naples, Italy
[106] Department of Physics and Astronomy, University of New Mexico, Albuquerque, NM, USA
[107] Institute for Mathematics, Astrophysics and Particle Physics, Radboud University Nijmegen/Nikhef, Nijmegen, The Netherlands
[108] Nikhef National Institute for Subatomic Physics and University of Amsterdam, Amsterdam, The Netherlands
[109] Department of Physics, Northern Illinois University, DeKalb, IL, USA
[110] Budker Institute of Nuclear Physics, SB RAS, Novosibirsk, Russia
[111] Department of Physics, New York University, New York, NY, USA
[112] Ohio State University, Columbus, OH, USA
[113] Faculty of Science, Okayama University, Okayama, Japan
[114] Homer L. Dodge Department of Physics and Astronomy, University of Oklahoma, Norman, OK, USA
[115] Department of Physics, Oklahoma State University, Stillwater, OK, USA
[116] Palacký University, RCPTM, Olomouc, Czech Republic
[117] Center for High Energy Physics, University of Oregon, Eugene, OR, USA
[118] LAL, Univ. Paris-Sud, CNRS/IN2P3, Université Paris-Saclay, Orsay, France
[119] Graduate School of Science, Osaka University, Osaka, Japan
[120] Department of Physics, University of Oslo, Oslo, Norway
[121] Department of Physics, Oxford University, Oxford, UK
[122] [(a)]INFN Sezione di Pavia, Pavia, Italy; [(b)]Dipartimento di Fisica, Università di Pavia, Pavia, Italy
[123] Department of Physics, University of Pennsylvania, Philadelphia, PA, USA
[124] National Research Centre "Kurchatov Institute" B.P. Konstantinov Petersburg Nuclear Physics Institute, St. Petersburg, Russia
[125] [(a)]INFN Sezione di Pisa, Pisa, Italy; [(b)]Dipartimento di Fisica E. Fermi, Università di Pisa, Pisa, Italy
[126] Department of Physics and Astronomy, University of Pittsburgh, Pittsburgh, PA, USA
[127] [(a)]Laboratório de Instrumentação e Física Experimental de Partículas-LIP, Lisbon, Portugal; [(b)]Faculdade de Ciências, Universidade de Lisboa, Lisbon, Portugal; [(c)]Department of Physics, University of Coimbra, Coimbra, Portugal; [(d)]Centro de Física Nuclear da Universidade de Lisboa, Lisbon, Portugal; [(e)]Departamento de Fisica, Universidade do Minho, Braga, Portugal; [(f)]Departamento de Fisica Teorica y del Cosmos and CAFPE, Universidad de Granada, Granada, Spain; [(g)]Dep Fisica and CEFITEC of Faculdade de Ciencias e Tecnologia, Universidade Nova de Lisboa, Caparica, Portugal
[128] Institute of Physics, Academy of Sciences of the Czech Republic, Prague, Czech Republic
[129] Czech Technical University in Prague, Prague, Czech Republic
[130] Faculty of Mathematics and Physics, Charles University in Prague, Prague, Czech Republic
[131] State Research Center Institute for High Energy Physics (Protvino), NRC KI, Moscow, Russia

[132] Particle Physics Department, Rutherford Appleton Laboratory, Didcot, UK
[133] [(a)]INFN Sezione di Roma, Rome, Italy; [(b)]Dipartimento di Fisica, Sapienza Università di Roma, Rome, Italy
[134] [(a)]INFN Sezione di Roma Tor Vergata, Rome, Italy; [(b)]Dipartimento di Fisica, Università di Roma Tor Vergata, Rome, Italy
[135] [(a)]INFN Sezione di Roma Tre, Rome, Italy; [(b)]Dipartimento di Matematica e Fisica, Università Roma Tre, Rome, Italy
[136] [(a)]Faculté des Sciences Ain Chock, Réseau Universitaire de Physique des Hautes Energies-Université Hassan II, Casablanca, Morocco; [(b)]Centre National de l'Energie des Sciences Techniques Nucleaires, Rabat, Morocco; [(c)]Faculté des Sciences Semlalia, Université Cadi Ayyad, LPHEA-Marrakech, Marrakech, Morocco; [(d)]Faculté des Sciences, Université Mohamed Premier and LPTPM, Oujda, Morocco; [(e)]Faculté des Sciences, Université Mohammed V, Rabat, Morocco
[137] DSM/IRFU (Institut de Recherches sur les Lois Fondamentales de l'Univers), CEA Saclay (Commissariat à l'Energie Atomique et aux Energies Alternatives), Gif-sur-Yvette, France
[138] Santa Cruz Institute for Particle Physics, University of California Santa Cruz, Santa Cruz, CA, USA
[139] Department of Physics, University of Washington, Seattle, WA, USA
[140] School of Physics, Shandong University, Shandong, China
[141] Department of Physics and Astronomy, Shanghai Key Laboratory for Particle Physics and Cosmology, Shanghai Jiao Tong University (also affiliated with PKU-CHEP), Shanghai, China
[142] Department of Physics and Astronomy, University of Sheffield, Sheffield, UK
[143] Department of Physics, Shinshu University, Nagano, Japan
[144] Fachbereich Physik, Universität Siegen, Siegen, Germany
[145] Department of Physics, Simon Fraser University, Burnaby, BC, Canada
[146] SLAC National Accelerator Laboratory, Stanford, CA, USA
[147] [(a)]Faculty of Mathematics, Physics and Informatics, Comenius University, Bratislava, Slovakia; [(b)]Department of Subnuclear Physics, Institute of Experimental Physics of the Slovak Academy of Sciences, Kosice, Slovak Republic
[148] [(a)]Department of Physics, University of Cape Town, Cape Town, South Africa; [(b)]Department of Physics, University of Johannesburg, Johannesburg, South Africa; [(c)]School of Physics, University of the Witwatersrand, Johannesburg, South Africa
[149] [(a)]Department of Physics, Stockholm University, Stockholm, Sweden; [(b)]The Oskar Klein Centre, Stockholm, Sweden
[150] Physics Department, Royal Institute of Technology, Stockholm, Sweden
[151] Departments of Physics and Astronomy and Chemistry, Stony Brook University, Stony Brook, NY, USA
[152] Department of Physics and Astronomy, University of Sussex, Brighton, UK
[153] School of Physics, University of Sydney, Sydney, Australia
[154] Institute of Physics, Academia Sinica, Taipei, Taiwan
[155] Department of Physics, Technion: Israel Institute of Technology, Haifa, Israel
[156] Raymond and Beverly Sackler School of Physics and Astronomy, Tel Aviv University, Tel Aviv, Israel
[157] Department of Physics, Aristotle University of Thessaloniki, Thessaloniki, Greece
[158] International Center for Elementary Particle Physics and Department of Physics, The University of Tokyo, Tokyo, Japan
[159] Graduate School of Science and Technology, Tokyo Metropolitan University, Tokyo, Japan
[160] Department of Physics, Tokyo Institute of Technology, Tokyo, Japan
[161] Tomsk State University, Tomsk, Russia
[162] Department of Physics, University of Toronto, Toronto, ON, Canada
[163] [(a)]INFN-TIFPA, Trento, Italy; [(b)]University of Trento, Trento, Italy
[164] [(a)]TRIUMF, Vancouver, BC, Canada; [(b)]Department of Physics and Astronomy, York University, Toronto, ON, Canada
[165] Faculty of Pure and Applied Sciences, and Center for Integrated Research in Fundamental Science and Engineering, University of Tsukuba, Tsukuba, Japan
[166] Department of Physics and Astronomy, Tufts University, Medford, MA, USA
[167] Department of Physics and Astronomy, University of California Irvine, Irvine, CA, USA
[168] [(a)]INFN Gruppo Collegato di Udine, Sezione di Trieste, Udine, Italy; [(b)]ICTP, Trieste, Italy; [(c)]Dipartimento di Chimica Fisica e Ambiente, Università di Udine, Udine, Italy
[169] Department of Physics and Astronomy, University of Uppsala, Uppsala, Sweden
[170] Department of Physics, University of Illinois, Urbana, IL, USA

[171] Instituto de Fisica Corpuscular (IFIC) and Departamento de Fisica Atomica, Molecular y Nuclear and Departamento de Ingeniería Electrónica and Instituto de Microelectrónica de Barcelona (IMB-CNM), University of Valencia and CSIC, Valencia, Spain
[172] Department of Physics, University of British Columbia, Vancouver, BC, Canada
[173] Department of Physics and Astronomy, University of Victoria, Victoria, BC, Canada
[174] Department of Physics, University of Warwick, Coventry, UK
[175] Waseda University, Tokyo, Japan
[176] Department of Particle Physics, The Weizmann Institute of Science, Rehovot, Israel
[177] Department of Physics, University of Wisconsin, Madison, WI, USA
[178] Fakultät für Physik und Astronomie, Julius-Maximilians-Universität, Würzburg, Germany
[179] Fakultät für Mathematik und Naturwissenschaften, Fachgruppe Physik, Bergische Universität Wuppertal, Wuppertal, Germany
[180] Department of Physics, Yale University, New Haven, CT, USA
[181] Yerevan Physics Institute, Yerevan, Armenia
[182] Centre de Calcul de l'Institut National de Physique Nucléaire et de Physique des Particules (IN2P3), Villeurbanne, France

[a] Also at Department of Physics, King's College London, London, UK
[b] Also at Institute of Physics, Azerbaijan Academy of Sciences, Baku, Azerbaijan
[c] Also at Novosibirsk State University, Novosibirsk, Russia
[d] Also at TRIUMF, Vancouver, BC, Canada
[e] Also at Department of Physics and Astronomy, University of Louisville, Louisville, KY, USA
[f] Also at Physics Department, An-Najah National University, Nablus, Palestine
[g] Also at Department of Physics, California State University, Fresno, CA, USA
[h] Also at Department of Physics, University of Fribourg, Fribourg, Switzerland
[i] Also at Departament de Fisica de la Universitat Autonoma de Barcelona, Barcelona, Spain
[j] Also at Departamento de Fisica e Astronomia, Faculdade de Ciencias, Universidade do Porto, Porto, Portugal
[k] Also at Tomsk State University, Tomsk, Russia, Russia
[l] Also at Universita di Napoli Parthenope, Naples, Italy
[m] Also at Institute of Particle Physics (IPP), Canada
[n] Also at National Institute of Physics and Nuclear Engineering, Bucharest, Romania
[o] Also at Department of Physics, St. Petersburg State Polytechnical University, St. Petersburg, Russia
[p] Also at Department of Physics, The University of Michigan, Ann Arbor, MI, USA
[q] Also at Centre for High Performance Computing, CSIR Campus, Rosebank, Cape Town, South Africa
[r] Also at Louisiana Tech University, Ruston, LA, USA
[s] Also at Institucio Catalana de Recerca i Estudis Avancats, ICREA, Barcelona, Spain
[t] Also at Graduate School of Science, Osaka University, Osaka, Japan
[u] Also at Department of Physics, National Tsing Hua University, Taiwan
[v] Also at Institute for Mathematics, Astrophysics and Particle Physics, Radboud University Nijmegen/Nikhef, Nijmegen, The Netherlands
[w] Also at Department of Physics, The University of Texas at Austin, Austin TX, USA
[x] Also at CERN, Geneva, Switzerland
[y] Also at Georgian Technical University (GTU), Tbilisi, Georgia
[z] Also at Ochadai Academic Production, Ochanomizu University, Tokyo, Japan
[aa] Also at Manhattan College, New York, NY, USA
[ab] Also at Hellenic Open University, Patras, Greece
[ac] Also at Academia Sinica Grid Computing, Institute of Physics, Academia Sinica, Taipei, Taiwan
[ad] Also at School of Physics, Shandong University, Shandong, China
[ae] Also at Department of Physics, California State University, Sacramento, CA, USA
[af] Also at Moscow Institute of Physics and Technology State University, Dolgoprudny, Russia
[ag] Also at Section de Physique, Université de Genève, Geneva, Switzerland
[ah] Also at Eotvos Lorand University, Budapest, Hungary
[ai] Also at Departments of Physics and Astronomy and Chemistry, Stony Brook University, Stony Brook, NY, USA
[aj] Also at International School for Advanced Studies (SISSA), Trieste, Italy

[ak] Also at Department of Physics and Astronomy, University of South Carolina, Columbia, SC, USA
[al] Also at School of Physics and Engineering, Sun Yat-sen University, Guangzhou, China
[am] Also at Institute for Nuclear Research and Nuclear Energy (INRNE) of the Bulgarian Academy of Sciences, Sofia, Bulgaria
[an] Also at Faculty of Physics, M.V. Lomonosov Moscow State University, Moscow, Russia
[ao] Also at Institute of Physics, Academia Sinica, Taipei, Taiwan
[ap] Also at National Research Nuclear University MEPhI, Moscow, Russia
[aq] Also at Department of Physics, Stanford University, Stanford, CA, USA
[ar] Also at Institute for Particle and Nuclear Physics, Wigner Research Centre for Physics, Budapest, Hungary
[as] Also at Flensburg University of Applied Sciences, Flensburg, Germany
[at] Also at University of Malaya, Department of Physics, Kuala Lumpur, Malaysia
[au] Also at CPPM, Aix-Marseille Université and CNRS/IN2P3, Marseille, France
[*] Deceased